IL NUOVO CIMENTO

1959

IL

NUOVO CIMENTO

PERIODICO ITALIANO DI FISICA

fondato a Pisa nel 1855 da C. Matteucci e R. Piria
dal 1897 Organo della Società Italiana di Fisica
è pubblicato
sotto gli auspici del Consiglio Nazionale delle Ricerche
a cura del Direttore
GIOVANNI POLVANI
Presidente della Società
e
dei Vicedirettori
M. Conversi e N. Dallaporta
con la collaborazione di un Comitato di redazione
costituito dai professori
G. Bernardini, G. Bolla, A. Borsellino, E. Caianiello, P. Caldirola,
G. Careri, M. Cini, R. Deaglio, B. Finzi, S. Franchetti,
F. Fumi, A. Giacomini, L. Giulotto, D. Graffi, G. Occhialini,
E. Perucca, L. A. Radicati, C. Salvetti, G. Salvini, M. Simonetta,
G. Toraldo di Francia, M. Verde, G. Wataghin.

Segretario di Redazione
R. Corbi

Redazione
Bologna, Via Irnerio n. 46
presso l'Istituto di Fisica dell'Università

Direzione
Milano, Via Saldini n. 50
presso l'Istituto di Fisica dell'Università

IL
NUOVO CIMENTO

ORGANO DELLA SOCIETÀ ITALIANA DI FISICA

SOTTO GLI AUSPICI DEL CONSIGLIO NAZIONALE DELLE RICERCHE

VOLUME XII

Serie decima

Anno centesimoquinto

1959

PRINTED IN ITALY

NICOLA ZANICHELLI EDITORE
BOLOGNA

IL
NUOVO CIMENTO
ORGANO DELLA SOCIETÀ ITALIANA DI FISICA
SOTTO GLI AUSPICI DEL CONSIGLIO NAZIONALE DELLE RICERCHE

VOL. XII, N. 1 *Serie decima* 1° Aprile 1959

Interactions of the Heavy Nuclei of Cosmic Rays in Carbon.

Y. HIRASHIMA
Department of Physics, Rikkyo University - Tokyo

(ricevuto il 15 Dicembre 1958)

Summary, — The fragmentation probabilities of the heavy nuclei of cosmic rays have been investigated in carbon. Emulsion chambers consisting of carbon and photographic nuclear emulsions exposed in Japan ($\lambda = 25$ °N) were used. The charges of the heavy nuclei with $Z > 3$ were determined by measuring the δ-ray densities. The fragmentation probabilities into the light nuclei are $P_{HL} = 0.35 \pm 0.08$ and $P_{ML} = 0.35 \pm 0.08$. The abundances at the balloon flight altitudes observed by several groups were extrapolated to the top of the atmosphere by using the fragmentation probabilities in carbon obtained in the present work. The ratio of the light nuclei to the medium nuclei at the top of the atmosphere is probably in the range from ~ 0.1 to ~ 0.2.

1. – Introduction.

The composition of the heavy nuclei of cosmic rays at the top of the atmosphere is an important information for deducing the origin of cosmic rays and the structure of the galaxy, and it can be discussed in relation to the origin of elements [1-9]. Many workers have investigated, especially, the abundance

(1) H. L. BRADT and B. PETERS: *Phys. Rev.*, **77**, 54 (1950).
(2) H. L. BRADT and B. PETERS: *Phys. Rev.*, **80**, 943 (1950).
(3) S. HAYAKAWA: *Progr. Theor. Phys.*, **15**, 111 (1956).
(4) V. L. GINSBURG and M. I. FRADKIN: *Žurn. Èksp. Teor. Fiz. SSSR*, **31**, 523 (1956).
(5) V. L. GINSBURG: *Usp. Fiz. Nauk SSSR*, **62**, 37 (1957).
(6) H. E. SUESS and H. C. UREY: *Rev. Mod. Phys.*, **28**, 53 (1956).
(7) E. M. BURBIDGE, G. R. BURBIDGE, W. A. FOWLER and F. HOYLE: *Rev. Mod. Phys.*, **29**, 547 (1957).
(8) M. KOSHIBA, G. SCHULTZ and M. SCHEIN: *Nuovo Cimento*, **9**, 1 (1958).
(9) S. HAYAKAWA, K. ITO and Y. TERASHIMA: *Suppl. Progr. Theor. Phys.*, no. 6, 1 (1958).

of lithium, beryllium, and boron in the primary cosmic rays during recent years ([2,8,10-18]); but their results are not in complete agreement. This discrepancy seems to be due partly to the difficulty of accurate determination of the fragmentation probabilities of the heavy primary cosmic rays by air nuclei, as well as to the difficulty of accurate determination of the charges of heavy nuclei. The fragmentation probabilities have been investigated by several groups ([2,8,17,19-23]); but these results are not in complete agreement, either. Experimental data on the fragmentation probabilities based on many statistics were obtained for the case in which the nuclei of the emulsion were targets. Either the fragmentation probabilities obtained experimentally by analyzing the interactions having few heavy prongs from a target nucleus, say $N_h \leqslant 6$ or 7, or the fragmentation probabilities by air nuclei inferred from experimental data of the fragmentation probabilities by all kinds of emulsion nuclei were used in extrapolation of the abundances of the heavy primary cosmic rays to the top of the atmosphere. In the former case, 43% of the events with $N_h \leqslant 7$ are known to be peripheral collisions with heavy targets in emulsion ([17]). A collision with the periphery of a heavy target nucleus in emulsion is not identical with a head-on collision with a light target nucleus. In the latter case, NOON and KAPLON ([20]) extrapolated the observed fragmentation probabilities in emulsion to the corresponding values in air by using a simple model. However, this was only a simple method of extrapolation to the values in air, namely Noon and Kaplon's own method, or Eisenberg's ([24]). RADJOPADHYE and WADDINGTON ([22]) deduced with care the values of the fragmentation probabilities by the light nuclei in emulsion from the experimental data in emulsion, but these results were obtained by an experiment in which the kind of a target nucleus was not defined.

In the present work, the fragmentation probabilities by carbon nuclei have

---

([10]) A. D. DAINTON, P. H. FOWLER and D. W. KENT: *Phil. Mag.*, **43**, 729 (1952).
([11]) M. F. KAPLON, J. H. NOON and G. W. RACETTE: *Phys. Rev.*, **96**, 1408 (1954).
([12]) H. FAY: *Zeits. f. Naturfor.*, **10***a*, 572 (1955).
([13]) W. R. WEBBER: *Nuovo Cimento*, **4**, 1285 (1956).
([14]) J. H. NOON, A. J. HERTZ and B. J. O'BRIEN: *Nuovo Cimento*, **5**, 854 (1957).
([15]) T. H. STIX: *Phys. Rev.*, **95**, 782 (1954).
([16]) C. J. WADDINGTON: *Phil. Mag.*, **2**, 1059 (1957).
([17]) R. CESTER, A. DEBENEDETTI, C. M. GARELLI, B. QUASSIATI, L. TALLONE and M. VIGONE: *Nuovo Cimento*, **7**, 371 (1958).
([18]) ROCHESTER GROUP: *Uchusen Kenkyu, Japan*, **3**, 75 (1958).
([19]) K. GOTTSTEIN: *Phil. Mag.*, **45**, 347 (1954).
([20]) J. H. NOON and M. F. KAPLON: *Phys. Rev.*, **97**, 769 (1955).
([21]) P. H. FOWLER, R. R. HILLIER and C. J. WADDINGTON: *Phil. Mag.*, **2**, 293 (1957).
([22]) V. Y. RAJOPADHYE and C. J. WADDINGTON: *Phil. Mag.*, **3**, 19 (1958).
([23]) V. D. HOPPER, J. E. LABY and Y. K. LIM: *Nuovo Cimento*, **7**, 552 (1958).
([24]) Y. EISENBERG: *Phys. Rev.*, **96**, 1378 (1954).

been observed. As carbon nuclei are the closest to air nuclei, the author has regarded the fragmentation probabilities obtained by analyzing the interactions of the heavy primary cosmic rays in carbon as those in air. In order to obtain the fragmentation probabilities by carbon nuclei, emulsion chambers containing carbon plates were used.

In this paper the heavy nuclei were divided into three groups: the light group, L, $3 \leqslant z \leqslant 5$; the medium group, M, $6 \leqslant Z \leqslant 9$; and the heavy group H, $10 \leqslant Z$.

With the values of the fragmentation probabilities by carbon nuclei, the abundances of the heavy primary cosmic rays at balloon flight altitudes obtained recently by the several groups have been extrapolated to the top of the atmosphere, as the balloon flight altitude in the present experiment was low, and was not appropriate to an observation of the abundance of the heavy primary cosmic rays.

2. – Experimental procedure.

Six emulsion chamber units were utilized, each unit consisting of nine carbon plates (20 cm×15 cm×0.8 cm) and nine Ilford G-5 coated photographic nuclear emulsions (20 cm×15 cm×200 μm), piled up alternatively. (All of these units were a part of the emulsion chambers exposed in 1956 as « Emulsion Chamber Project » in Japan ([25]).) The exposure details were reported in ref. ([25]). The main feature of the exposure is that the emulsion chambers were exposed with horizontal orientation of the emulsion surfaces. The balloon flights were made at Shizuoka and Kobe ($\lambda = 25°$ N, probable cut-off energy of the heavy primary cosmic rays ~ 5 GeV/nucleon) at atmospheric depths from 25 g/cm² to 50 g/cm².

A total area of 1800 cm² of the top emulsion plates were scanned, and tracks were picked out which have a δ-ray density of > 2.5 per 100 μm. 460 tracks were found having this criterion, and they were followed through the emulsion chamber until they left the emulsion chamber, whether the incident particle interacted in the emulsion chamber or not. Some of these tracks were not found in the next emulsion plate under the top plate when the tracks were followed to the next plate successively. This disappearance is due to the difficulty of following tracks to the next plate, caused by track distortion and stop of the low energy particles in the carbon plate just under the top emulsion plate. In the analysis of the interaction mean free paths and fragmen-

([25]) O. Minakawa, Y. Nishimura, Y. Tsuzuki, H. Yamanouchi, H. Aizu, H. Hasegawa, Y. Ishii, S. Tokunaga, Y. Fujimoto, S. Hasegawa, J. Nishimura, K. Niu, K. Nishikawa, K. Imaeda and M. Kazuno: preprint.

tation probabilities, therefore, the top emulsion plates were excluded. In the case where a track was found in the next plate, however, it was hardly difficult to follow the track successively. The tracks of projected length < 50 μm were excluded in the analysis because of difficulty of analysis, and also excluded were those of projected length > 500 μm, because the particles passed through a large thickness of the atmosphere to undergo an appreciable amount of the ionization loss, and they might be not relativistic in energy, and because it was difficult to follow the tracks of such a large projected length to the next plate.

To determine the charges of the heavy nuclei with $Z \geqslant 3$, the densities of δ-rays with four or more grains were measured. To distinguish between protons, α-particles, and heavier nuclei with $Z \geqslant 3$, the grain densities were measured. It could be assumed, as many other authors have done, that all the analyzed nuclei had relativistic energies because the cut-off energy of the heavy primary cosmic rays was especially high under our exposure conditions ($\lambda = 25°$ N, cut-off energy ~ 5 GeV/nucleon). The δ-ray density of a relativistic nucleus with a multiple charge can be expressed as follows

$$N_\delta = aZ^2 + b \,, \tag{1}$$

where N_δ is the δ-ray density per 100 μm. The δ-ray density was calibrated by using the secondary protons and α-particles resulting from the break-ups of the heavy primary cosmic rays. The secondary protons, α-particles and heavier nuclei with $Z \geqslant 3$ were divided by the grain densities per 100 μm, g: the protons, $g \leqslant 2g_0$; the α-particles, $2g_0 < g \leqslant 5g_0$; and the heavier nuclei with $Z \geqslant 3$, $5g_0 < g$; where g_0 was the plateau value of the grain density, and was found to be 21.3 ± 0.3 per 100 μm. As the separation among the protons, the α-particles, and the heavier nuclei with $Z \geqslant 3$ by the grain densities was perfectly done, constants a and b in equation (1) were determined as follows by using the δ-ray densities of the secondary protons and α-particles: $a = 0.096 \pm 0.013$ and $b = 0.100 \pm 0.035$.

Since it was not possible to observe the heavy prongs from carbon target nuclei, care was taken in identifying the interactions in carbon plates. At the time of following the tracks, the vicinities of the tracks were carefully scanned. The tracks which had an angular spread of $< 3°$ from the direction of the track of the primary particle were identified as secondary fragments. These secondary tracks were nearly parallel, as the primary nuclei had high energies owing to the high cut-off energy of ~ 5 GeV/nucleon in our exposure conditions. Taking into consideration the fact that NAKAGAWA *et al.* ([26]) had observed energetic lithium fragments emitted from the nuclear

([26]) S. NAKAGAWA, E. TAMAI and S. NOMOTO: *Nuovo Cimento*, **9**, 780 (1958).

stars, other than in the evaporation process, amounting to 250 MeV, it is reasonable to take the angular spread of $< 3°$ as the criterion of the secondary fragments. The mixing of π-mesons within such an angle is slight. In the case of Waddington's experiment ([16]), 90% of the singly charged particles emitted within an angle of 5° were protons belonging to the incoming nucleus.

Great care was taken in identifying the interactions producing one heavily ionized track and one thin track. In some cases one thin track attached to the heavily ionized track is not a track made by a secondary proton from the heavy primary nucleus to be attributed to the nuclear interaction in carbon, there being a possibility for such a thin track to be a track made by a knock-on electron. The momentum of the knock-on electron is considerably lower than that of the secondary proton, and the multiple scattering of the electron is very large. Owing to this large multiple scattering of the electron, the knock-on electrons could be distinguished from the protons. The frequency of the knock-on electron which is emitted forwards with an angular spread of $< 3°$ from the direction of the track of the primary particle is $\sim 2.4 \cdot 10^{-4} Z^2$ g^{-1} cm^2, if the spin is not taken into account and if the kinetic energy of the heavy primary nucleus is ~ 3.5 GeV/nucleon. Several tens of knock-on electrons with an angular spread of $< 3°$, therefore, were expected to be observed in our case. Such a knock-on electron has a kinetic energy of ~ 18 MeV (when the primary energy is ~ 3.5 GeV/nucleon, and the angular spread of $< 3°$). The root mean square angle of the multiple scattering of the knock-on electron with kinetic energy of ~ 18 MeV amounts to ~ 0.3 radian after penetration of one pair of carbon plate and backing glass plate. Even if the knock-on electron had a kinetic energy of 270 MeV (when the primary energy is 10^3 GeV/nucleon, and the angular spread of 3°), the root mean square angle of the multiple scattering of the electron amounts to ~ 0.02 radian after penetration of one pair of plates; while in the case of the secondary proton with a kinetic energy of ~ 3.5 GeV by break-up of the heavy primary nucleus, the root mean square angle of the multiple scattering amounts to ~ 0.001 radian. (In these estimations, the observed mean path length of the particles in penetration of one pair of carbon plate and backing glass plate was used.) Therefore, if a track underwent multiple scattering deflection of > 0.005 radian after penetration of one pair of plates, it was taken to be the track of the knock-on electron, and with this criterion, the knock-on electrons with a large angle deflection could be almost perfectly eliminated in identifying the nuclear interactions. The 46 knock-on electrons which were eliminated with this criterion have been observed.

112 interactions were found in which the heavy primary cosmic rays with $Z \geqslant 6$ had broken up. There were 5 events which were missed under the third emulsion plates in following the tracks, but they are few in proportion to the total number of interactions. It was expected to observe the events in

which the primary nuclei had broken up into thin tracks only. 9 events which had only thin tracks as a result of the interaction, were found among the 112 events. An isolated thin track is apt to be missed on account of the high density of background fog and slow electrons, as will be shown in later discussion. The 5 events which were missed in following the tracks can be regarded as interactions of such a type. For the 5 missed events, the variation of the δ-ray density along the tracks were measured. For example, in the event which showed the largest increase of δ-ray density among the 5 events, the increase of the δ-ray density in the lowest emulsion plate with the track belonging to this event over that in the top emulsion plate did not exceed 20%, and this is within the statistical error. On the other hand, if the heavy nucleus had stopped at the carbon plate, when the increase of the δ-ray density is estimated using the relation between the range and the δ-ray density by BRADT and PETERS ([27]), neglecting the difference between carbon and emulsion caused by the density effect of the collision loss, then the increase of the δ-ray density in the lowest emulsion plate at the range not to exceed 1.9 g/cm² would have amounted to 110% in comparison with the δ-ray density in the top place at the range of 9.6 g/cm². Hence, it is apparent that these 5 events can not be considered to be stopped events, but rather missed events in which the primary nuclei broke up into thin tracks only.

The final confirmation of the identification of the nuclear interactions was performed by comparing the observed interaction mean free path in our experiment with the empirical expression of the interaction mean free path given by BRADT and PETERS ([1]).

3. – Results and discussion.

The characteristics of each of the 117 interactions in carbon which were produced by the heavy primary nuceli with $Z \geqslant 6$ are shown in Table I. The interactions with sodium, silicon, and oxygen nuclei in the thin backing glass (1.3 mm thick) could not be distinguished from the interactions with carbon nuclei, but this is of no great consequence, for sodium, silicon, and oxygen nuclei are few in number, compared with carbon nuclei in the emulsion chambers, and not so different from carbon nuclei in size, as silver and bromine nuclei are. It is not inappropriate, therefore, to have to include the interactions with nuclei in glass. The interactions produced by the fragments from the other interactions are included in Table I. The interactions are listed according to the charge of the heavy primary nucleus.

([27]) H. L. BRADT and B. PETERS: *Phys. Rev.*, **74**, 1828 (1948).

TABLE I. — *Characteristics of each of the* 117 *interactions in carbon produced by the heavy primary nuclei with* $Z > 6$. (n_2 and n_s represent the numbers of α-particles and thinly ionizing particles with an angular spread of $< 3°$ respectively).

Primary nucleus	Fragments H	M	L	n_2	n_s
Ti	Na			2	4
K	Al				3
	Na		Li	2	1
	A			1	1
	Al			1	2
A			Be	4	2
				1	3
	Al				12
Cl			Be	2	6
			B	1	5
S	Al			1	1
			B. Li	3	2
				3	12
P			Li	2	14
			B		17
			Be	2	
Si		C		4	
	Mg			1	
			B	4	2
		C			4
Al		O		2	3
		O	Li		1
			B	1	3
Mg	Mg			1	
		F		1	2
			Be		1
				2	5
			Be	1	9
Na				2	7
		C		1	
				1	3
	Na				1
			Be	2	4
				3	1
Na		N	2		
					?(*)
		O		1	1
				3	6
				2	3
				1	1
			Li		4
				2	5
		N		1	
Ne			Be		4
			Be	1	
		C		1	2
		N			1
		C		2	1
		O		1	
				2	
					?
		C			2
			Li	1	
			B	2	
		F		1	1
				1	7
		F		1	
F			Li		3
		C			5
			Li	4	
				3	1
					1
					6
					5
			Li	1	2
					16
					2
				2	1
				3	5
					3
				4	
					?

(*) Events which had been missed in following the tracks. These can be regarded as interactions by which the primary nuclei broke up into thin tracks only (see text).

TABLE I (*continued*).

Primary nucleus	Fragments H	Fragments M	Fragments L	n_α	n_t	Primary nucleus	Fragments H	Fragments M	Fragments L	n_α	n_t
O			Li	1		N					?
				1	1				Li	2	
			Be	2	1				B		2
				3	1				Li	1	
		C			1				Be		1
				1	1						
		N			1	C					2
				1	2				B	1	
			Be		4					2	
				3	3					2	2
			Li	1					Be	1	
				1	1					1	1
					2				B	1	
		C		1						1	1
										1	
N				2	2						2
				4	4				Be	1	
			Li		1					1	2
		C			1				B		2
			Li		4					3	1
				2						3	1
				1	1				Be		1
			B		1						?
			B		1						

In order to obtain the value of the fragmentation probability of the primary nuclei belonging to the L group, P_{LL}, the 12 interactions in carbon which were produced by the L group fragments from other interactions were available. The characteristics of each of those interactions are listed in Table II.

TABLE II. – *Characteristics of each of the* 12 *interactions in carbon produced by* L *group fragments from other interactions.*

Primary nucleus	Fragments L	n_α	n_t	Primary nucleus	Fragments L	n_α	n_t
B		1	2	Be			2
		1					4
	Li		2			1	1
		1	3		Li		1
			3				
				Li			?
Be		2					?

As for the 117 interactions produced by the heavy primary nuclei with $Z \geqslant 6$, the observed primary charges were compared with the sums of the charges of the secondary particles with the angular spread of $< 3^{\circ}$. The distributions of the differences between the primary charge and the sum of the charges of the secondary particles with the angular spread of $< 3^{\circ}$, $\Delta Z = Z_{1ry} - \sum Z_{2ry}$, are shown in Fig. 1-*a* and Fig. 1-*b* for the H group and

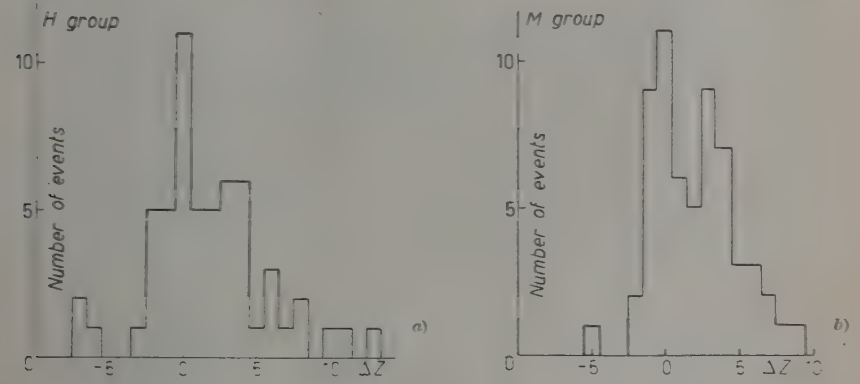

Fig. 1.

the M group respectively of the primary nuclei. It seems that the large area of the positive region of ΔZ is due to having missed the thin tracks produced by the protons, for the isolated thin tracks were likely to be missed in the present experiment. When the incoming heavy nuclei have broken up into many secondary fragments, the detection of the heavy fragments, especially important L group fragments, is easy, and the protons are apt to be missed, but the missed protons are not so important to the fragmentation probabilities to be used in extrapolation of the abundance of the heavy primary cosmic rays to the top of the atmosphere. The determination of charges, however, becomes a problem. In order to obtain the correct fragmentation probabilities into the L nuclei, P_{HL} and P_{ML}, especially the correct determination of the charges of the L nuclei is important. At first glance, Fig. 1-*a* and Fig. 1-*b* seem to show that the charge determination is rough, but the spreads of the distribution are attributable mainly to having missed the protons, to the mixture of π-mesons, and to the inexact charge determination of the comparatively heavy nuclei.

In order to show the degree of accuracy in the charge determination, the distribution of the δ-ray densities N_δ for the individual nuclei with $3 \leqslant Z \leqslant 14$ which were used to obtain the fragmentation probabilities is shown in Fig. 2.

The δ-ray densities for the incident heavy nuclei and those for the fragments were collected without distinction, so the distribution in Fig. 2 does not represent the distribution of the δ-ray densities of the incoming heavy nuclei.

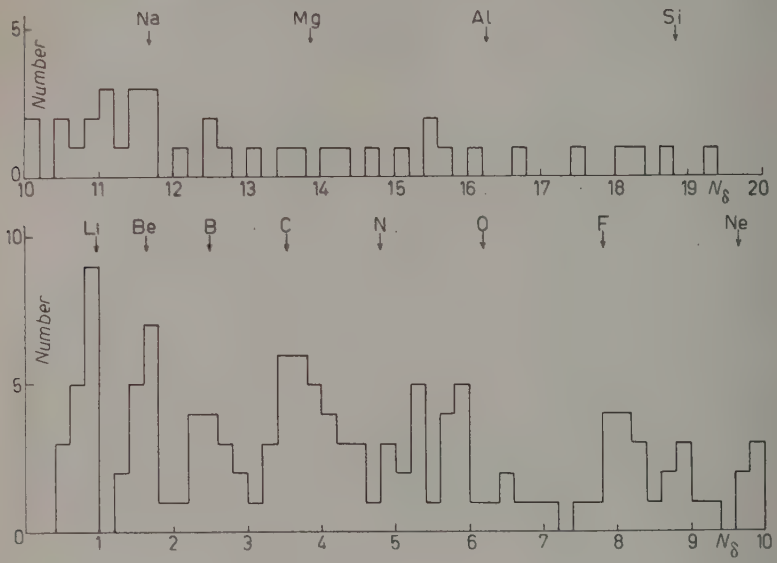

Fig. 2.

The clear separation of the δ-ray density peaks is observed as far as carbon, although the positions of the higher δ-ray density peaks are not well defined. The positions of the observed peaks agree closely with the predicted positions from the charge calibration as far as carbon. The distinction between boron nuclei and carbon nuclei is important in the determination of the fragmentation probabilities into the L nuclei, P_{HL} and P_{ML}. In our experiment the charge determination undergoes little distortion as far as carbon.

TABLE III. *Interaction mean free paths in the present work, together with calculated values in carbon.*

Charge group	$\bar{Z}$	Present work		Calculated value in carbon (g/cm²)
		Observed value in emulsion chambers (g/cm²)	Observed value in carbon (g/cm²)	
H	12.8	19.2 ± 4.0	18.0 ± 4.4	18.3
M	7.2	29.3 ± 5.9	28.3 ± 7.0	24.0

The observed interaction mean free paths in the emulsion chambers were (19.2 ± 4.0) g/cm² for the H nuclei and (29.3 ± 5.9) g/cm² for the M nuclei. To obtain the values of the interaction mean free paths in carbon, the modification of the interaction mean free paths by eliminating the contribution of the backing glass is necessary. The observed interaction mean free paths in glass by BRADT and PETERS [2] were used in this modification. In Table III, the interaction mean free paths in carbon are compared with the values calculated by using the empirical expression of the cross-section proposed by BRADT and PETERS [1] and confirmed by many experimenters [17,20-22,24,28]:

$$\sigma = (R_i + R_t - 2\Delta R)^2, \qquad R = r_0 A^{\frac{1}{3}} \qquad (r_0 = 1.45 \cdot 10^{-13} \text{ cm}), \tag{2}$$

where R_i is the radius of the incoming nucleus, R_t is the radius of the target nucleus, and ΔR has the empirical value of $0.85 \cdot 10^{-13}$ cm. The experimental values are in good agreement with the calculated values within experimental error, so it can reasonably be concluded that there have been little mistakes made in the identification of the nuclear interactions.

TABLE IV. – *Total numbers of fragments with $Z > 3$, α-particles, and thinly ionizing particles, resulting from the break-ups of the heavy nuclei.*

Primary nuclei	Number of interactions	Fragments			n_α	n_t
		H	M	L		
H	57	10	16	20	76	169
M	60	—	5	21	62	96
L	12	—	—	2	6	18

In Table IV are presented the total numbers of the fragments with $Z > 3$, α-particles, and thinly ionizing particles with the angular spread of $< 3°$ (which are mostly protons from the break-ups of the primary nuclei).

Table V shows the fragmentation probabilities obtained in the present work, together with those obtained by the several groups. In this Table V, it is shown that the fragmentation probabilities into the L nuclei, P_{HL} and P_{ML}, obtained in the present work, have intermediate values between the value obtained by the Rochester group and HOPPER *et al.*, and those by the Bristol group, the Chicago group, and the Turin group.

(28) F. B. MCDONALD: *Phys. Rev.*, **104**, 1723 (1956).

TABLE V. – *Fragmentation probabilities obtained in the present work, together with those obtained by the several groups.*

	P_{HH}	P_{HM}	P_{HL}	$P_{H\alpha}$	P_{MM}	P_{ML}	$P_{M\alpha}$	P_{LL}	$P_{L\alpha}$
Present work (in carbon)	0.18 ± 0.06	0.28 ± 0.07	0.35 ± 0.08	1.33 ± 0.15	0.08 ± 0.04	0.35 ± 0.08	1.03 ± 0.13	0.17 ± 0.12	0.50 ± 0.20
Rochester — NOON and KAPLON [20] ($N_h \leqslant 7$)	0.18 ± 0.06	0.23 ± 0.06	0.52 ± 0.08	2.00 ± 0.20	0.09 ± 0.03	0.38 ± 0.06	1.33 ± 0.12	—	—
Rochester — NOON and KAPLON [20] (derived for air)	0.25	0.27	0.48	2.07	0.13	0.42	1.42	0.13	—
HOPPER *et al.* [23] ($N_h \leqslant 6$ in water loaded emulsion)	0.19 ± 0.11	0.25 ± 0.13	0.31 ± 0.14	2.25 ± 0.38	0.11 ± 0.07	0.47 ± 0.16	0.79 ± 0.20	0.40 ± 0.20	1.00 ± 0.32
Bristol — FOWLER *et al.* [21] ($N_h \leqslant 7$)	0.20 ± 0.08	0.50 ± 0.13	0.17 ± 0.07	1.33 ± 0.26	0.16 ± 0.04	0.18 ± 0.04	0.98 ± 0.11	0.16 ± 0.07	0.45 ± 0.13
Bristol — RAJOPADHYE and WADDINGTON [22]	0.29 ± 0.11	0.46 ± 0.15	0.21 ± 0.09	1.23 ± 0.40	0.17 ± 0.06	0.23 ± 0.07	1.27 ± 0.28	0.12 ± 0.07	0.79 ± 0.26
KOSHIBA *et al.* [8] ($N_h < 6$)	0.21 ± 0.12	0.21 ± 0.12	0.29 ± 0.14	1.57 ± 0.34	0.13 ± 0.08	0.17 ± 0.09	0.87 ± 0.20	0.06 ± 0.06	0.47 ± 0.16
CESTER *et al.* [17] ($N_h < 7$)	0.34 ± 0.09	0.27 ± 0.08	0.14 ± 0.06	—	0.19 ± 0.04	0.23 ± 0.04	—	0.15 ± 0.06	—

It must be noted that the impact parameter may play an important role as regards the fragmentation of the heavy primary nuclei, the fragmentation being increased when the impact parameter decreases. Including peripheral collisions with the heavy nuclei, silver and bromine (when the fragmentation probabilities are obtained by picking out the interactions with $N_h \leqslant 6$ or 7 in the emulsion), emphasizes the case of the large impact parameter, and would result in an overestimate of P_{HH}, P_{MM}, and P_{LL}, and in an underestimate of P_{HL} and P_{ML}.

The abundances of the heavy primary nuclei at balloon flight altitudes observed recently by several groups have been extrapolated to the top of the atmosphere by using the diffusion equations given by KAPLON *et al.* ([11]):

$$\mathrm{d}N_{\mathrm{I}}(x)/\mathrm{d}x = -N_{\mathrm{I}}(x)/\lambda_{\mathrm{I}} + \sum_{\mathrm{I}'>\mathrm{I}} N_{\mathrm{I}'}(x) P_{\mathrm{I}'\mathrm{I}}/\lambda_{\mathrm{I}'}\,, \qquad \mathrm{I}, \mathrm{I}' = \mathrm{H}, \mathrm{M}, \mathrm{L}, \tag{3}$$

where $N_{\mathrm{I}}(x)$ is the abundance of the I group nuclei after passing through x g/cm² of air, and $P_{\mathrm{I}'\mathrm{I}}$ is the fragmentation probability. The solutions are:

$$\begin{cases} N_{\mathrm{H}}(x) = N_{\mathrm{H}}^{0} \exp\left[-x/\lambda_{\mathrm{H}}'\right], \\ N_{\mathrm{M}}(x) = N_{\mathrm{M}}^{0} \exp\left[-x/\lambda_{\mathrm{M}}'\right] + (\alpha_{\mathrm{HM}} P_{\mathrm{HM}}/\lambda_{\mathrm{H}})\left[N_{\mathrm{H}}^{0} \exp\left[-x/\lambda_{\mathrm{M}}'\right] - N_{\mathrm{H}}(x)\right], \\ N_{\mathrm{L}}(x) = N_{\mathrm{L}}^{0} \exp\left[-x/\lambda_{\mathrm{L}}'\right] + (\alpha_{\mathrm{ML}} P_{\mathrm{ML}}/\lambda_{\mathrm{M}})\left[N_{\mathrm{M}}^{0} \exp\left[-x/\lambda_{\mathrm{L}}'\right] - N_{\mathrm{M}}(x)\right] + \\ \qquad + (\alpha_{\mathrm{HL}}/\lambda_{\mathrm{H}})(P_{\mathrm{HL}} + P_{\mathrm{HM}} P_{\mathrm{ML}} \alpha_{\mathrm{ML}}/\lambda_{\mathrm{M}})\left[(N_{\mathrm{H}}^{0} \exp\left[-x/\lambda_{\mathrm{L}}'\right] - N_{\mathrm{H}}(x)\right], \end{cases} \tag{4}$$

where

$$N_{\mathrm{I}}^{0} = N_{\mathrm{I}}(0)\,,$$

$$\alpha_{\mathrm{IJ}} = \lambda_{\mathrm{I}}'\lambda_{\mathrm{J}}'/(\lambda_{\mathrm{J}}' - \lambda_{\mathrm{I}}') > 0\,, \qquad \lambda_{\mathrm{J}}' > \lambda_{\mathrm{I}}'\,,$$

and

$$\lambda_{\mathrm{I}}' = \lambda_{\mathrm{I}}/(1 - P_{\mathrm{II}})\,.$$

The author has used the values of the fragmentation probabilities P_{IJ} in carbon obtained in the present work and the interaction mean free paths λ_{I} in air given by KAPLON *et al.* ([11]), $\lambda_{\mathrm{H}} = 18.0$ g/cm², $\lambda_{\mathrm{M}} = 26.5$ g/cm², and $\lambda_{\mathrm{L}} = 31.5$ g/cm².

The ratios of the abundances of the L nuclei and the H nuclei to the M nuclei at the top of the atmosphere, $N_{\mathrm{L}}^{0}/N_{\mathrm{M}}^{0}$ and $N_{\mathrm{H}}^{0}/N_{\mathrm{M}}^{0}$, obtained by using our experimental data for the fragmentation probabilities in carbon are shown in Table VI, together with the ratios of the abundances at the top of the atmosphere obtained by the other groups themselves. It may be concluded that the ratio of the abundances of the L nuclei to the M nuclei at the top of the

atmosphere, N_L^0/N_M^0, is in the range from ~ 0.1 to ~ 0.2, although it varies somewhat with the data of the abundances at balloon flight altitude of the particular group used. (The ratio N_L^0/N_M^0 by the Kobe group deviates a bit from this range.)

TABLE VI. – *Ratios of the abundances of the heavy primary cosmic rays at the top of the atmosphere.*

Group	Flight altitude (g/cm²)	Obtained by using the fragmentation probabilities in carbon	Obtained by the other groups themselves
Chicago [8]	10	$N_L^0/N_M^0 = 0.22 \pm 0.07$ $N_H^0/N_M^0 = 0.42 \pm 0.08$	$N_L^0/N_M^0 = 0.30 \pm 0.06$ $N_H^0/N_M^0 = 0.42 \pm 0.08$
Bristol [14]	15	$N_L^0/N_M^0 = 0.15 \pm 0.06$ $N_H^0/N_M^0 = 0.40 \pm 0.06$	$N_L^0/N_M^0 = 0.37 \pm 0.07$ $N_H^0/N_M^0 = 0.41 \pm 0.06$
Turin [17]	17	$N_L^0/N_M^0 = 0.08 \pm 0.05$ $N_H^0/N_M^0 = 0.54 \pm 0.09$	$N_L^0/N_M^0 = 0.30 \pm 0.09$ $N_H^0/N_M^0 = 0.51 \pm 0.11$
Rochester [18] (*)	—	—	$N_L^0/N_M^0 = 0.12 \pm 0.02$ $(N_L^0/N_M^0 = 0.34 \pm 0.07)$ $N_H^0/N_M^0 = 0.36 \pm 0.09$
Bombay [29] (**)	6.6	$N_L^0/N_M^0 = 0.16$ $N_M^0/N_H^0 = 2.81$	$N_L^0/N_M^0 = 0.075 \pm 0.08$ $N_M^0/N_H^0 = 3.45 \pm 0.65$
Kobe [30] (*,*)	14	$N_L^0/N_M^0 = 0.43 \pm 0.15$ $N_M^0/N_H^0 = 1.52 \pm 0.38$	$N_L^0/N_M^0 = 0.27 \pm 0.06$ $N_M^0/N_H^0 = 2.46 \pm 0.54$

(*) As the author did not have the observed data at the flight altitude, the abundances could not be extrapolated to the top of the atmosphere by using the fragmentation probabilities in carbon. The value of the ratio N_L^0/N_M^0 in parentheses is that obtained by using the fragmentation probabilities given by the Bristol group.

(**) Values obtained by the Bombay group itself were extrapolated to the top of the atmosphere from the zenith angle distribution.

(*,*) The fragmentation probabilities given by the Rochester group were used in the extrapolation by the Kobe group itself to the top of the atmosphere.

In order to take into account the slight possibility—if indeed any—that, in our following the tracks, some interactions of the type by which the heavy primary nucleus broke up into one proton and one residual heavy nucleus might have been missed, an estimation was made of how many such inter-

[29] M. V. APPA RAO, S. BISWAS, R. R. DANIEL, K. A. NEELAKANTAN and B. PETERS: *Phys. Rev.*, **110**, 751 (1958).

[30] M. MIYAGAKI: private communication.

actions would have been missed. Even if some of such interactions were missed, the number of the missed interactions would be at most 7 for the M group nuclei, judging from the difference between the observed and the calculated interaction mean free paths of the M group nuclei. On the other hand, for the H group nuclei, from such a judgment, it seems that no interaction of the H nucleus was missed. If the 7 interactions are added to the interactions of the M nuclei, the fragmentation probabilities will be the following: $P_{MM} = 0.15 \pm 0.05$, $P_{ML} = 0.34 \pm 0.07$, and $P_{M\backslash} = 0.93 \pm 0.12$, with the assumption that the charge distribution of the incident M nuclei in the 7 interactions is identical with the charge distribution of the primary M nuclei in Table I. Even using these values of the fragmentation probabilities, N_L^0/N_M^0 will be the following: the Chicago group, 0.24 ± 0.07; the Bristol group, 0.17 ± 0.06; the Turin group, 0.14 ± 0.06; the Bombay group, 0.16; the Kobe group, 0.46 ± 0.15. The variation in the ratio of the abundance of the L nuclei to M nuclei, N_L^0/N_M^0, resulting from taking into account the 7 interactions estimated as missed interactions, is not serious.

It is important to know by using the ratios of the abundances at the top of the atmosphere how much of interstellar matter the heavy primary cosmic rays traverse from a source to the top of the atmosphere. It is necessary prior to that, however, to obtain accurate values for the fragmentation probabilities in hydrogen based on many statistics and without the bias in the impact parameter.

* * *

We should like to express our sincere thanks to Professor S. NAKAGAWA for his constant interest and encouragement. We are indebted to Professor J. NISHIMURA for his suggestions and discussions on this subject. Thanks are due also to Professor H. HASEGAWA and to Mr. K. NIU for their discussions and assistances.

RIASSUNTO (*)

Le probabilità di frammentazione dei nuclei pesanti dei raggi cosmici sono state studiate in carbonio. Si sono usate camere ad emulsione consistenti di carbonio ed emulsioni nucleari esposte in Giappone ($\lambda = 25^\circ$ N). Le cariche dei nuclei pesanti con $Z \geqslant 3$ sono state determinate misurando le densità dei raggi δ. Le probabilità di frammentazione in nuclei leggeri sono $P_{HL} = 0.35 \pm 0.08$ e $P_{ML} = 0.35 \pm 0.08$. Le abbondanze osservate da diversi gruppi ad altezze aerostatiche sono state estrapolate alla sommità dell'atmosfera usando le probabilità di frammentazione in carbonio ottenute nel presente lavoro. Il rapporto dei nuclei leggeri a quelli di peso medio alla sommità dell'atmosfera è probabilmente da ~ 0.1 a ~ 0.2.

(*) *Traduzione a cura della Redazione.*

Nuclear Interactions of Neutral K-Mesons of Long Lifetime. - II.

V. Bisi, R. Cester, A. Debenedetti, C. M. Garelli, N. Margem (*)
B. Quassiati and M. Vigone

Istituto di Fisica dell'Università - Torino
Istituto Nazionale di Fisica Nucleare - Sezione di Torino

(ricevuto il 7 Gennaio 1959)

Summary. — This work follows a previous study of the interactions of long lived neutral K-mesons, already published. The increased statistics allows us to check the results previously obtained and to determine the cross section for charge exchange of the θ_2^0 particles in the eigenstate of strangeness -1.

1. – Introduction.

In a previous work (paper I) (1), we studied the interactions of θ_2^0 in the modes θ^0 and $\bar{\theta}^0$. In that work a volume of 8.5 cm³ was scanned and a sufficient statistics was obtained to evaluate, at least as an order of magnitude, the flux of θ_2^0 particles incident on the stack, and their probability of interacting in the modes θ^0 and $\bar{\theta}^0$. This was done starting from the number of K^+ and hyperfragments produced.

The rather low number of K^- found, on the contrary, did not permit to evaluate the magnitude of the cross-section for the reaction:

$$\bar{\theta}^0 + n \to K^- + p \,. \tag{1}$$

(*) On leave of absence from the Centro Brasileiro de Pesquísas Físicas, Rio de Janeiro.

(1) V. Bisi, R. Cester, A. Debenedetti, C. M. Garelli, B. Quassiati, L. Tallone and M. Vigone: *Nuovo Cimento*, **9**, 864 (1958).

As very little is known ([2-4]) about the cross-section for charge exchange of K^-, we decided to study this problem by means of the inverse reaction (1). To this purpose we made a more rapid scanning than the previous one, looking only for capture stars. In the additional scanned volume of 14.5 cm³ we found:

2 τ and 1 τ',
7 K^-,
7 Σ^- captured at rest,
1 Σ^+ decaying at rest and 1 Σ^+ decaying in flight,
2 hyperfragments and 6 GOKS,

all emitted from stars in emulsion.

Adding these results to those of paper I it is possible, not only to calculate the magnitude of the charge exchange cross-section of $\bar{\theta}^0$, but also to check the previous result on the ratio θ^0 mode/$\bar{\theta}^0$ mode.

Details on the exposure and methods for the particles' identification are described in paper I which deals also with the problem of the possible neutron contamination.

2. - Experimental results.

The data of θ_2^0 interaction events found in the total scanned volume of 23 cm³ are given in Tables I, II-*A*, II-*B*, II-*C*.

The features of the stars from which K^- and K^+ are emitted are in agreement with the assumption that these stars are produced respectively in the two interactions:

(1) $$\theta^0 + p \to K^+ + n\,,$$

(2) $$\bar{\theta}^0 + n \to K^- + p\,,$$

In fact in Table I there are 6 cases (1, 2, 3, 4, 11, 12) that are readily interpreted according to reaction (1) while the remaining stars, characterized by the presence of an energetic proton, can be due, as already pointed out in paper I, to a double interaction of the θ^0 inside the nucleus.

In the stars emitting K^- (Table II-*A*) an energetic proton, in agreement with reaction (2) is always found among the prongs.

([2]) J. HORNBOSTEL and G. T. ZORN: *Phys. Rev.*, **109**, 165 (1958).

([3]) F. H. WEBB, E. L. ILOFF, F. H. FEATHERSTON, W. W. CHUPP, G. GOLDHABER and S. GOLDHABER: *Nuovo Cimento*, **8**, 899 (1958).

([4]) *Report of the Annual International Conference on High Energy Physics at CERN* (1958), p. 177.

TABLE I.

Event no.	Strange particle produced	Parent star		Strange particle		Calculated kinetic energy of θ^0 from reaction $\theta^0 + p \rightarrow K^+ + n$ (MeV)	Remarks
		no. of prongs	Total visible kinetic energy (MeV)	Angle in the L.S. with the θ^0 beam	Kinetic energy (MeV)		
1	K^+	1	85	43°	85	130	—
2	τ^+	4	65	46°	41	95	—
3	K^+	1	74	163°	74	300	—
4	K^+	1	28	70°	28	70	—
5	K^+	5	130	142°	48	—	One fast proton of 72 MeV kinetic energy is emitted from the parent star
6	τ'^+	4	324	179°	48	—	One fast proton of 254 MeV kinetic energy is emitted from the parent star
7	K^+	8	323	65°	6	—	One fast proton of 195 MeV kinetic energy is emitted from the parent star
8	K^+	6	547	139°	58	—	One fast proton of 440 MeV kinetic energy is emitted from the parent star
9	K^+	9	180	7°	41	—	One stopping π^- of 34 MeV and a proton of 71 MeV are emitted from the parent star
10	τ^+	3	> 250	112°	55	—	One minimum ionization track, not identified, is emitted from the parent star
11	τ'^+	1	86	26°	86	99	—
12	τ^+	1	68	38°	68	157	—

TABLE II-*A*.

Event no.	Parent star		Strange particle					Remarks	
	Strange particle produced	no. of prongs	Total visible kinetic energy (MeV)	Kinetic energy (MeV)	Track length (μm)	Angle in L. S. with the 6° beam	Capture star: no. of prongs	Capture star: Visible energy (MeV)	On the capture star	On the parent star
1	K^- (at rest)	8	118	41	10500	127°	2	23	One π^+ of 22 MeV kinetic energy is emitted	—
2	K^- (at rest)	3	>270	65	24300	88°	3	48	—	One grey track is probably due to an energetic proton
3	K^- (at rest)	10	138	8	545	40°	2+ recoil	52	One π^- of 52 MeV kinetic energy is emitted	—
4	K^- (at rest)	8	>250	2	62	129°	3	31	One π^- of 24 MeV kinetic energy is emitted	One relativistic prong, not identified, is emitted
5	K^- (at rest)	3	255	32	7000	123°	3	111	—	One proton of 148 MeV kinetic energy, is emitted
6	K^- (at rest)	4	104	18	2600	44°	3	30	—	One proton of 72 MeV kinetic energy, is emitted
7	K^- (in flight)	3	351	35 (*)	6100	107°	2	11	One π^- of 10 MeV kinetic energy is emitted	One proton of 230 MeV kinetic energy, is emitted
8	K^- (at rest)	11	183	3	140	99°	2	36	One π^-_e of 33 MeV kinetic energy is emitted	One proton of 76 MeV kinetic energy, is emitted

(*) From gap measurements.

TABLE II-*B*.

Event no.	Strange particle produced	Parent star			Strange particle						Remarks
								Capture star or decay mode			
		no. of prongs	Total visible kinetic energy (MeV)	Emission of a π	Kinetic energy (MeV)	Track length (μm)	Angle in L. S. with the θ^0 beam	no. of prongs	Visible energy (MeV)	Mode of decay	
1	Σ^- (at rest)	5	102	no	65	12400	53°	2			
2	Σ^- (at rest)	10	246	no	4	110	158°	4	6		Auger electron visible in the capture star
3	Σ^- (at rest)	7	73	no	5	135	83°	1	10		
4	Σ^- (at rest)	7	50	no	4	90	25°	2	108		
5	Σ^- (at rest)	11	150	no	10	430	85°	2	30		
6	Σ^- (at rest)	5	>530	π^+ ?	27	1560	131°	1	46		
7	Σ^- (at rest)	3	214	no	36	4200	45°	2	2		
8	Σ^- (at rest)	5	68	no	33	1410 + +875	53°	2	2		The Σ^- suffers an inelastic scattering before being captured at rest
9	Σ^- (at rest)	6	105	no	8	330	112°	4	16		
10	Σ^- (at rest)	3	>440	π^+ ?	36	4200	69°	2	72		
1	Σ^+ (decaying in flight)	1	134	no	134	29200	75°			$\Sigma^+ \rightarrow p + \pi^0$	
2	Σ^+ (decaying in flight)	1	72	no	72	1880	32°			$\Sigma^+ \rightarrow p + \pi^0$	
3	Σ^+ (decaying in flight)	2	155	no	137	19900	160°			$\Sigma^+ \rightarrow p + \pi^0$	
4	Σ^+ (decaying in flight)	3	18	no	~ 8	140	133°			$\Sigma^+ \rightarrow p + \pi^0$	
5	Σ^+ (decaying at rest)	5	152	no	85	19400	45°			$\Sigma^+ \rightarrow p + \pi^0$	Range of the proton: 1630 μm
								Interaction star			
								no. of prongs	Visible energy (MeV)		
6	Σ^+ (interacting in flight)	3	132	no	69	2200	154°	1	90		$\pi^\pm$ emitted from the interaction star

TABLE II-*C*.

Event no.	Strange particle produced	Parent star			Strange particle		Secondary star			Remarks
		no. of prongs	Total visible kinetic energy (MeV)	Emission of a π	Track length (μm)	Angle in L. S. with the θ^0 beam	no. of prongs	Visible energy (MeV)	Mode of decay	
1	H.F.	4	30	no	280	61°	2	2.2	non mesonic	—
2	H.F.	9	94	no	136	62°	2{p, p}	88{84, 4}	non mesonic	Kinematics in agreement with: $^4He_\Lambda \rightarrow 2p+2n$
3	H.F.	7	>172	π^-	40	61°	3	18	non mesonic	—
4	H.F.	4	18	no	160	26°	6	11	non mesonic	—
5	H.F.	9	415	no	5	38°	2	69	non mesonic	—
6	H.F.	6	70	no	24	94°	2	12	non mesonic	—

In Table II-*B* the interactions leading to $\Sigma^\pm$ are listed. The events 1 ... 10 are certainly Σ^- captured at rest: in two cases a relativistic track is present in the parent star, which can very likely be interpreted as a π^1.

3. – θ^0 flux (a) as deduced from charge exchange processes.

In paper I an estimate of the θ^0 flux was obtained starting from the number of K^+ decaying at rest in the scanned volume. The result was depending on the estimate of the scanning efficiency. This was deduced studying the dip angle distribution of the light secondaries and should be taken as an upper limit since we assumed that all light secondaries with dip angle $\gtrsim 45°$ were detected.

The scanning efficiency can also be derived from the known ratio K^1/τ with the reasonable assumption that all τ and τ' decays have been detected. The increased statistics makes this calculation meaningful.

(a) The expressions θ^0 and $\bar{\theta}^0$ flux are used for brevity and stand in place of number per cm² of θ_2^0 times the probability to be in the eigenstate of strangeness +1 and −1 respectively.

In the total scanned volume (previous work: 8.5 cm³, present work: 14.5 cm³) 3 τ and 2 τ' were found. Taking for the K^+/τ ratio the value [5] 11.5 we estimated the number of K^+ decaying at rest in the scanned volume to be 62, that is (2.7 ± 0.9) K^+/cm^3. This has to be compared with the value $N_{K^+}/cm^3 = 1.4 \pm 0.4$ found in paper I and shows that the scanning efficiency has been previously overestimated.

Since the additional scanned volume lies in the same region of the stack as the volume scanned in the previous research, the geometrical loss due to the finite size of the stack is that evaluated in paper I (89%) [b].

The θ^0 incident flux integrated over the time of exposure turns out to be:

$$\varphi_{\theta^0} = \frac{N_{K^+}}{cm^3} \lambda_{c.e.} = 25 \cdot 170 = (4200 \pm 1400)/cm^2 ,$$

where $\lambda_{c.e.}$ is the effective mean free path for charge exchange as calculated in paper I and the quoted error is the statistical one.

4. - $\bar{\theta}^0$ flux [a] as deduced from the number of Σ^- hyperons.

An estimate of the $\bar{\theta}^0$ flux is done starting from the number of Σ^- captured at rest in the scanned volume. This calculation is now possible owing to the increased statistics.

In the total volume 10 Σ^- captured at rest were found. This number must be corrected for scanning losses. These are mainly due to the fact that scanning by area for capture stars, Σ_ϱ events and capture stars with one low energy prong were not detected. Events of this type were estimated by other authors [6] to occur in $\sim 70\%$ of all captures. Assuming 100% efficiency for detection of other kinds of capture stars, the number of Σ^- captured at rest in the scanned volume should have been 33.

In order to deduce the primary flux from this number, we must estimate the percentage of interacting $\bar{\theta}^0$ giving rise to a Σ^- which will be captured at rest in the scanned volume. This could be done by the following considerations.

As in paper I we assume the $\bar{\theta}^0$ to be the charge symmetric particle of the

---

[5] *Proceedings of the Seventh Annual Rochester Conference*, VIII-24.

[b] For the discussion on the contamination due to strange particles produced by high energy neutrons, see Paper I, Sect. 3.

[6] W. F. Fry, J. Schneps, G. A. Snow, M. S. Swami and D. C. Wold: *Phys. Rev.*, **107**, 257 (1957).

K^- ([c]), so that informations on the cross sections and on the branching ratios in the strong interactions of the $\overline{\theta}^0$ can be obtained from the results on K^- interactions.

The elementary interactions of the $\overline{\theta}^0$ in emulsion are:

(1) $$\overline{\theta}^0 + p \to \Sigma^+ + \pi^0$$

(2) $$\to \Sigma^0 + \pi^+$$

(3) $$\to \Lambda^0 + \pi^+$$

(4) $$\overline{\theta}^0 + n \to \Sigma^+ + \pi^-$$

(5) $$\to \Sigma^- + \pi^+$$

(6) $$\to \Sigma^0 + \pi^0$$

(7) $$\to \Lambda^0 + \pi^0$$

To these, inelastic $\overline{\theta}^0$ reemission and charge exchange processes must be added; these can be estimated to be of the order of 10% of all $\overline{\theta}^0$ interactions ([d]).

If we consider the bubble chamber data of ALVAREZ *et al.* ([8]) and make use of charge independence, we expect the fraction of interacting $\overline{\theta}^0$ giving as a product of the reaction inside the nucleus a Σ^- hyperon to be 24% ([e]).

From the results on K^- interactions in complex nuclei ([3]) it is known that only 42% of charged hyperons are not converted in Λ^0 in nuclear matter by the reaction: $\Sigma + \mathcal{N} = \Lambda^0 + \mathcal{N}$.

The energy spectrum of the Σ^- emitted from the nucleus has been then calculated under the following assumptions:

1) The centre of mass distribution of the produced Σ^- particles is isotropic.

2) The θ_2^0 primary spectrum is that calculated in paper I (Fig. 1-*b'*).

([c]) Recently PAIS ([7]) has proposed a scheme in which θ^0 and K^- (or θ^0 and K^+) do not belong anymore to the same charge doublet. If this scheme is proved to hold, our calculations must be revised.

([7]) A. PAIS: *Relative parity of charged and neutral* K*-particles*. Preprint.

([d]) From the results of K^- interacting in flight ([3]), the inelastic reemissions are estimated to occur in 4% of the cases. An estimate of the charge exchange cross section of θ^0 is given in Sect. 5 of the present work and is found to be of the order of (5÷6)% of the total cross section.

([8]) L. W. ALVAREZ, H. BRADNER, P. FALK-VAIRANT, J. D. GOW, A. H. ROSENFELD, F. T. SOLMITZ and R. D. TRIPP: *Nuovo Cimento*, **5**, 1026 (1957).

([e]) If the decrease of the Σ^-/Σ^+ ratio with increasing energy, as indicated by the Berne group ([9]), is confirmed, this percentage will have to be reduced and our calculation revised.

From the total spectrum we have to subtract all the particles which did not come to rest before decaying, because they were not detected according to our scanning criteria.

If we calculate the probability of a Σ^- to decay in flight as a function of the energy, it turns out that practically all hyperons having an energy greater than 100 MeV decay in flight and that the number of Σ^- captured at rest is 9.5% of the total spectrum, that is $9.5\% \times 24\% \times 42\% = 1\%$ of all $\bar{\theta}^0$ interactions.

Taking for the $\bar{\theta}^0$ interaction mean free path the value obtained for low energy K^- ([3,9]), $\lambda = 27$ cm, we obtained the $\bar{\theta}^0$ flux value:

$$\varphi_{\bar{\theta}^0} = \frac{N_{\Sigma^-}}{\mathrm{cm}^3} \lambda \frac{1}{1\%} = \frac{33}{23} \cdot 27 \cdot 100 = (3900 \pm 950)/\mathrm{cm}^2 ,$$

where the quoted error is the statistical one.

The flux value obtained is in amazingly good agreement with the θ^0 flux and this supports the Gell-Mann and Pais scheme.

5. – $\bar{\theta}^0$ charge exchange cross section.

In the total scanned volume 16 K^- captured at rest were observed. 8 of these, followed back through the stack, were found to originate in emulsion from stars with a neutral primary. If we assume these events to be due to the charge exchange of a $\bar{\theta}^0$ ([b]) an estimate of the cross-section for this process can be obtained.

This calculation requires a rather accurate estimate of the losses in detecting K^- captures. These are due both to scanning losses and to the geometrical limitation arising from the finite size of the stack.

The first effect was accounted for with the following considerations.

1) 28% of all K^- captures (K_e, one prong stars, large stars ([10])) were missed.

2) K^- captures occurring in the upper and lower layer of the plates are very difficult to observe. These layers have been estimated to be $\sim 10\%$ of the total volume.

([9]) E. Lohrmann, M. Nikolić, M. Schneeberger, P. Waloschek and H. Winzeler: *Nuovo Cimento*, **7**, 163 (1958); Y. Eisenberg, W. Koch, E. Lohrmann, M. Nikolić, M. Schneeberger and H. Winzeler: *Nuovo Cimento*, **9**, 745 (1958).

([10]) G. L. Bacchella, A. Berthelot, A. Bonetti, O. Goussu, F. Levy, M. René, D. Revel, J. Sacton, L. Scarsi, G. Tagliaferri and G. Vanderhaeghe: *Nuovo Cimento*, **8**, 215 (1958). K$^-$-stack Collaboration: *Padua Conference*, II-5 (1957).

3) The scanning efficiency of other types of capture stars depends mainly on the dip of the primary K^- track. The dip angle distribution of the last 50 μm of the K^- tracks observed (16 including the ones coming from outside the stack) was analysed. The scanning efficiency can be estimated comparing the observed distribution with the true one supposed to be isotropic. The same analysis has also been made for 100 π^- tracks whose captures at rest were observed by area scanning carried on by the same observers (50 π^- in the same stack and 50 π^- in a stack exposed to the cosmic radiation). In all cases the efficiency has been found to be $\sim 65\%$.

The total scanning losses amount then to 58%.

The evaluation of the losses due to the finite size of the stack has been carried out as in paper I (Section **6**) assuming an average energy loss $\Delta T/T = 50\%$ [3] and gives a geometrical efficiency of detection of 9%.

The total number of K^- produced by charge exchange of $\bar{\theta}^0$ in the scanned volume is then estimated to be $N_{K^-} = 210$, that is $N_{K^-}/\mathrm{cm}^3 = 9$.

This leads to a $\bar{\theta}^0$ charge exchange mean free path in the energy interval (0÷400) MeV of:

$$\lambda_{c.e.} = \frac{\varphi_{\bar{\theta}^0}}{N_{K^-}/\mathrm{cm}^3} = (460 \pm 180)\ \mathrm{cm}\,,$$

where for the incident flux we have taken the value averaged over the results of Sections **3** and **4** and where the error is the statistical one.

6. – Conclusions.

From a study of the interactions of long lived θ_2^0 in emulsion we have derived the following conclusions:

1) The probabilities that θ_2^0 particles interact in the modes θ^0 and $\bar{\theta}^0$ are equal within the experimental errors.

2) The cross-section for charge exchange of the $\bar{\theta}^0$ mode is of the order of (5÷6)% of the total $\bar{\theta}^0$ inelastic cross-section.

These conclusions are correct if charge independence in the conventional sense holds true.

* * *

We are glad to express our thanks to Prof. G. WATAGHIN who planned and carried out the exposure at the Berkeley bevatron and helped us with constant interest during this work.

We are grateful to Dr. E. LOFGREN for his valuable advice and co-operation, and to Dr. CHUPP and Dr. GOLDHABER for help during the exposure.

We express our appreciation to Mr. G. ALGOSTINO, Mr. V. BORRELLI, Mr. M. GRECO and Mr. P. TROSSERO for their accuracy in the difficult task of scanning the plates.

One of us (N.M.) is supported by a fellowship of the Conselho Nacional de Pesquísas, Brasil.

RIASSUNTO

Questo lavoro è la continuazione di uno studio sulle interazioni dei mesoni K neutri a vita lunga, già pubblicato. La maggiore statistica permette di confermare i risultati già ottenuti e di determinare la sezione d'urto per scambio carica delle particelle θ_2^0 nell'autostato di stranezza -1.

IL NUOVO CIMENTO Vol. XII, N. 1 1° Aprile 1959

Interaction of 4.2 Gev π^--Mesons with Nuclear Emulsion.

P. Abrahamson (*), J. Ben-Arieh and G. Yekutieli

Department of Physics, The Weizmann Institute of Science - Rehovoth

G. Alexander

Department of Physics, The Weizmann Institute of Science - Rehovoth
Department of Physics, Atomic Energy Establishment - Rehovoth

(ricevuto l'8 Gennaio 1959)

Summary. — 1425 interactions of 4.2 GeV π^--mesons with emulsion nuclei, found by area scanning were studied. A total mean free path of (32.4 ± 4) cm was obtained. The mean multiplicity per star was found to be 1.72 for charged pions and 2.48 for fast protons. These figures were compared with the statistical model of Fermi. The angular distributions and energy spectra of the secondary particles were obtained and confronted with the corresponding results for 5 GeV π^--p interactions.

Introduction.

One of the basic problems in the study of the pion-nucleus interaction is the question whether this interaction can be described by a cascade of pion-nucleon and nucleon-nucleon collisions. In the present work the interaction of 4.2 GeV negative pions with emulsion nuclei is studied. The characteristic features of the pion-nucleus interaction, such as multiplicity, energy spectra and angular distributions of the secondary pions and protons are measured and compared with those of a pion-proton collision. The results obtained may serve both as a guide and a test for a comprehensive theory of a pion-nucleus interaction.

(*) Now at the Technion, Haifa.

1. – Experimental.

A stack of 60 pellicles of G-5 emulsion, each of $15 \times 7.5 \times 0.06$ cm^3 was exposed to the 4.2 GeV π^--meson beam of the Bevatron for the purpose of studying the meson interaction with the emulsion nuclei. The beam entered the stack from its 7.5 cm edge travelling in the emulsion parallel to the 15 cm edge. The muon and electron contamination of the pion beam at the entrance to the emulsion was estimated to be $\sim 5\%$. The beam was well collimated and its density was ~ 3300 particles per cm^2, which corresponds to an average of two tracks per one vision field of 100×100 μm^2. The low density exposure unfortunately made the measurements of relative scattering of the pion beam unpractical and we were not able to measure the $p\beta c$ free of spurious scattering. In fact, multiple scattering measurements on individual tracks of 4.2 BeV pions described later, show that the emulsion used in the present experiment was not free of spurious scattering.

For scanning purposes every track in the emulsion travelling in the direction of the beam with a blob density below 19 blobs per 100 μm was considered as a 4.2 GeV pion. Five plates were scanned under low power magnification for stars produced by the 4.2 GeV pions. Only stars with the following criteria were accepted for the analysis.

a) The stars were found at least 50 μm (unprocessed emulsion) from the surface or glass of the plate, and at least 3 mm from any cut edge.

b) The stars had a visible pion primary.

The stars were classified and analyzed according to the ionization value of their prongs. In order to ensure that no light ionizing tracks were missed in the first scan a second scan has been performed on the stars found and an appropriate correction has been applied.

TABLE I.

$h =$		Nuclear scatters	0	1÷2	3÷5	6	Total
Along the track scanning	No.	8	5	14	20	45	92
	%	9	5	15	22	49	100
Area scanning	No.	0	0	95	403	930	1425
	%	0	0	5	21	49	75
EDWARDS *et al.* [6] Along the track scanning	%	13.4		21.4	22.1	43.3	100.2

The percentage figures were calculated on the assumption that the scanning efficiency for stars of $N_h \geq 3$ is 100 %.

It is known that under low power magnification area scanning is not efficient for the detection of scattering events and stars of $N_h \leqslant 2$. To obtain an unbiased sample of interaction events 29.82 meters of pion track were followed under high power magnification for nuclear events. In this way 92 nuclear events were obtained, including nuclear scattering events, and they are classified in Table I. Comparison of the two scanning methods shows that while in area scanning scatters and $N_h = 0$ stars are missed completely, 1 and 2 prongs events were partly found and all stars with $N_h \geqslant 3$ were observed.

2. – The interaction mean free path.

The interaction mean free path λ of 4.2 GeV negative pions in nuclear emulsion was evaluated in two ways:

a) by measuring the average distance travelled by a particle before it produced a nuclear interaction and

b) by measuring the attenuation of the pion beam in the nuclear emulsion.

The first method involves the knowledge of the pion beam purity. In the present experiment the beam consisted of 95% pions, the rest being electrons and muons. 29.82 meters of pion tracks were followed and 92 nuclear events were discovered of which 8 were nuclear scattering. This corresponds to a mean free path of (32.4 ± 4) cm for all types of events and (35.5 ± 4) cm for absorption only.

The attenuation of the pion beam was measured by the attenuation of the pion produced stars in the emulsion. The nuclear interactions found in the scanning were divided into two groups according to the distance x_i travelled by their primary pion in the emulsion. 788 stars with primaries length of $(0.3 < x_i < 7.2)$ cm were assembled in group I and the 637 with primaries of $(7.8 < x_i < 14.7)$ cm were assembled in group II. Now as all primaries have the same potential range in both boundaries, the expected ratio 637/1425 is equal to $\exp[-a/\lambda]$ where $a = 7.5$ cm is the distance between the mid lines of the two boundaries. In this way an interaction m.f.p. of $\lambda = (35.4 \pm 4)$ cm was found. This last value is independent of the scanning efficiency as long as the efficiency is the same for both boundaries, which is the case in the present experiment.

Shadow scattering of small angles is of the same order of magnitude as the angular dispersion of the beam and will not contribute to the attenuation of the beam in the nuclear emulsion. Hence the m.f.p. of 34.5 cm obtained from the beam attenuation corresponds to the m.f.p. for nuclear absorption. Our results are compared with those of others in Table II.

TABLE II.

Author	E_π (GeV)	λ_{total} (cm)	λ_{abs} (cm)
SCHEIN *et al.* [1]	3 (*)	35.5 ± 5	—
CLARK and MAJOR [2] .	4.2 (*)	31.9 ± 4.7 (**)	38.7 ± 3.5
MARQUES *et al.* [3] . .	4.3 (*)	33.7 ± 4.7	36.2 ± 4.7
Present experiment . .	4.3 (*) 4.2 (*,*)	32.4 ± 4 —	35.5 ± 4 35.4 ± 4

(*) By scanning along the track.

(**) CLARK and MAJOR applied a correction of 30 % for missing cases of scattering, and obtained a value of 27.1 ± 2.4 cm.

(*,*) By attenuation measurements.

3. – Measurements.

3·1. *Classification of stars.* – In course of the scanning procedure, in each star the number of prongs has been counted and divided visually into three classes:

a) Shower particles denoted by s;

b) Grey prongs denoted by g;

c) Heavy ionizing prongs denoted by h.

It was found later on, when accurate measurements were done that this visual classification was very much the same for the different observers. Hence we could assign a correspondence between the visual division

$$I_{min} \leqslant I_s \leqslant 2 \times I_{min} ; \qquad 2 \times I_{min} < I_g < 4 \times I_{min} ; \qquad 4 \times I_{min} < I_h .$$

where I_{min} is the minimum ionization value. In addition to this classification the dip angle and the projected angle were taken for all s and g prongs and for the primary pion. These measurements were used to determine the spatial angular distributions of the different particles.

3·2. *Calibration of the stack.* – In all the plates used in this experiment a ionization evaluation has been done on the primary pion beam tracks by means of blob counting. On the average in each plate a total number of 4 000 blobs

(1) M. SCHEIN, D. M. HASKIN and R. G. GLASSER: *Nuovo Cimento*, **3**, 131 (1956).

(2) J. O. CLARK and J. V. MAJOR: *Phil. Mag.*, **2**, 37 (1957).

(3) M. MARQUES, N. MARGEM and G. A. B. GARNIER: *Nuovo Cimento*, **5**, 291 (1957).

on 4 tracks was counted and a mean b_{π^-} has been found. The value obtained in the different plates did not differ more than 3% from the average. This 4.2 GeV pion beam ionization point was however not suitable as reference point as the ionization behaviour in the relativistic rise region is not well known and no accurate experimental calibration has yet been made. Hence we scanned the stack for $\mu \to e$ decay events and determined the « plateau » value which was then reduced to the minimum value by the ratio $b_{\text{Pl}}/b_{\text{min}} = 1.12$ (Reference (4)). As some of the ionization evaluations were performed by blob counting and some by grain counting, it was necessary to convert the blob data into their grain equivalent. This was done by the use of the known relation $g = b \exp[K/\bar{G}]$, $\bar{G}$ being the mean gap length and K a constant that was determined experimentally by counting blobs and grains on a few tracks in different plates.

3·3. *Ionization measurements of the prongs.* – All s and g tracks emerging from the interaction stars were subjected to ionization determination provided they had a potential range of not less than 3 mm in the plate.

The tracks assigned as s tracks were blob counted as this method seems more reliable (Reference (4)) and depending less on the observer than grain counting. The blob densities thus obtained were converted to grain densities and normalized to the minimum value.

The tracks classified under g particles were not suitable for blob counting, and grain counting was preferred. To eliminate the personal differences that are known to exist in grain counting, each observer calibrated the plates he used. All tracks that were found to have a ionization value exceeding the value of $4 \times g_{\text{min}}$ were not included in the analysis. Few particles were traced to rest and the energy determined by the range confirmed the energy value obtained by ionization determination. Throughout this work we assumed a statistical error of 3% on the ionization value obtained by grain and blob counting.

3·4. *Multiple scattering.* – Multiple scattering was measured by the coordinate method on Cooke M4000 and the results were evaluated automatically on the WEIZAC electronic computer. We used a standard programme which evaluated the results measured on a basic cell s and multiples of this basic cell ($1s$, $2s$, ..., $8s$). During this procedure a $4\bar{D}$ rigorous rejection was used, and a noise elimination for $2s$ to $8s$ against $1s$ was carried out. At the same time the statistical error of each $\bar{\alpha}$ was computed. A set of $7\bar{\alpha}$ of different cell size was obtained for each track, of which we chose one which was already in the convergent region and had a sufficiently small statistical error.

(4) G. ALEXANDER and R. H. W. JOHNSTON: *Nuovo Cimento*, **5**, 363 (1957).

A sample of 38 primary 4.2 GeV pions tracks were subjected to multiple scattering on basic cell of 400 μm and evaluated up to 3200 μm and a value of (3.7 ± 0.4) GeV was obtained for the highest cell size. The results indicate a certain amount of noise and spurious scattering which hindered measurements by multiple scattering on tracks of $p\beta c$ above 1.5 GeV with the present experimental condition.

All tracks that were subjected to ionization measurements were scattered. The s particles on a basic cell size of 100 μm and the g particles on a basic cell size of 50 μm. The results were used only for identification purposes, while the energy was estimated by the ionization value.

3·5. *Identification of the secondaries.* – The number of the K-mesons to be produced in the interaction of the 4.2 GeV pion with nucleons is very small and estimated to be not more than few per cent of the charged secondaries (References [5], [6]). Hence in this work K-meson production was not considered, we assumed throughout the present experiment that charged particles were either protons or pions.

Identification of a secondary to be either a proton or a pion was determined by the $p\beta c$ versus ionization method, using the calibrated curve obtained by ALEXANDER and JOHNSTON [4]. This method could be applied for values of $p\beta c$ below 1.5 GeV where in this experiment the noise and the spurious scattering was of no importance; particles with a $p\beta c$ value above 1.5 GeV and with $g > g_{\min}$ were left unidentified.

The identification has been performed in the following way:

a) Particles having an ionization value above the minimum, their mass was determined by the $p\beta c$ versus ionization method and identified accordingly.

b) All particles with minimum ionization were identified as pions.

In this way only protons within the energy region of $94 < E_p < 1000$ MeV and pions of energy $14 < E_\pi < 1400$ MeV were identified. (1400 MeV is the energy of a pion with a ionization value of $\sim 1.03 \times I_{\min}$, according to STILLER and SHAPIRO [7]). The energy of the identified particles was determined by the ionization value where it was possible, namely for $g \gtrsim 1.03 \times g_{\min}$ and by multiple scattering for pions of minimum ionization up to 1250 MeV.

3·6. *Geometrical correction.* – The selection criterion that only tracks with a length of more than 3 mm per plate were accepted for measurements intro-

---

[5] G. MAENCHEN, W. B. FOWLER, W. M. POWELL and R. W. WRIGHT: *Phys. Rev.*, **108**, 850 (1957).

[6] B. P. EDWARDS, A. ENGLER, M. W. FRIEDLANDER and A. A. KAMAL: *Nuovo Cimento*, **5**, 1188 (1957).

[7] B. STILLER and M. M. SHAPIRO: *Phys. Rev.*, **92**, 735 (1953).

duced a geometrical bias. This bias depends on the angle ϑ that the secondary makes with the direction of the primary π-meson. A correction factor $F(\vartheta)$ was calculated on the assumption that tracks with the same angle ϑ are equally distributed around the direction of the primary pion. $F(\vartheta)$ expresses the fraction of the secondary particles with the angle ϑ that are measurable; its values are shown in Table III.

TABLE III.

$l \sin \vartheta$	$F(\vartheta)$
$x > l \sin \vartheta$	1
$2d - x > l \sin \vartheta > x$	$\frac{1}{2} + \frac{1}{\pi} \arcsin\left(\frac{x}{l \sin \vartheta}\right)$
$l \sin \vartheta > x\,; \quad 2d - x$	$\frac{1}{\pi}\left[\arcsin\left(\frac{x}{l \sin \vartheta}\right) + \arcsin\left(\frac{2d - x}{l \sin \vartheta}\right)\right]$

where: x = depth of the emulsion from the surface in mm;
l = 3 mm, minimum track length accepted;
$2d$ = 0.6 mm, the emulsion thickness (unprocessed).

4. – Results and analysis.

4·1. *Angular distributions and energy spectra.* – In Figs. 1 and 2 the angular distributions of secondary particles identified as pions and protons are plotted.

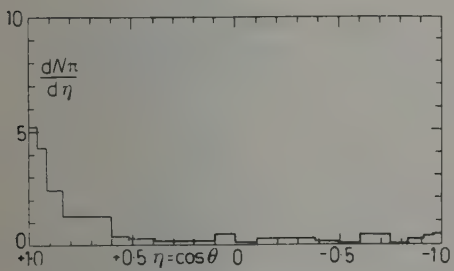

Fig. 1. – Angular distribution of secondary pions.

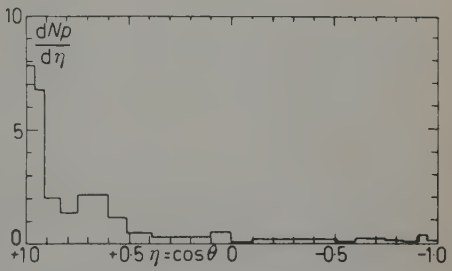

Fig. 2. – Angular distribution of secondary protons.

The median angles of the distributions $\vartheta_{\frac{1}{2}}$ are 33.5° and 32.3° respectively. If we assume that all pions are ejected forward and backward with the same probability from a single center of mass system, moving with a velocity β_c,

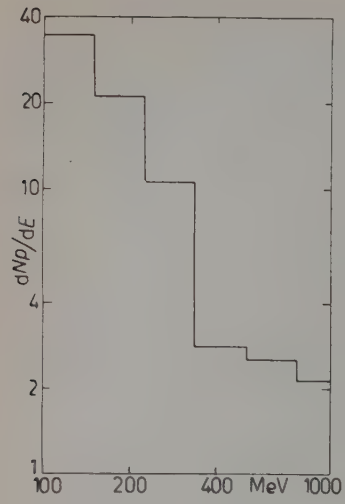

Fig. 3. – Energy spectrum of secondary protons between 100 and 1000 MeV.

then the following relation is valid:

$$\frac{1}{\gamma_c} = \sqrt{1-\beta_c^2} = \operatorname{tg} \vartheta_{\frac{1}{2}} .$$

Using the results of $\vartheta_{\frac{1}{2}}$ obtained for the pions one finds a value of $\gamma_c = 1.55$. Assuming that all the pions emerged from a single collision between a pion and a particle of a mass M at rest and equating the velocity of this center of mass with the one obtained from the angular distribution, one finds for the mass of the target particle a value of $M = 1.5$ GeV. If indeed all mesons were produced in a single pion nucleon collision, the expected mass should be 0.94 GeV, the nucleonic mass. The higher mass value of 1.5 GeV obtained indicates that the pions were produced either in more than a single two particles collision, or in a collision involving more than two particles.

The energy spectra of the protons and the pions emitted from the interaction between the 4.2 GeV π-mesons and the emulsion nuclei are shown in Figs. 3 and 4. The pion spectrum is extended only up to 1250 MeV and contains 97 % of all secondary charged pions. The spectrum is compared with that obtained from MAENCHEN *et al.* [5] for 5 GeV π-p interaction, where only 66 % of the produced pions are lying in the region below 1250 MeV. It is interesting to observe that more pions emerge at low energy ($E_\pi < < 320$ MeV) from the 4.2 GeV π-nucleus interaction, and this in spite of the fact that the number of pions emerging from a star is lower than in the case of the 5 GeV π-p interaction.

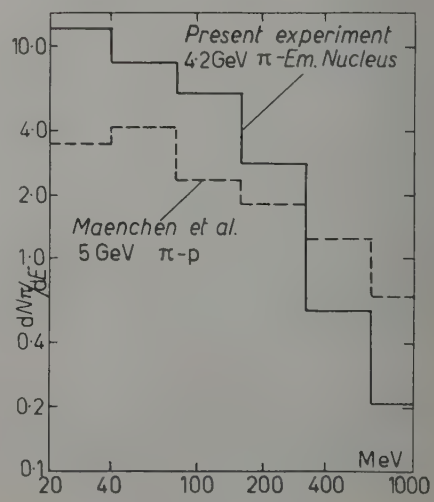

Fig. 4. – Energy spectra of secondary pions between 20 and 100 MeV. ——— Present experiment; ------- MAENCHEN *et al.*

4·2. *Meson production.* – The identified particles were corrected for the geometrical bias and the average number of pions and protons for all s and g particles were found to be $\overline{\pi}(s+g) = 0.41$ and $\overline{p}(s+g) = 0.59$. In our star sample found by area scanning the average number of $s+g$ tracks per star is 4.2, which means, 1.72 charged pions and 2.48 protons are produced per interaction. For comparison with these experimental figures, the number of charged pions and protons produced in single collision of a 4.2 GeV π^--meson with a representative emulsion nucleus ($\overline{A} = 74.1$; $\overline{Z} = 31.9$) were calculated. These calculations were carried out according to the statistical model of Fermi and charge independence assumption for $E_{\pi^-} = 4.2$ GeV in two cases:

a) The interaction volume corresponds to the pion Compton wave length $R_0 = 1.4 \cdot 10^{-13}$ cm;

b) For a larger interaction volume of $R = 1.19 \times R_0$, corresponding to the volume needed to give at 5 GeV π^--meson interaction the multiplicity of pions found experimentally by MAENCHEN *et al.* [5].

The results are summarized in Table IV.

TABLE IV.

Secondary particle	Present experiment	Theory	
		R_0	$1.19 \times R_0$
$\pi^{\pm}$	1.71	1.87	2.1
p	2.48	0.41	0.42

It appears from Table IV that the number of pions that emerge from interaction at 4.2 GeV with an emulsion nucleus is smaller than the expected one from a pion nucleon interaction at the same energy.

4·3. *Multiplicity.* – The observed stars found by scanning were divided in groups of h (evaporation prongs), and for each group the average number of shower particles $\langle s \rangle$ and grey particles $\langle g \rangle$ were calculated. The results are presented in Table V. As we known from comparison with the sample of stars obtained by along the track scanning, the first group of $N_h \leqslant 2$ is detected only with an efficiency of $\sim 25\%$ while the other groups have a detection efficiency of about 100%. An interesting feature of the data is that $\langle s \rangle$ is almost constant for stars of small and large N_h, while $\langle g \rangle$ is increasing with N_h. If we discuss the pion nucleon interaction in terms of a pion nucleon cascade, the number of non-evaporation protons is not more than the number of collisions in the cascade. In our case all s and g particles identified as

protons are of energy above 94 MeV and hence are of non-evaporation nature. Now the average number of nucleons ejected per star with energy above 94 MeV will be $N_{Nu} = (\bar{A}/\bar{Z})(\langle p\rangle_{em} - \langle p\rangle_{Nu}) + 1$; where $\langle p\rangle_{em}$ is the average number of protons ejected in a pion-emulsion nucleus collision, and $\langle p\rangle_{Nu} = 0.41$ (see Table IV) is the average number of protons ejected in a pion-nucleon interaction in the emulsion nucleus.

TABLE V.

$h =$	$1 \div 2$	$3 \div 5$	$6 \div 8$	$9 \div 11$	$12 \div 15$	>6
s	2.18	2.24	2.39	2.24	2.12	2.03
g	1.18	1.26	1.85	2.50	3.10	3.40
$s+g$	3.36	3.50	4.24	4.74	5.22	5.43
$\bar{p}(s+g)$ (*)	1.98	2.07	2.50	2.80	3.08	3.20
N_{Nu}	4.72	4.98	6.03	6.76	7.35	7.70

(*) $\bar{p}(s+g) = \langle p\rangle_{em}$.

The number of $\langle p\rangle_{em}$ can be estimated in the following way for the different star size. The number of identified protons among the $s+g$ particles is given in Section 4·2 and is equal to 0.59. This ratio is not necessarily the same for small and large stars, however, as the number of identified protons is too small to be divided according to N_h, we took the above figure of 0.59 to obtain the value of $\langle p\rangle_{em}$ for all the different star groups. The values of N_{Nu} and $\langle p\rangle_{em} = \bar{p}(s+g)$ calculated as above are given in Table V.

5. – Conclusions.

In concluding one has to bear in mind that our results are obtained from a special sample of interactions, namely including all stars with $N_h \geqslant 3$ and 30% of the stars with $N_h = 1, 2$. These nuclear events constitute only 75% of all emulsion nucleus interactions, and are made of those interactions in which the energy transfer to the nucleus was rather large.

Both the angular distribution and the energy spectrum of ejected pions show that these pions are the result of a complex interaction between the primary pion and the nucleons in the target nucleus. The results presented in Sections 4·2 and 4·3 may serve as a guide to a cascade model in the π^--nucleus interaction. The constant value of $\langle s\rangle$ for the different groups of stars with different N_h and the observation that pions produced in π-nucleus

interaction are not more than in π^--p collision, show that pion production takes place mostly in the primary π-nucleon collision. In the further stages of the cascade, processes of pion production and absorption do not change appreciably the pion multiplicity, but energy is transferred from the pions to the nucleus. This process is reflected in the large number of low energy pions emerging from the interactions. The marked increase of $\overline{p}(s+g)$ with N_h show that in the second and later collisions mostly nucleons are added to the cascade. From the average number of the fast nucleons ($E_p \leqslant 94$ MeV) emerging, one may estimate the number of high energy collisions that take place in the cascade. This number ranges from 4.72 for stars of $N_h = 1, 2$ up to 7.7 for stars with $N_h \geqslant 16$, with an average number of 6 collisions per cascade for the present star sample.

Actually more collisions from which nucleons with energy below 94 MeV emerge, take place in the cascade. Part of these low energy nucleons escape the nucleus barrier and contribute directly to the h prongs, others are trapped to excite the nucleus. Subsequently the nucleus is de-excited by an evaporation process in which low energy nucleons and other low A particles are ejected. The charged evaporation particles make the majority of the h prongs. A comprehensive understanding of the experimental results, however, calls for a detailed study of the cascade development in the nucleus, which will take in account all the possible elementary interactions. Such a study programme will be even more important for interactions in higher energy range than the one dealt with here, where the production of mesons may occur in considerable amount in all the cascade stages.

* * *

The plates used in this experiment were kindly supplied by the Rochester emulsion group, for which we thank Professor M. F. Kaplon. We wish to acknowledge the assistance of the scanning team, consisting of Mrs. R. Gottesmann, Miss R. Herzog and Mrs. E. Mashiach. We are also grateful to Mr. E. Bogart for participating in part of this work.

RIASSUNTO (*)

Si sono studiate 1425 interazioni di mesoni π di 4.2 GeV con nuclei dell'emulsione trovate con esplorazione areale. Si è ottenuto un cammino libero medio totale di (32.4 ± 4) cm. La molteplicità media per stella fu trovata di 1.72 pei pioni carichi e 2.48 pei protoni veloci. Tali cifre furono confrontate col modello statistico di Fermi. Si sono rilevate le distribuzioni angolari e gli spettri energetici delle particelle secondarie e confrontate coi corrispondenti risultati per le interazioni π -p di 5 GeV.

(*) *Traduzione a cura della Redazione.*

Asymptotic Conditions in Quantum Field Theories.

G. F. Dell'Antonio and P. Gulmanelli

Istituto di Scienze Fisiche dell'Università - Milano
Istituto Nazionale di Fisica Nucleare - Sezione di Milano

(ricevuto il 9 Gennaio 1959)

Summary. — On the ground of quite general hypotheses, as Lorentz invariance of the theory and causality, and restricting oneself to the case in which no zero-mass particles occur, one proves that it is possible to define in the ordinary field theory « asymptotic states» according to Haag. The proof is mainly based on the integral representations of the generalized singular functions.

1. – Introduction.

Many efforts have been made in the last few years (1) to work out formulations of field theories in which the « asymptotic states » (*i.e.*, the states in the remote future and past) are introduced in a clear cut way. In Haag's (1) approach, this asymptotic states are shown to exist, provided a suitable assumption is made on the space behaviour of certain vacuum expectation values, in which all times are taken equal. In the particular case in which the state is composed of only two « localized systems », it is moreover proved that general requirements, such as causality, Lorentz invariance and simple spectral conditions, are sufficient to assure the correct space behaviour. The purpose of the present note is to extend the proof to the general case, in which an arbitrarily large number of « localized systems » is considered.

(1) K. Nishijima: *Progr. Theor. Phys.*, **10**, 549 (1953); **12**, 279 (1954); **13**, 305 (1955); *Phys. Rev.*, **111**, 995 (1958); H. Ekstein: *Nuovo Cimento*, **4**, 1017 (1956); R. Haag (preprint and Varenna lecture notes). See also H. Lehmann, K. Symanzik and W. Zimmermann: *Nuovo Cimento*, **1**, 205 (1955).

2. – Basic assumptions and definitions.

The theoretical scheme we shall use stands on the following postulates:

α) The whole theory is Lorentz-invariant.

β) The energy-momentum four vector associated with a physically realizable state lays in the future light cone.

γ) Apart from the vacuum, there is no other state belonging to a zero-mass representation of the inhomogeneous Lorentz group. Our proof is thus restricted to theories where no zero-mass particle exists [2].

δ) All relevant theoretical quantities can be written in terms of a complete system of operators $A_i(x)$; for the sake of simplicity we shall suppose all operators to be scalar quantities.

ε) The operators

$$C_i(x) = \int g(x-y) A_i(y)\, \mathrm{d}y \,, \tag{1}$$

where $g(z)$ is a Laurent-Schwartz function (infinitely differentiable and with finite support), are local observables.

η) Causality is built in with the aid of the commutation relations:

$$[A_i(x), A_j(y)] = 0 \qquad \text{for} \quad (x-y)^2 > 0. \tag{2}$$

(Here, and in the following, the metric is $x^2 = \boldsymbol{x}^2 - x^{0^2}$.) Since $A(x)$ need not have a direct physical meaning, postulate η) could turn out to be too stringent. We shall not go further here into this problem.

θ) Finally, quantities as

$$\langle 0 \,|\, C_{i_1}(x_1) \ldots C_{i_n}(x_n) \,|\, 0 \rangle \tag{3}$$

are assumed to be finite for any configuration of the points $x_1, \ldots, x_n$.

We now turn to the « spatial condition » which plays a fundamental role in Haag's approach.

Using completeness, formula (3) may be written as follows

$$\sum_{\alpha_1 \ldots \alpha_{n-1}} \langle 0 \,|\, C_{i_1}(x_1) \,|\, \alpha_1 \rangle \langle \alpha_1 \,|\, C_{i_2}(x_2) \,|\, \alpha_2 \rangle \ldots \langle \alpha_{n-1} \,|\, C_{i_n}(x_n) \,|\, 0 \rangle \,. \tag{3'}$$

([2]) See however, in this connection, note ([3]).

Call « truncated part » of (3') what survives when all those terms are subtracted in which *at least one* of the intermediate states α_i is the vacuum state (3). With this notations, the « spatial asymptotic condition » is given the following form

$$\lim_{R\to\infty} R^m \langle 0 | C_{i_1}(x_1) \dots C_{i_n}(x_n) | 0 \rangle_T = 0 \qquad (x_1^0 = x_2^0 = \dots = x_n^0) \tag{4}$$

for arbitrary m.

T stands for « truncated », and R is the radius of the smallest sphere enclosing all points $x_1, \dots, x_n$.

We want to show that condition (4) is verified in those field theories, which satisfy postulates $\alpha), \dots, \theta)$.

3. - On the reduction formulae for the singular functions.

We shall start proving the following formula (4):

$$\lim_{R\to\infty} R^m \langle 0 | A_{i_1}(x_1) \dots A_{i_n}(x_n) | 0 \rangle_T = 0 \qquad (x_1^0 = x_2^0 = \dots = x_n^0) \,. \tag{4'}$$

To prove (4') we shall use an integral representation of vacuum expectation values of field operators, worked out in great detail by KÄLLÉN, WIGHTMAN and WILHELMSSON (5). By means of this representation, we can write (notations are the same as in K.W.):

$$\langle 0 \; A_1(x_1) \dots A_{n+1}(x_{n+1}) | 0 \rangle_T = i^n \int_{\varrho_{kl}} \dots \int^{\infty} \prod_{k,l}^{n} \mathrm{d}a_{kl} \, G(-a_{kl}) \, \Delta_{n-1}^{(+)}(\xi_k ; a_{kl}) \,, \tag{5}$$

where $\xi_k = x_k - x_{k+1}$ and

$$\varrho_{kl} > 0 \qquad (k, l = 1, \dots, n). \tag{5'}$$

---

(3) This definition is equivalent to that given by Haag.

(4) In the following we shall treat the l.h.s. of (4') as if it were a function. Strictly speaking it is a distribution: it is possible, however, to regard it as a limit of a function, when some suitable parameters ε_i are let go to zero. As the $\lim_{R\to\infty}$ commutes with $\lim_{\varepsilon_i \to 0}$ (modifications occur only in the neighbourhood of the light cone), the asymptotic behaviour we shall deduce is valid in a « strong sense » for the distribution.

(5) G. KÄLLÉN and A. WIGHTMAN: preprint (1958); D. HALL and A. WIGHTMAN: *Dan. Mat. Phys. Medd.*, **31**, n. 5 (1957); G. KÄLLÉN and H. WILHELMSSON: preprint 1958; hereafter referred to as K.W.

The «generalized function» $\Delta^{(+)}_{n+1}$ is defined as follows:

$$\Delta^{(+)}_{n+1}(\xi_k; a_{kl}) = \tag{6}$$

$$= \frac{(-i)^n}{(2\pi)^{3n}} \int \dots \int \mathrm{d}p_1 \dots \mathrm{d}p_n \exp\left[i \sum p_k \xi_k\right] \prod_{k \leq l}^{n} \delta(p_k p_l + a_{kl}) \prod_{k}^{n} \theta(p_k) .$$

The lower limits of integration in (5) and the related condition (5)′ are a consequence of postulate γ) and of the definition of «truncated part».

It is easily seen from (5) that the spatial behaviour of the vacuum expectation values may be deduced from that of the corresponding «generalized function», provided the commutability of the operations $\lim_{R\to\infty}$ and $\int \mathrm{d}a_{kl}$ is assured.

We state now the following *lemma*, the proof of which is given in Appendix I.

Given $N+1$ points x_i in a three-dimensional space (6), it is always possible to find a permutation $k_1, \dots, k_{N+1}$ of the indices $1, \dots, N+1$ and three vectors y_1, y_2, y_3 in such a way that the following four relations hold

$$\xi_i = \sum_{1}^{3}{}_{\alpha} c_{i\alpha} y_\alpha \; ; \qquad \xi_i \in \{\xi\} \; ; \qquad \xi_i = x_{k_i} - x_{k_{i+1}} , \tag{7}$$

where

$$0 < c_{i_\alpha} \leqslant 1 \tag{8}$$

for each value of the indices i, α;

$$\xi_i \to R\xi_i \Rightarrow y_\alpha \to R y_\alpha \qquad (\alpha = 1, 2, 3), \ (i = 1, \dots, N), \tag{9}$$

$$\xi_i \to R\xi_i \Rightarrow y_\alpha \to f_\alpha(R) y_\alpha , \quad (i = 1, \dots, M < N), \ (\alpha = 1,2,3,), \tag{10}$$

where $f_\alpha(R) \div R$ for R large enough.

As a consequence of (9) and (10), $\lim_{R\to\infty} c_{i_\alpha} \neq 0$ $(\alpha = 1, 2, 3)$ for *at least one* value of the index i.

By means of (7), (6) may be written as follows:

$$\Delta^{(+)}_{n+1}(\xi_k; a_{kl}) = \tag{11}$$

$$= \frac{(-i)^n}{(2\pi)^{3n}} \int \dots \int \mathrm{d}p_1 \dots \mathrm{d}p_n \exp\left[i \sum_{1}^{3}{}_{\alpha} p'_\alpha y_\alpha\right] \prod_{k \leq l}^{n} \delta(p_k p_l + a_{kl}) \prod_{k}^{n} \theta(p_k) ,$$

$$p'_\alpha = \sum_i p_i c_{i_\alpha} . \tag{11′}$$

p'_α are, by condition (8), time-like vectors with positive time component.

(6) We assume that the set $\{\xi\}$ does not belong to a plane; if it does, our lemma has to be modified in an obvious way, which amounts essentially in letting the index α run from 1 to 2, instead of 1 to 3, (See Appendix I).

Assume, now, that p'_α ($\alpha = 1, 2, 3$) are linearly independent, and choose among the p_i, a vector p_m such that the set $\{p'_\alpha\}$ is a complete set (7) (*i.e.* every p_i can be expressed as a linear combination of p'_α; this is connected with the four dimensions of the p-space).

With formal manipulations, eq. (11) is given now the form (see K.-W. eq. (15)):

$$(12)\quad \Delta^{(-)}_{n-1}(\xi_k; a_{kl}) = \frac{(-i)^{n-4}}{(2\pi)^{3(n-4)}}(-D)^{(n-4)/2}\prod_{k_1\le k_2=5}^{n}\delta(Da'_{k_1k_2} - \sum_{\lambda,\lambda'=1}^{4} a'_{k_1\lambda}\Delta'_{\lambda\lambda'}a'_{\lambda' k_2})\cdot$$

$$\cdot\prod_{k=4}^{n}\theta(a'_{1k})\,\frac{1}{D_c}\,\frac{(-i)}{(2\pi)^3}\,\frac{1}{\sqrt{-D}}\,\theta(-D)\,\Delta^{(+)}_4(y; a')\,,$$

where

$$D_c = \det\|d_{ik}\| \qquad (i,k=1,\ldots,n), \qquad d_{k_i} = \begin{cases} c_{ik} & k=1,2,3,\\ \delta_{ik} & \text{otherwise,}\end{cases}$$

$$(12')\quad \begin{cases} a'_{k_1k_2} = \sum_{i,l}^{n} d_{k_1 i}d_{k_2 l}a_{il}\,,\\ D = \det\|a'_{\lambda\lambda'}\| \quad (\lambda,\lambda'=1,\ldots,4) \quad \Delta'_{\lambda\lambda'} \equiv \text{cofactor of } a'_{\lambda\lambda'} \text{ in} D \end{cases}$$

and

$$(13)\quad \Delta^{(-)}_4(y; a') = \frac{i}{(2\pi)^9}\int dp_1\ldots\int dp_3 \exp\Big[i\sum_1^3 p_i y_i\Big]\prod_{k\le l}^{3}\delta(p_k p_l + a'_{kl})\prod_k^3\theta(p_k)\,.$$

Recalling (9) and (10), it is easily seen from (12) that the behaviour of $\Delta^{(-)}_{n-1}(\xi; a)$ for large values of the (three dimensional) vectors ξ (or of some of them) is the same as the behaviour of $\Delta^{(+)}_4(y; a')$ for large values of the vectors y.

We want to stress that postulate γ) and relations (8), (9), (10) imply (8)

$$(14)\quad \min_{d_p,\, R \text{ arbitrary}} a'_{\alpha\beta} = \varrho_{\alpha\beta}\,, \qquad \varrho_{\alpha\beta} \geqslant c > 0\,,$$

(7) A p_m which satisfies this requirement can always be found, if the set $\{p_i\}_{i=1,\ldots,N}$ does not belong to a three dymensional manyfold. In the latter case, the following developments have to be modified in an obvious way.

(8) Condition γ) is sufficient, but by no means necessary. Relation (14) can be proved under the following weaker assumptions: 1) *at least one* of the sets of intermediate states in (3'), *e.g.* $\{|\alpha_{\bar{k}}\rangle\}$, due to the operation of some selection rule, does not contain states belonging to a zero-mass representation of the Lorentz group, and different from the vacuum. 2) When only a subset $\{\xi_i\} \subset \{\xi_i\}$ contains vectors which are made indefinitely large (cfr. (10); $\{\xi_i\} \equiv \xi_1, \ldots, \xi_M$), the sequence $x_1, \ldots, x_N$ has to be chosen « well ordered » (see App. I) and moreover the vector $\xi_{\bar{k}} (\equiv x_{\bar{k}} - x_{\bar{k}+1})$ (« corresponding » to the aforementioned set $\{|\alpha_{\bar{k}}\rangle\}$ of intermediate states) has to satisfy the relation $\xi_{\bar{k}} \in \{\xi_i\}$.

where d_p is the domain within which the energy-momentum four-vectors $p_1, \ldots, p_n$ may vary.

Relation (14) is essential in deriving the asymptotic behaviour of $\langle 0 | A_1(x_1) \ldots A_n(x_n) | 0 \rangle_T$ from that of the generalized functions; as it will become clear when we shall give the asymptotic behaviour of $\Delta_4^+(x; a)$, rel. (14) assures the commutability of the operations $\lim_{R\to\infty}$ and $\int da_{kl}$ (cfr. discussion after eq. (6)).

For completeness, we shall now treat briefly the case in which the vectors p'_α defined in (11′) are not linearly independent.

Suppose they do not lay on the same line, and that p'_1 and p'_2 are linearly independent (this is of course always possible; it is a mere matter of labelling).

Then we write

$$p'_3 = \sum_1^2 b_i p'_i$$

and, by a procedure completely analogous to that followed before, we get a formula which is essentially equal to (12) with the following change in notations:

$$d_{ki} = \begin{cases} c_{ik} & k = 1, 2; \\ \delta_{ik} & \text{otherwise}; \end{cases}$$

$$\text{(15)} \qquad \Delta_4^{(+)}(y; a') = \frac{-i\pi}{(2\pi)^3} \frac{1}{\sqrt{a'^2_{12} - a'_{11} a'_{22}}} \theta(D_0)\theta(a'_{13}) \Delta_3^{(+)}(y'_1, y'_2; a'_{11}, a'_{12}, a'_{22});$$

$$y'_i = y_i + b_i y_3 \qquad i = 1,2,$$

$$D_0 = \det \| a'_{ik} \| \qquad i, k = 1, 2, 3.$$

As y_1, y_2, y_3 are taken as linearly independent (9), $y'_i \neq 0$, $i = 1, 2$, and moreover

$$\text{(16)} \qquad \xi_i \to R\xi_i \Rightarrow y'_j \to R y'_j . \qquad (i = 1,\ldots,n) \quad (j = 1,2)$$

Formulae (12), (15), (16) show that, in this case, the asymptotic behaviour of $\Delta_{n+1}^{(+)}$ is given by the asymptotic behaviour of $\Delta_3^{(+)}$.

---

(9) For the sake of brevity, we do not cover here the case in which the vectors y_1, y_2, y_3 lay on a plane (or on a line). All conclusions reached in this chapter are valid in that case too, and are moreover deduced in an easier way, due to the particularly simple form our lemma takes when a relation like $\sum m_i y_i = 0$ holds. See Appendix I, second part.

It is now easily seen that, when all vectors p_i, $(i = 1, 2, 3)$, have the same direction, one is led back to the asymptotic behaviour of $\Delta_2^{(-)}$.

Finally, all considerations made in connection with (14) are still valid in these two cases.

Summing up the results of this chapter, we see that, in order to prove (4') it will be sufficient to show that

1) $\lim_{R\to\infty} R^k \Delta_4^{(-)}(x; a) = 0$ for all m $(k = 2, 3, 4)$, R being the radius of the smallest sphere enclosing the points x_i;

2) one is allowed to interchange the operations $\lim_{R\to\infty}$ and $\int da_{ik}$ in (5).

3·1. *Spatial behaviour of* $\Delta_4^{(-)}$. – The integral representation for the $\Delta_4^{(-)}$ functions can be written in the following form [10]:

$$(17)\quad \Delta_4^{(+)}(\xi; a) = \frac{i}{4(2\pi)^4}\int_{-\infty}^{-\infty} \frac{H_0^{(2)}(t)\,t\,dt}{\sqrt{(t^2 - Q)^2 - P^2}^{\frac{1}{2}} - St^2}\,\vartheta(D_0)\vartheta(a_{12}^2 - a_{11}a_{22})\vartheta(a_{12})\vartheta(a_{13}),$$

where: $Q = I_1$,

$$P = 2(I_1^2 - I_2),$$

$$S = \tfrac{32}{3}(I_1^3 - 3I_1 I_2 + 2I_3),$$

$$I_k = \mathrm{Sp}\left[(-AX)^k\right]; \quad A = \|a_{ik}\|; \quad X = \|\xi_i\xi_k\| \qquad (i, k = 1, 2, 3).$$

It can be shown that $S < 0$, and that $S = 0$, if and only if the vectors ξ_k or p_i are not linearly independent (cf. Appendix II). In either case by a discussion similar to that of Section 3 one is led back to study the spatial behaviour of the $\Delta_2^{(+)}$ function (cf. Section 3·2).

We shall therefore confine ourselves to the negative values of S.

Due to (9), (10), we are interested in the case in which it is possible to express all the ξ_i variables as

$$(18)\qquad \xi_i = R\chi_i,$$

i.e., the case in which all distances go at the end to infinity.

---

[10] Eq. 17 is a specialization of formula (44) in K.W. Use can be made of this formula, because of the analiticity of the generalized singular functions in the products $\xi_i\xi_k$, when all vectors ξ_i are spacelike. Cfr. F. DYSON: *Phys. Rev.*, **110**, 579 (1958); G. KÄLLÉN and A. WIGHTMAN: ref. quoted in (5).

Because of (18) and of the form of Q, P, S as functions of the scalar products $\xi_i\xi_k$, eq. (17) becomes:

$$(19)\quad \Delta_4^{(+)}(\xi;a) = \frac{i}{4(2\pi)^6}\frac{1}{R^2}\int_{-\infty}^{+\infty}\frac{H_0^{(1)}(Rt')t'\,dt'}{\sqrt{[(t'^2-q)^2-p]^2-st'^2}}\theta(D_0)\theta(a_{12}^2-a_{11}a_{22})\theta(a_{12})\theta(a_{13}),$$

where

$$t = Rt'; \qquad q = \frac{Q}{R^2}; \qquad p = \frac{P}{R^4}; \qquad s = \frac{S}{R^6}.$$

and

$$q,\ p,\ s \text{ remain finite when } R \to \infty.$$

It is easily seen that the roots of the equation

$$(19')\qquad [(t'^2-q)^2-p]^2 - st'^2 = 0$$

are in general out of the real axis ([11,12]) and always symmetric with respect to it. Roots not on the imaginary axis are symmetric with respect to it too.

We can now perform the integration in eq. (19) by the method of residua. The function under the sign of integral is analytic in the upper half-plane of the (complex) variable t', after the introduction of a suitable number (two) of cuts, so chosen as to connect pairs of the branch points of the algebroid function $\sqrt{[(t'^2-q)^2-p]^2-st'^2}$.

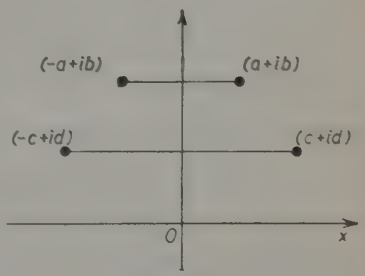

Fig. 1.

The properties of the Hankel functions, for positive imaginary part of the argument, allow us to reexpress (19) in the form of an integral along the chosen cuts. The explicit computation of that integral would not be in general an easy task; for our purposes it will suffice, however, to find an expression depending on R and dominant with respect to it.

Let us take, for instance, the case in which the branch points are: $a-ib$; $-a+ib$; $c+id$; $-c+id$ $(b>0,\ d>0)$.

The cuts are chosen as shown in Fig. 1.

([11]) The only exception is the root $t'=0$, which appears when $p=q^2$. One easily realizes that this case can be treated on the same lines as the general one, the only formal difference being that one of the two cuts runs now from one of the roots of (19') to infinity.

([12]) The hypothesis of the absence of zero mass particles plays here an important role. It can be replaced, however, by a weaker assumption; see note ([8]).

Then eq. (19) becomes:

$$(20)\quad \Delta_4^{(+)}(\xi; a_{ik}) = \frac{i}{2(2\pi)^6}\frac{1}{R^2}\Bigg(\int_{-a}^{a} \frac{H_0^{(1)}[(Rx + ibR)]\cdot(x+ib)\,\mathrm{d}x}{\sqrt{[(x^2-2ibx-b^2-q)^2-p]^2-s(x^2-2ibx-b^2)}} + \\ - \int_{-e}^{e} \frac{H_0^{(1)}[(Rx + idR)]\cdot(x+id)\,\mathrm{d}x}{\sqrt{[(x^2+2idx-d^2-q)^2-p]^2-s(x^2+2idx-d^2)}}\Bigg).$$

By the aid of the addition formulae for Hankel functions [13] we can rewrite the r.h.s. of eq. (20) as a sum of products of Hankel functions with imaginary argument (ibR, idR) by integrals for which dominant functions may be easily found. Only Hankel functions with real argument will appear in the integrands. It then follows that the $\Delta_4^{(+)}$ function is smaller than a sum of terms which go to zero faster than any power of $1/R$ for $R \to \infty$. *I.e.*

$$(21)\qquad \lim_{R\to\infty} R^m \Delta_4^{(+)}(\xi; a_{ik}) = 0\,.$$

In order to legitimate the interchange of the two processes of integration and limes in eq. (5), we still have to prove that the convergence is uniform in the variables a_{ik}. Let us note first of all that

$$b \equiv b(a_{ik})\,; \qquad d \equiv d(a_{ik})$$

and introduce besides the notations

$$\bar{b} = \min_{a_{ik}} \{b(a_{ik})\}\,, \qquad \bar{d} = \min_{a_{ik}} \{d(a_{ik})\}\,.$$

Recalling that $a_{ik} \geqslant \varrho_{ik} > 0$, one sees immediately that $\bar{b}$ and $\bar{d}$ do exist and are different from zero. Let us call $\bar{a}_{ik}$ the point (not necessarily unique) for which $b = \bar{b}$ and $d = \bar{d}$. It is then evident from eq. (20) that, if

$$R^m \Delta_4^{(+)}(\xi; \bar{a}_{ik}) < \varepsilon \qquad \text{for } R > R_0,$$

it also holds:

$$R^m \Delta_4^{(+)}(\xi; a_{ik}) < \varepsilon \qquad \text{for } R > R_0 \text{ and all } a_{ik}. \qquad \text{Q.E.D.}$$

We wish to remark that all our conclusions do not depend of course on the particular choice we have made for the cuts in the complex plane of the variable t' (cf. formula (19)).

---

[13] Cfr. *e.g.* *Higher Transcendental Functions*, vol. 2 (New York, 1953), p. 101.

3·2. *Spatial behaviour of* Δ_3^-. – The asymptotic behaviour of the Δ_3^- functions can be studied along the same lines we have followed in the preceding Section. In this case, however, there are some simplifying circumstances: the function to be integrated is now analytic in the upper half-plane of the complex variable t, except at two points, where it shows a pole [14]: the integral reduces then to the sum of the residua at the two poles and the result is the one well known [15]:

$$(22)\quad \Delta_3^{(+)}(\xi_1, \xi_2; a) =$$

$$= \frac{-2i\sqrt{a_{12}^2 - a_{11}a_{22}}}{(4\pi)^3}\frac{}{\sqrt{P}}\left[H_0^{(1)}(\sqrt{Q - \sqrt{P}}) - H_0^{(1)}(\sqrt{Q - \sqrt{P}})\right]\cdot\vartheta(a_{12}^2 - a_{11}a_{22}) .$$

where the imaginary part of the arguments of the Hankel functions is taken to be positive and

$$Q = -\sum_{i,k}^{1,2} a_{ik}\xi_i\xi_k , \qquad (a_{12} = a_{21})$$

$$P = 4[a_{12}^2 - a_{11}a_{22}][(\xi_1\cdot\xi_2)^2 - (\xi_1)^2(\xi_2)^2] .$$

Here is $P \geqslant 0$: we are interested though only in the case $P = 0$, because if $P = 0$ then it is possible to express Δ_3^- by means of Δ_2^- [16].

One sees immediately that $P \to \infty$, when at least one of the vectors ξ_i tends to infinity. From (22) one has then:

$$(23)\qquad \lim_{R\to\infty} R^m \Delta_3^{(+)}(\xi_1, \xi_2; a) = 0$$

for all m. The proof goes as follows:

Let us put $\xi_i = R\chi_i$ and take the limes for $R \to \infty$. It is easily seen that $Q \div R^2$, $P \div R^4$; $q \equiv Q R^2$ and $p \equiv P R^4$ depend only on the angles between the vectors ξ_i and, of course, on the values of a_{ik}. Eq. (22) can be rewritten in the following form:

$$(22')\quad \Delta_3^{(+)}(\xi_1, \xi_2; a) =$$

$$= \frac{-2i\sqrt{a_{12}^2 - a_{11}a_{22}}}{(4\pi)^3}\frac{}{R^2\sqrt{q}}\left[H_0^{(1)}(R\sqrt{q - \sqrt{p}}) - H_0^{(1)}(R\sqrt{q - \sqrt{p}})\right]\cdot\vartheta(a_{12}^2 - a_{11}a_{22}) .$$

---

(14) The two singular points coincide, if and only if Δ_3^- can be expressed by means of $\Delta_2^{(+)}$. The asymptotic behaviour of $\Delta_2^{(+)}$ is well known.

(15) Cfr. K.W.: A. WIGHTMAN and D. HALL: *Phys. Rev.*, **99**, 674 (1955).

(16) Cfr. note (14).

In eq. (22'), the imaginary part of the arguments of $H_0^{(1)}$ must be taken as positive; eq. (23) follows then immediately from the known behaviour of the Hankel-functions.

A discussion completely analogous to that of Section 3·1 leads to the conclusion, that the limes (23) is uniform with respect to the parameters a_{ik}.

4. – Proof of eq. (4).

By the definition (1) of the quasi-local operator $C(x)$, eq. (4) may be rewritten as follows:

$$(4'') \quad \lim_{R\to\infty} R^m \int g_{i_1}(x_1 - y_1) \dots g_{i_n}(x_n - y_n) \langle 0 | A_{i_1}(y_1) \dots A_{i_n}(y_n) | 0 \rangle_T \mathrm{d}y_1 \dots \mathrm{d}y_n = 0 .$$

We recall that $g(z)$ are Lorentz-Schwartz functions, *i.e.* infinitely differentiable and with finite support around the origin.

By making use of the properties of the $g(z)$ functions one can derive the asymptotic behaviour (for $R \to \infty$) of the *function* $\langle 0 | C(x_1) \dots C(x_n) | 0 \rangle_T$ from that of the *distribution* $\langle 0 | A(x_1) \dots A(x_n) | 0 \rangle_T$.

Let S_i be the support of $g_i(z)$ and $\varrho_i (\equiv \max_{S_i} \sqrt{\boldsymbol{z}^2 + z_0^2})$ the supremum of the « distance » of the border S_i from its origin. Define $\varrho \equiv \max \{\varrho_i\}$. Let $x_i - x_j = R z_{i,j}$ be the distance between any two of the point arguments of the $C_i(x)$; it is then easily seen that only those set of points may give contribution to the integral, for which the following inequalities are satisfied:

$$(24) \qquad R - 2\varrho \leqslant |\boldsymbol{y}_i - \boldsymbol{y}_j| \leqslant R + 2\varrho \; ; \qquad |y_i^0 - y_j^0| < 2\varrho \qquad i \neq j \;\; (i, j = 1, \dots n).$$

Let $\mathcal{M}_R$ be the totality of the n-ples for which (24) holds.

The asymptotic behaviour of $\langle 0 | A(y_1) \dots A(y_n) | 0 \rangle_T$ has been derived in Section 3 for the case in which

$$(25) \qquad y_1^0 = y_2^0 = \dots = y_n^0 .$$

The results of Section 3 may, however, be easily extended, by use of the reduction formulae and of the integral representation of $\Delta_5^{(+)}$, to hold true when the less stringent condition (24) is satisfied.

We have therefore

$$(26) \qquad \lim_{R\to\infty} R^m \langle 0 | A(y_1) \dots A(y_n) 0 | \rangle_T = 0 \quad \text{for arbitrary } m, \text{ if } (y_1, \dots, y_n) \in \mathcal{M}_R .$$

The asymptotic behaviour of $\langle 0 | C_{i_1}(x_1) \dots C_{i_n}(x_n) | 0 \rangle_T$ we had to prove, follows now immediately from (26) and from the circumstance that contributions to the integral in (4'') only come from n-ples which belong to $\mathcal{M}_R$.

We end noting that it would not be difficult to prove, that the same asymptotic behaviour holds for vacuum expectation values of operators $B(x)$, defined as

$$B_i(x) \equiv \int A_i(y) f(x-y)\, \mathrm{d}y \,,$$

where $f(z)$ are functions infinitely differentiable, different from zero only for $|z^0| < \varrho$ and such that

$$\lim_{|\boldsymbol{z}| \to \infty} |\boldsymbol{z}|^n f(z) = 0 \,.$$

* * *

We want to thank Proff. P. Caldirola and A. Loinger for their kind interest and useful discussions.

Appendix I

This Appendix is devoted to the proof of the following

Lemma. – Given, in an M-dimensional Euclidean [17] space, $N+1$ points $(N > M)$ [18], it is always possible to order them so that, if ξ_i $(\equiv x_i - x_{i+1})$, $i = 1, \dots, N$, are the differences between «adiacent» points, the following relations hold:

$$\xi_i = \sum_1^M{}_\alpha c_{i_\alpha} y_\alpha \qquad 0 < c_{i_\alpha} \leqslant 1 \,, \tag{A.1}$$

where y_α, $\alpha = 1, \dots, M$, are vectors suitably chosen. Moreover

$$\xi_i \to R\xi_i \Rightarrow y_\alpha \to R y_\alpha \,, \qquad (i = 1, \dots, N),\ (\alpha = 1, \dots, M), \tag{A.2}$$

$$\xi_i \to R\xi_i \Rightarrow y_\alpha \to f(R) y_\alpha \,, \qquad (i = 1, \dots, N' < N),\ (\alpha = 1, \dots, M), \tag{A.3}$$

$f(R) \div R$ for R large enough.

---

[17] This limitation is not essential.

[18] For $M = N$ the lemma is quite trivial, as one can always choose, in (A.1), $c_{i_\alpha} = \delta_{i_\alpha}$ (Kronecker-δ), and each ordering works. When $M > N$, the points lay in fact on an N-dimensional surface, and one is led back to the case $M = N$.

Proof. – For the sake of simplicity, we shall prove the lemma for the case $M = 3$, in which the geometrical arguments we shall use are more intuitive. The generalization to $M > 3$ is obtained just changing some words (plane, pyramid, etc.) in an obvious way.

We have therefore $N+1$ points $x_1, \ldots, x_{N+1}$ in a three dimensional Euclidean space; let us first assume that they do not lay on a plane. The second part of this appendix will deal with the latter case.

Choose a set $\{\pi_i\}_{i=1,\ldots,N+1}$ of parallel planes each containing one and only one of the points x_i. This is always possible, as the set $\{\eta_j\}$ of the lines which join two points of the set $X = \{x_i\}$ is composed of $[(N+1)(N+2)]/2$ elements; our requirement is satisfied by each set $\{\pi_i\}$ whose normal is not orthogonal to *any* line of the set $\{\eta_j\}$.

Let σ be a line normal to thet set $\{\pi_i\}$; we fix arbitrarily a point P and a direction on σ, and order the planes π_i according to the increasing distance from P of their intersections with σ. We choose now, for the points x_i, the ordering of the corresponding [19] planes

Let us change the indices so that $x_1, \ldots, x_N$ is now the right order. It is easily seen that vectors $x_\alpha - x_{\alpha+1}$ $(\alpha = 1, \ldots, N)$ drawn from the arbitrary point P lay all on the same side with respect to the plane passing through P and parallel to $\{\pi_i\}$

It is therefore possible to construct a pyramid with triangular basis and vertex at the point P, so that all vectors ξ_i lay in the interior of it.

Let us choose, on the edges of this pyramid, three vectors y_1, y_2, y_3 whose length is given by the maximum value of the covariant components of the set $\{\xi_i\}$ $(\xi_\alpha \equiv x_\alpha - x_{\alpha+1})$.

Obviously, the following relations hold:

$$\xi_i = \sum_i^3{}_\alpha c_{i\alpha} y_\alpha , \qquad 0 < c_{i\alpha} \leqslant 1 , \qquad (i = 1, \ldots, N) .$$

This proves the first part of the lemma (formula (A.1)). Relation (A.2) is a direct consequence of the way in which the vectors y_1, y_2, y_3 have been constructed.

For the validity of relation (A.3) it is however necessary that the sequence $x_1, \ldots, x_{N+1}$, ordered according to the previously stated criterion, be moreover a « well ordered » one.

This expression has the following meaning: if I is any set of points, whose distances are held finite in the limit $R \to \infty$, we shall term « well ordered » a sequence $x_1, \ldots, x_{N+1}$ for which

$$x_i, x_j \in I \Rightarrow x_k \in I , \qquad i < k < j .$$

It may easily be seen that it is always possible to choose, among all ordered solutions, a particular one which is « well ordered » too.

« Well ordering » is just a device to prevent the pyramid to degenerate

[19] By plane π corresponding to a point x is meant here the plane to which the point belongs.

into a plane, in the limit $R \to \infty$; in this limit, y_1, y_2, y_3 would no longer be a complete system, and a much more careful discussion would be required.

The importance of choosing a well ordered sequence is perhaps more clearly exhibited by the following example. Let $A_1(x)$, $A_2(x)$ be two electromagnetic currents and $B(x)$ a « neutral » field.

Consider the following vacuum expectation value

(A.4) $\quad \langle 0 | A_1(\boldsymbol{t}_1, 0) A_2(\boldsymbol{t}_2, 0) B(\boldsymbol{t}_3, 0) | 0 \rangle_T .$

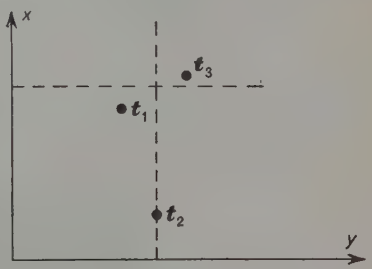

Fig. 2.

Let $|\boldsymbol{t}_1 - \boldsymbol{t}_2| \to \infty$, $|\boldsymbol{t}_2 - \boldsymbol{t}_3| \to \infty$, $|\boldsymbol{t}_3 - \boldsymbol{t}_1| \to$ $\to$ finite value.

The sequence $\boldsymbol{t}_1$, $\boldsymbol{t}_2$, $\boldsymbol{t}_3$ is an ordered one.

(The set $\{\pi_i\}$ is here, *e.g.*, parallel to the xz plane).

Using completeness, (A.4) can be expressed as

$$\text{(A.5)} \qquad \sum_{\alpha_1 \alpha_2} \langle 0 | A_1(\boldsymbol{t}_1, 0) | \alpha_1 \rangle \langle \alpha_1 | A_2(\boldsymbol{t}_2, 0) | \alpha_2 \rangle \langle \alpha_2 | B(\boldsymbol{t}_3, 0) | 0 \rangle_T ,$$

where $\{|\alpha_1\rangle\}$ contains states with zero mass, but $\{|\alpha_2\rangle\}$ does not. As $|\boldsymbol{t}_2 - \boldsymbol{t}_3| \equiv$ $\equiv R \to \infty$, one would be led to think that (A.5) goes to zero more rapidly than any inverse power of R.

Yet, this is not the case, as one easily realizes, rewriting (A.4) in the following form (using postulate η) and completeness

$$\text{(A.6)}\ (^{20}) \qquad \sum_{\beta_1 \beta_2} \langle 0 | A_2(\boldsymbol{t}_2, 0) | \beta_1 \rangle \langle \beta_1 | A_1(\boldsymbol{t}_1, 0) | \beta_2 \rangle \langle \beta_2 | B(\boldsymbol{t}_3, 0) | 0 \rangle_T .$$

Now, since $|\boldsymbol{t}_1 - \boldsymbol{t}_3|$ remains finite, the whole « asymptotic behaviour » when $R \to \infty$ is due to the separation between A_1 and A_2; as $\{|\beta_1\rangle\}$ contains states with zero mass, it can be proved, using *e.g.* the explicit formula for $\Delta_3^{(+)}$ given in (22) of the text, that $\lim_{R \to \infty} R^2 \cdot (\text{A.6}) = \text{finite} \neq 0$.

This is exactly what one would expect, as the particular situation, which we are studying in this example, is that of two systems, interacting via electromagnetic forces, which are moved far apart, the effect of the interaction being studied as a function of the distance.

For completeness, we shall now sketch briefly what happens when all points $x_1, \ldots, x_{N+1}$ lay on a plane π.

Draw on π a line σ such that all projections ν_i on σ of the points x_i are distinct. Choose arbitrarily on σ an origin and a direction, and order the set $\{x_i\}$ according to the increasing distance of ν_i from the origin.

Let $\{x_\nu\}$ be the ordered sequence and let it be « well ordered » too. The vectors $\xi_\alpha \equiv x_\nu - x_{\nu-1}$, drawn from a point P, lay all on the same half-plane, with respect to the normal ϱ to σ, passing through the point P.

---

(20) Notice that $\boldsymbol{t}_2$, $\boldsymbol{t}_1$, $\boldsymbol{t}_3$ is a « well ordered » sequence (choose now for σ the x-axis).

Let $\overline{y}_1$, $\overline{y}_2 \in \{\xi_\alpha\}$ be those vectors which make the largest and smallest angle with σ (arbitrarily oriented). Call y_1, y_2 two new vectors, which have the same direction of $\overline{y}_1$ and $\overline{y}_2$ respectively, and as length the maximum of the covariant components of $\{\xi_\alpha\}$ on the direction of $\overline{y}_1$ and $\overline{y}_2$ respectively.

With this notations, the following relations hold:

$$\xi_\alpha = c_{\alpha_1} y_1 + c_{\alpha_2} y_2 , \qquad 0 \leqslant c_{\alpha_i} \leqslant 1 , \qquad (\alpha = 1, \ldots, N) , \ (i = 1, 2). \tag{A.7}$$

In particular, there are two indices k, k' such that $c_{k_2} = c_{k'_1} = 0$. Using this fact, expression (A.7) can be rewritten in the following way:

$$\xi_\alpha = c_\alpha \xi_k + c'_\alpha \xi_{k'} ; \qquad c_\alpha \equiv \frac{c_{\alpha_1}}{c_{k_1}} > 0 ; \qquad c'_\alpha \equiv \frac{c_{\alpha_2}}{c_{k'_2}} > 0 . \qquad (\alpha \neq k, k'). \tag{A.8}$$

Relation (A.7) (or (A.8)) is the counter-part of formula (7) in the text, for the case in which all points lay on a plane.

We end noting that the choice of y_1 and y_2 parallel to $\overline{y}_1$ and $\overline{y}_2$ respectively leads to some formal simplifications: one has, however, to be careful in applying (A.7) when not all the distances ξ_α are made infinite. If one (or both) of the following relations holds

$$\lim_{R \to \infty} c_{k_1} = 0 , \qquad \lim_{R \to \infty} c_{k'_2} = 0 , \tag{A.9}$$

one has to choose the vectors y_1 and y_2 in such a way that all ξ_α lie in the *interior* of the angle $\widehat{y_1 y_2}$.

Appendix II

In the text we have stated that $S \leqslant 0$ and moreover that $S = 0$ if and only if the vectors ξ_k or p_k are linearly dependent. Let us consider the second case.

It may be seen that the relevant quantity is the determinant

$$V = \begin{vmatrix} p_1 \cdot p_1 & p_1 \cdot p_2 & p_1 \cdot p_3 \\ p_2 \cdot p_1 & p_2 \cdot p_2 & p_2 \cdot p_3 \\ p_3 \cdot p_1 & p_3 \cdot p_2 & p_3 \cdot p_3 \end{vmatrix} ,$$

i.e. $S \leqslant 0$ if $V \leqslant 0$, and viceversa.

If the vectors are linearly dependent, it is trivial to verify that $V = 0$. Conversely, if $V = 0$, there certainly exist two numbers α and β such that

$$\begin{aligned} p_1 \cdot (p_1 + \alpha p_2 + \beta p_3) &= 0 , \\ p_2 \cdot (p_1 + \alpha p_2 + \beta p_3) &= 0 , \\ p_3 \cdot (p_1 + \alpha p_2 + \beta p_3) &= 0 , \end{aligned}$$

and this relations together imply, as it may be seen by an elementary analysis

$$p_1 + \alpha p_2 + \beta p_3 = 0 .$$

Suppose now that the vectors p_k are linearly independent.
We may always decompose p_2 and p_3 in the following way:

$$p_2 = c_2 p_1 + p_2' ,$$

$$p_3 = c_3 p_1 + p_3' ,$$

where p_2' and p_3' are such vectors that

$$p_2' \cdot p_1 = 0 , \qquad p_3' \cdot p_1 = 0 ,$$

and $p_1^2 < 0$.
One has then

$$V = \begin{vmatrix} p_1^2 & 0 & 0 \\ 0 & p_2'^2 & p_2' \cdot p_3' \\ 0 & p_3' \cdot p_2' & p_3'^2 \end{vmatrix} ,$$

together with

$$p_2'^2 > 0 , \qquad p_3'^2 > 0 .$$

If now $p_2' \cdot p_3' \neq 0$, by means of a decomposition of, say, p_3' analogous to the preceding one, V becomes

$$V = \begin{vmatrix} p_1^2 & 0 & 0 \\ 0 & p_2'^2 & 0 \\ 0 & 0 & p_3''^2 \end{vmatrix} < 0 . \quad \text{q.e.d.}$$

The proof runs along the same lines for the ξ_k vectors.

RIASSUNTO

Sulla base di ipotesi molto generali, come Lorentz invarianza della teoria e causalità e con la restrizione al caso dell'assenza di particelle di massa nulla, si dimostra che è possibile definire nell'ordinaria teoria di campo « stati asintotici » secondo Haag. La dimostrazione si basa in gran parte sulle rappresentazioni integrali delle funzioni singolari generalizzate.

IL NUOVO CIMENTO Vol. XII, N. 1 1° Aprile 1959

The Supplementary Condition in Quantum Electrodynamics.

D. J. Candlin

Faculty of Mathematics - University of Cambridge (*)

(ricevuto il 22 Gennaio 1959)

Summary. — The difficulties of the supplementary condition are completely analogous to those of the momentum of the centre of mass in non-relativistic bound-state problems. It is unnecessary to introduce an indefinite metric or limiting procedures.

1. – Introduction.

We consider an electromagnetic field A_μ in interaction with a prescribed (conserved) electric current field J_μ. The equations of motion derived from the Lagrangian density

$$L = -\frac{1}{2}\frac{\partial A_\mu}{\partial x_\nu}\frac{\partial A_\mu}{\partial x_\nu} + J_\mu A_\mu \,, \tag{1}$$

are equivalent to Maxwell's equations when the supplementary condition

$$\frac{\partial A_\mu}{\partial x_\mu} = 0 \,, \tag{2}$$

is fulfilled. In the quantum theory, this cannot be postulated as an operator equation, since it is incompatible with the canonical commutation relations

$$[A_\mu(\boldsymbol{x}, t), \dot{A}_\nu(\boldsymbol{y}, t)] = i\delta_{\mu\nu}\delta_3(\boldsymbol{x} - \boldsymbol{y}) \,. \tag{3}$$

(*) Present address: Tait Institute of Mathematical Physics, University of Edinburgh.

It is therefore considered as a condition

$$\frac{\partial A_\mu}{\partial x_\mu}| \ ) = 0 \,, \tag{4}$$

on the physically admissible states.

The operator $\partial A_\mu/\partial x_\mu$ has a continuous spectrum, so that the states satisfying (4) are not normalizable. This is a considerable disadvantage when one wants to use the creation and annihilation operators, and has led to the introduction of an indefinite metric (1) or a limiting procedure (2). Both of these methods are open to criticism, and I wish to point out that the usual conclusion of these methods, that one need consider only transverse protons and the Coulomb interaction, can be reached in a more conventional way.

An analogous difficulty arises in calculating the energy levels of an isolated system, for instance an atomic nucleus. The interactions between the particles are invariant under a translation of the co-ordinate axes, and the energy can be split into two parts, the kinetic energy of the centre of mass with a continuous spectrum, and the discrete energies of the motion relative to that centre, which are the quantities of physical interest. It is not convenient to separate the centre of mass motion by replacing one of the particle co-ordinates by the co-ordinate of the centre of mass, for this would destroy the symmetry of the equations under interchange of particles. We therefore would like to impose the subsidiary condition that the total momentum of the system be zero, in the order that the Hamiltonian might have the discrete internal energies as its eigenvalues. However, we cannot normalize states in which the total momentum is zero. Instead, we can choose any supplementary condition which leads to a normalizable state and does not affect the relative co-ordinates of the particles. A possible choice of this condition is

$$\sum_{n=1}^{A} (\boldsymbol{p}_n - im\omega \boldsymbol{r}_n)\Psi = 0 \,,$$

where ω is an arbitrary positive constant, or, in terms of the center of mass co-ordinate,

$$(\boldsymbol{P} - iM\omega \boldsymbol{R})\Psi = 0 \,. \tag{5}$$

---

(1) S. N. Gupta: *Proc. Phys. Soc.*, **63**, 681 (1950); **64**, 850 (1951); K. Bleuler: *Helv. Phys. Acta*, **23**, 567 (1950); K. Bleuler and W. Heitler: *Progr. Theor. Phys.* **5**, 600 (1950).

(2) R. Utiyama, T. Imamura, S. Sunakawa and T. Dodo: *Progr. Theor. Phys.*, **6**, 587 (1951).

If we hold the relative co-ordinates constant, a state satisfying (5) will vary as

$$\exp\left[-\tfrac{1}{2}M\omega\boldsymbol{R}^2/\hbar\right],$$

and the expectation value of the kinetic energy of the centre of mass will be

$$\left(\Psi\left|\frac{\boldsymbol{P}^2}{2M}\right|\Psi\right)=\frac{3}{4}\hbar\omega\,. \tag{6}$$

This term will appear in all energy calculations with states satisfying (5), and will not affect the relative energies of the internal motion [3].

The condition (5) is not invariant under the fundamental group, that of translations of the axes, but we may replace (5) by

$$(\boldsymbol{P}-iM\omega(\boldsymbol{R}+\boldsymbol{\Lambda}))\Psi=0\,, \tag{5'}$$

where $\boldsymbol{\Lambda}$ is any constant vector, without affecting our argument, or even the expectation (6). A translation of the axes replaces (5) by one of the set (5'), which is equally satisfactory.

In the next Section, this method is applied to quantum electrodynamics. The translation group of the nuclear problem is replaced by that of the gauge transformations, and the symmetry group of the permutations of nucleons (which we wish to preserve explicitly) is replaced by the Lorentz group.

2. – Formal development.

Introduce the operators

$$\begin{cases} \chi_1(x)=\operatorname{div}\boldsymbol{A}(x)+\dot{A}_0(x)\,, \\ \chi_2(x)=\operatorname{div}\dot{\boldsymbol{A}}(x)+\nabla^2A_0(x)\,, \\ \varphi_1(x)=-\dfrac{1}{2}\displaystyle\int_{y_0=x_0}G(\boldsymbol{x}-\boldsymbol{y})\left(\nabla^2A_0(y)-\operatorname{div}\dot{\boldsymbol{A}}(y)\right)\mathrm{d}^3y\,, \\ \varphi_2(x)=-\dfrac{1}{2}\displaystyle\int_{y_0=x_0}G(\boldsymbol{x}-\boldsymbol{y})\left(\operatorname{div}\boldsymbol{A}(y)-\dot{A}_0(y)\right)\mathrm{d}^3y\,, \end{cases} \tag{7}$$

where G is the Green function for Laplace's equation,

$$G(\boldsymbol{x}-\boldsymbol{y})=-\left(4\pi\left|\boldsymbol{x}-\boldsymbol{y}\right|\right)^{-1}.$$

---

[3] S. Gartenhaus and C. Schwartz: *Phys. Rev.*, **108**, 482 (1957).

By the canonical commutation relations

$$\text{(8)} \qquad \begin{cases} [\chi_1(\boldsymbol{x}, t),\ \varphi_1(\boldsymbol{y}, t)] = -i\delta_3(\boldsymbol{x}-\boldsymbol{y}) , \\ [\chi_2(\boldsymbol{x}, t),\ \varphi_2(\boldsymbol{y}, t)] = -i\delta_3(\boldsymbol{x}-\boldsymbol{y}) , \end{cases}$$

while all other pairs of χ and φ operators commute for equal times.

The spatial part of A_μ may be split into longitudinal and transverse parts

$$\boldsymbol{A}(x) = \boldsymbol{A}_L(x) + \boldsymbol{A}_T(x) ,$$

where

$$\boldsymbol{A}_L(x) = \int_{y_0 = x_0} G(\boldsymbol{x}-\boldsymbol{y}) \operatorname{grad} \operatorname{div} \boldsymbol{A}(y)\, \mathrm{d}^3y ,$$

and

$$\boldsymbol{A}_T(x) = -\int_{y_0 = x_0} G(\boldsymbol{x}-\boldsymbol{y}) \operatorname{curl} \operatorname{curl} \boldsymbol{A}(y)\, \mathrm{d}^3y .$$

The set of operators χ_1, χ_2, φ_1, φ_2 at a given time is equivalent to the set $\boldsymbol{A}_L$, $\dot{\boldsymbol{A}}_L$, A_0, $\dot{A}_0$, from equations (7).

The Hamiltonian is

$$H(t) = \frac{1}{2}\int_{x_0 = t} (\dot{\boldsymbol{A}}^2 - \boldsymbol{A}\cdot\nabla^2\boldsymbol{A} - \dot{A}_0^2 + A_0\nabla^2 A_0)\, \mathrm{d}^3x - \int_{x_0 = t} (\boldsymbol{J}\cdot\boldsymbol{A} - J_0 A_0)\, \mathrm{d}^3x = H_T(t) + H_{LS}(t),$$

where

$$H_T(t) = \frac{1}{2}\int_{x_0 = t} (\dot{\boldsymbol{A}}_T^2 - \boldsymbol{A}_T\cdot\nabla^2\boldsymbol{A}_T)\, \mathrm{d}^3x - \int_{x_0 = t} \boldsymbol{J}\cdot\boldsymbol{A}_T \mathrm{d}^3x ,$$

and

$$\text{(9)} \qquad H_{LS}(t) = \int_{x_0 = t} (\nabla\chi_1\cdot\nabla\varphi_2 - \varphi_1\chi_2 - J_0\varphi_1 - \operatorname{div}\boldsymbol{J}\,\varphi_2)\, \mathrm{d}^3x +$$

$$+ \frac{1}{2}\int_{y_0 = x_0 = t} (J_0(x) G(\boldsymbol{x}-\boldsymbol{y})\,\chi_2(y) - \operatorname{div}\boldsymbol{J}(x) G(\boldsymbol{x}-\boldsymbol{y})\,\chi_1(y))\ \mathrm{d}^3x\, \mathrm{d}^3y .$$

In the unquantized theory, we must set

$$\text{(10)} \qquad \chi_1 = \chi_2 + J_0 = 0 .$$

so that

$$H_{LS}(t) = -\frac{1}{2}\int_{x_0=y_0=t} J_0(x)G(x-y)J_0(y)\,\mathrm{d}^3x\,\mathrm{d}^3y - \int_{x_0=t}\varphi_2 \operatorname{div} \boldsymbol{J}\,\mathrm{d}^3x. \tag{11}$$

The second term vanishes if the given charge density J_0 does not vary with time. If, however, it is derived from a quantized matter field, this term can be cancelled in the usual way by a phase transformation $\psi \to \exp[ie\varphi_2]\psi$ in the Hamiltonian of that field.

In the quantized theory, we adopt supplementary conditions in which (10) hold not for the operators themselves but for their expectation values in states satisfying the conditions. Since χ_1 and φ_2 commute, and also χ_2 and φ_1, (11) will hold for the expectation values of H_{LS} and of φ_2. The second term again makes no physical contribution.

3. – Supplementary conditions.

It remains to show that we can find the supplementary conditions mentioned in the last paragraph, and that the scheme is invariant under inhomogeneous Lorentz transformations. Such conditions are

$$\begin{cases} C_1(\boldsymbol{x})\Psi = 0 \\ \text{and} \\ C_2(\boldsymbol{x})\Psi = 0 \end{cases} \tag{12}$$

for all $\boldsymbol{x}$, where

$$\begin{cases} C_1(\boldsymbol{x}) = \chi_1(\boldsymbol{x}, t_0) - 2i\omega\left(\varphi_1(\boldsymbol{x}, t_0) + \frac{1}{2}\int G(\boldsymbol{x}-\boldsymbol{y})J_0(\boldsymbol{y}, t_0)\,\mathrm{d}^3y - B_1(\boldsymbol{x})\right), \\ \text{and} \\ C_2(\boldsymbol{x}) = \chi_2(\boldsymbol{x}, t_0) + J_0(\boldsymbol{x}, t_0) + 2i\omega\nabla^2(\varphi_2(\boldsymbol{x}, t_0) - B_2(\boldsymbol{x})), \end{cases} \tag{13}$$

t_0 being any fixed time. $B_1(\boldsymbol{x})$ and $B_2(\boldsymbol{x})$ can be any Hermitian operators or functions such that the two supplementary conditions can be simultaneously satisfied by a normalizable state [4]. ω is an operator acting on the spatial arguments: if

$$f(\boldsymbol{x}) = \int F(\boldsymbol{k}) \exp[i\boldsymbol{k}\cdot\boldsymbol{x}]\,\mathrm{d}^3k,$$

---

[4] In general, this is achieved by choosing the B_i to commute with the χ_i and φ_i at time t_0, but in the next section we require greater generality to establish covariance.

then

$$\omega f(\boldsymbol{x}) = \int |\boldsymbol{k}| F(\boldsymbol{k}) \exp [(i\boldsymbol{k}\cdot\boldsymbol{x})] \, \mathrm{d}^3k .$$

Specifically,

$$\omega G(\boldsymbol{x} - \boldsymbol{y}) = [-2\pi^2(\boldsymbol{x} - \boldsymbol{y})^2]^{-1} .$$

The equations (12) and (13) are analogous in form to (5), and the matrix elements of the Hamiltonian and other observables [5] at time t_0 between states satisfying (12) take their correct physical values. That the same holds for observables at other times follows from the discussion of time-displacement invariance in the next section.

A change in the quantities $B_i(\boldsymbol{x})$ is a gauge transformation

$$A_\mu \to A_\mu + \partial_\mu \Lambda ,$$

where $\Lambda(x)$ is defined by

$$\Lambda(\boldsymbol{x}, t_0) = \delta B_2(\boldsymbol{x}) ,$$

$$\dot{\Lambda}(\boldsymbol{x}, t_0) = \delta B_1(\boldsymbol{x}) ,$$

$$\Box\Lambda = 0 .$$

In a scattering problem, we take the time t_0 before the source is effective, that is, $J_0(\boldsymbol{x}, t_0)$ is zero, and then in the gauge in which $B_1 = B_2 = 0$, our supplementary conditions reduce to the familiar prescription that no scalar or longitudinal photons are present at time t_0.

4. – Invariance properties.

Our equations (13) define the supplementary conditions in terms of the field operators on a particular space-like surface $t = t_0$. We must now show that the system is invariant under displacements and space-time rotations of this surface.

First, consider an infinitesimal displacement in time; suppose that $C_1'(\boldsymbol{x})$ and $C_2'(\boldsymbol{x})$ are defined by equations (13) except that t_0 is replaced by $t_0 + \varepsilon$ and B_i by B_i'. Then

$$C_1'(\boldsymbol{x}) = C_1(\boldsymbol{x}) + \varepsilon C_2(\boldsymbol{x})$$

---

[5] J. M. JAUCH and F. ROHRLICH: *The Theory of Photons and Electrons* (Cambridge, Mass. 1955), p. 85.

and

$$C_2'(\boldsymbol{x}) = C_2(\boldsymbol{x}) - \varepsilon\nabla^2 C_1(\boldsymbol{x}) \,, \tag{14}$$

provided

$$B_1'(\boldsymbol{x}) = B_1(\boldsymbol{x}) - \varepsilon\nabla^2 B_2(\boldsymbol{x})$$

and

$$B_2'(\boldsymbol{x}) = B_2(\boldsymbol{x}) - \varepsilon\left(B_1(\boldsymbol{x}) - \int G(\boldsymbol{x}-\boldsymbol{y})\, J_0(\boldsymbol{y}, t_0)\, \mathrm{d}^3y\right) .$$

That is, the change in the surface is equivalent to a change in the B_i, or a gauge transformation.

Secondly, we suppose that the conditions involve the field operators on a space-like hyperplane $t = t_0 - \boldsymbol{v}\cdot\boldsymbol{x}$, where $\boldsymbol{v}$ is an infinitesimal vector. The supplementary conditions are best defined in a Lorentz frame with co-ordinates $(\boldsymbol{x}', t')$, where

$$\boldsymbol{x}' = \boldsymbol{x} + \boldsymbol{v}t$$

and

$$t' = t + \boldsymbol{v}\cdot\boldsymbol{x} \,; \tag{15}$$

in this frame the hyperplane is $t' = t_0$, and the supplementary conditions take the form

$$C_i'(\boldsymbol{x}, t_0)\Psi = 0 \,, \tag{16}$$

where the operators C_i' are defined by equations (13) with all operators and co-ordinates primed. Making the infinitesimal Lorentz transformation back to the original frame, we obtain, to first order in v,

$$\begin{cases} C_1'(\boldsymbol{x}', t_0) = C_1(\boldsymbol{x}, t_0) \,, \\ C_2'(\boldsymbol{x}', t_0) = C_2(\boldsymbol{x}, t_0) - \boldsymbol{v}\cdot\operatorname{grad} C_1(\boldsymbol{x}, t_0) \,, \end{cases} \tag{17}$$

provided

$$B_1(\boldsymbol{x}) = B_1'(\boldsymbol{x}') + \boldsymbol{v}\cdot(\boldsymbol{A}_T(\boldsymbol{x}) - 2\operatorname{grad}\varphi_2(\boldsymbol{x}, t_0))$$

and

$$B_2(\boldsymbol{x}) = B_2'(\boldsymbol{x}') - \boldsymbol{v}\cdot\left\{\dot{\boldsymbol{A}}_T(\boldsymbol{x}) + \operatorname{grad}\left(2\varphi_1(\boldsymbol{x}, t_0) + B_1(\boldsymbol{x}) - \int G(\boldsymbol{x}-\boldsymbol{y}) J_0(\boldsymbol{y}, t_0)\, \mathrm{d}^3y\right)\right\} .$$

The change of surface is again equivalent to a change of gauge, this time involving the potential operators (4).

5. – The S-matrix.

The S-matrix is defined by

$$S_{ba} = U_{ba}(\infty, -\infty) , \tag{18}$$

$$U_{ba}(t, t_0) = (b\,|\,U(t, t_0)\,|\,a) , \tag{19}$$

$$i\dot{U}(t, t_0) = H(t)\,U(t, t_0) , \tag{20}$$

$$U(t_0, t_0) = 1 . \tag{21}$$

If $|a)$ is a physical state, then

$$P\,|a) = |a) , \tag{22}$$

where P is the projection operator on the manifold satisfying (12), and so (19) may be written

$$U_{ba}(t, t_0) = (b\,|\,U(t, t_0)P\,|a) = (b\,|\,P'(t)U(t, t_0)\,|a) , \tag{23}$$

where $P'(t) = U(t, t_0)P\,U(t, t_0)^{-1}$.
Further, (20) may be written

$$i\dot{U}_{ba}(t, t_0) = \sum_c (b\,|\,H(t)\,|c)\,U_{ca}(t, t_0) , \tag{24}$$

where the summation is over any complete set of states. If we choose this set to be eigenstates of $P'(t)$, and also use the same set for the final states $|b)$, only states $|b)$ and $|c)$ with $P' = 1$ will contribute to (22), according to (23). That is, $|b)$ and $|c)$ satisfy

$$C_1'(\boldsymbol{x}, t)\,|\,) = 0$$

and

$$C_2'(\boldsymbol{x}, t)\,|\,) = 0 , \tag{25}$$

where $C_i'(\boldsymbol{x}, t) = U(t, t_0)\,C_i(\boldsymbol{x})\,U(t, t_0)^{-1}$.

The $C_i'(\boldsymbol{x}, t)$ are thus the same as the $C_i(\boldsymbol{x})$, with the argument t_0 in the operators replaced by t, and it follows that in (24) $(b\,|\,H(t)\,|c)$ may be replaced by $(b\,|\,H'(t)\,|c)$, where

$$H'(t) = H_T(t) - \frac{1}{2}\int J_0(\boldsymbol{x}, t)\,G(\boldsymbol{x} - \boldsymbol{y})\,J_0(\boldsymbol{y}, t)\,\mathrm{d}^3x\,\mathrm{d}^3y ,$$

according to (11), if we take $B_2(\boldsymbol{x}) = 0$. In this form of (24) we must explicitly restrict the summation over states $|c)$ to those satisfying (25), but since the effective Hamiltonian H' contains no reference to the longitudinal and scalar potentials, we may replace our actual system by a model in which the corresponding degrees of freedom do not occur.

* * *

I am very grateful to Professor E. R. CAIANIELLO for the hospitality of the Istituto di Fisica Teorica dell'Università di Napoli, in which this work was begun.

RIASSUNTO (*)

Nei problemi non relativistici degli stati legati le difficoltà della condizione supplementare sono del tutto analoghe a quelle dell'impulso del centro di massa. Non è necessario introdurre una metrica indefinita o procedimenti di limite.

(*) *Traduzione a cura della Redazione.*

ITALIAN PHYSICAL SOCIETY

INTERNATIONAL SCHOOL OF PHYSICS

UNDER THE AUSPICES OF THE

MINISTRY OF EDUCATION

AND THE

NATIONAL RESEARCH COUNCIL

SUMMER COURSES 1959

VILLA MONASTERO

VARENNA SUL LAGO DI COMO

GENERAL INFORMATION

A) - In addition to the Courses which are listed above, seminars on questions related to the basic subjects of the different courses will be held by visiting scientists.

B) - The lectures, seminars, conferences and discussions will generally be held in English or French.

C) - The organization and direction of the Courses is entrusted to the Directors.

D) - Those wishing to attend a Course should send not later than 15 days before the beginning of the course (*i.e.* resp., before June 1st, June 15th, July 1st, August 19th) an application, furnishing the following information, which should be set out clearly and legibly: 1) Christian name and surname; 2) Date and place of birth; 3) Present address; 4) Degrees and other qualifications obtained, with name of university in each case; 5) Present professional activity; 6) List of publications in Physics (and for the 3rd Course 1959 also in Astrophysics); 7) Standard of knowledge of English and French - written and spoken; 8) Whether intending to stay at Varenna unaccompanied or with members of family and, in the former case, whether willing to share a room with other students. The applicant should send, together with his application, a note of reference from a University professor of Physics, or in case of the 3rd Course 1959, from a University professor of Astronomy, testifying the applicant's interest and preparation for the activities of the School.

E) - Each application will be considered by the President of the Italian Physical Society and by the Director of the School on the basis of the information submitted, with regard also to a fair distribution of the places available among students of various nations. The decisions on the admittance to the School will be made known to the applicants within 7 days of the expiring of the date fixed for the sending of applications (*i.e.* resp., June 8th, June 22nd, July 8th, August 26th).

F) - Students will oblige in arriving at Varenna in the afternoon of the day preceding the opening of the Course (*i.e.* resp., in the afternoon of June 14th, June 28th, July 14th, September 1st) and calling at the Hotel Victoria (Piazza del Municipio di Varenna) for lodgings, and receive information and papers concerning the Course.

G) - Accomodation for the students will be provided in rooms with 1 or 2 beds either in the guest quarters of the Villa Monastero or in hotels at Varenna. Meals will be had at the Villa itself or at a hotel in Varenna.

H) - Fees as per 10) should be paid not later than 5 days after the beginning of the course (*i.e.* before June 20th, July 4th, July 20th, September 7th respectively) to the management of the School, at Varenna, in Italian currency. A very limited number of scholarships may be granted to students whose economic conditions might otherwise prevent them from attending the School.

I) - The School will do everything possible to find suitable accomodation in local hotels for members of families accompanying the students. It should be noted, however, that, in view of the holiday season, local possibilities are limited. Members of students' families may avail themselves of the catering arrangements being organized for the School. All expenditure involved in the hotel accomodation, board etc. for students' relatives will be payable separately. These expenses will be, according to the hotel, from 2 800 to 3 600 Lire per person per day and are to be settled directly with the hotel management.

Milan, 28 April 1959

The Secretary of the Society
G. C. Dalla Noce

The President of the Society
G. Polvani

The Directors of the Summer Courses
S. R. De Groot, L. A. Radicati, G. Righini, H. Alfvén

IL NUOVO CIMENTO Vol. XII, N. 1 1° Aprile 1959

Cut-Off Models of the Proton.

R. Hofstadter (*)

CERN - Geneva

(ricevuto il 27 Gennaio 1959)

Summary. — It is demonstrated that the form factor fitting the electron-proton scattering data, which could formerly be described by an exponential density distribution, can also be given entirely equivalently by one of several cut-off proton models. Such models have a theoretically desirable asymptotic behaviour, according to present ideas of field theory.

Electron scattering experiments on protons show that the experimental cross-sections can be successfully described in terms of phenomenological form factors F_1 and F_2 (1). The present experiments do not furnish unique values of these form factors because of the experimental error in the absolute cross-sections amounting to a little less than $\pm$ 10% in F^2. If the postulate $F_1 = F_2 = F$ is made, which incidentally appears to be supported by experiment, the choice of a functional form of F is greatly narrowed. For the case of not-too-large momentum transfer F can also be described by an equivalent spatial charge density distribution obtained by a well-known Fourier transformation. A simple one-parameter charge distribution fitting the data very well corresponds to an exponential model with root-mean-square (r.m.s) radius $= 0.80 \cdot 10^{-13}$ cm. Two-parameter models can also be found which fit the data, but if they do not change sign, *i.e.* if they are monotonic the r.m.s. radius always lies near the value $0.80 \cdot 10^{-13}$ cm.

(*) John Simon Guggenheim Fellow on leave from Stanford University, Stanford (Ca.).

(1) R. Hofstadter, F. Bumiller and M. R. Yearian: *Rev. Mod. Phys.*, **30**, 482 (1958).

From a theoretical point of view the exponential model does not appear to be reasonable for a proton, at least in the framework of current field theory [2] If the Yukawa field is employed the charge or magnetic moment density for a static model should behave [3] according to equation (1):

$$\varrho = \frac{\varrho_0 \exp[-r/b]}{r^2}. \tag{1}$$

This density distribution was examined by CHAMBERS and HOFSTADTER [4] who found that it was inadequate to fit the experimental data for any sensible choice of r.m.s. radius. However, the author has recently found that the above density distribution, if modified at small radii ($r \leqslant 0.45 \cdot 10^{-13}$ cm) yields a form factor as consistent with the present experimental results as the one corresponding to the exponential density distribution. Furthermore the agreement is insensitive to the precise manner of changing ϱ at small radii.

For example if the charge density has the value zero up to a radius « d » and then follows the behaviour given by Eq. (1) the experiments are well fit with the constants $d = 0.307 \cdot 10^{-13}$ cm, $b = 0.404 \cdot 10^{-13}$ cm which provide an r.m.s. radius of $a = 0.82 \cdot 10^{-13}$ cm. The latter value is quite close to the value $a = 0.80 \cdot 10^{-13}$ cm given by the exponential model.

More generally one can successfully use the following density distribution:

$$\begin{cases} \varrho = \varrho_0 h\,, & 0 \leqslant r \leqslant d, \\ \varrho = \dfrac{\varrho_0 \exp[-r/b]}{r^2}\,, & d \leqslant r \leqslant \infty, \end{cases} \tag{2}$$

where the case of the cut-off model described above corresponds to putting $h = 0$.

The fact that one can find values of a finite cut-off ($h \neq 0$) fitting the experiments is reasonable since a finite density at small radii fixes only a small amount of charge near the center of the proton, unless the value of h is made very large. However, the value chosen for h does affect the value of b. We shall comment on this point a bit later. In any case the value of h is not critical and since the interpretation of the experiment in terms of static charge (or magnetic moment) density models may need modification [5] at distances of the order of $r = \hbar/Mc = 2.1 \cdot 10^{-14}$ cm, we do not regard the exact value of h as greatly significant. The result that a theoretically more acceptable

---

[2] J. BERNSTEIN and M. L. GOLDBERGER: *Rev. Mod. Phys.*, **30**, 465 (1958).

[3] See, for example, S. S. SCHWEBER, H. A. BETHE and F. DE HOFFMANN: *Mesons and Fields*, Vol. 1 (Evanston, Ill., 1955).

[4] E. E. CHAMBERS and R. HOFSTADTER: *Phys. Rev.*, **103**, 1454 (1956).

[5] D. R. YENNIE, M. M. LEVY and D. G. RAVENHALL: *Rev. Mod. Phys.*, **29**, 144 (1957).

charge distribution at larger radii can fit the experiments, provided only that the charge density is « smoothed over » at very small radii, which one expects anyway because of recoil and of the contributions of more massive virtual intermediate states, is thought to be significant.

The density distribution given in Eq. (2) corresponds to a form factor:

$$F(qa) = \frac{1}{1+\frac{1}{3}h_0 d_0} \cdot \left\{ \frac{h_0 d_0}{(d_0 s)^3} [\sin s d_0 - s d_0 \cos s d_0] - \frac{d_0 \exp[d_0]}{d_0 s} \operatorname{Im} E_1(d_0 + i s d_0) \right\}, \tag{3}$$

where

$$h = h_0 \frac{\exp[-d_0]}{d_0^2 b^2}, \tag{4}$$

$$d_0 = \frac{d}{b}, \tag{5}$$

$$s = qa/k. \tag{6}$$

and

$$k^2 = \frac{2 + 2d_0 + d_0^2 + \frac{1}{5}h_0 d_0^3}{1+\frac{1}{3}h_0 d_0}. \tag{7}$$

The variable q is the usual four-momentum-energy transfer and the parameter a is the r.m.s. radius. $E_1(z)$ is the exponential integral for complex arguments ([6]).

TABLE I.

Unit of $q^2 = 10^{26}$ cm^{-2} q^2	F^2		
	Exponential	Model C	Model B
0.207	.954	.952	.951
0.825	.842	.835	.820
1.87	.691	.680	.675
3.30	.522	.521	.518
5.15	.379	.370	.369
7.42	.264	.269	.265
10.1	.179	.180	.180
13.2	.119	.120	.114
16.7	.078	.077	.072
20.6	.052	.047	.042
25.0	.034	.028	.023

([6]) Tables of the exponential integral for complex arguments, U.S. Department of Commerce, Nat. Bur. Standards Applied Mathematics Series 51, (May 1958).

In Table I we compare the values of F^2 for the exponential model and for the cut-off Yukawa models. Fig. 1 shows the corresponding distribution of ϱ, when the latter is multiplied by $4\pi r^2$, for the three cases:

a) The exponential model for which $a = 0.80 \cdot 10^{-13}$ cm.

b) The «zero» cut-off model for which $h = 0$, $d = 0.307 \cdot 10^{-13}$ cm, $b = 0.404 \cdot 10^{-13}$ cm and $a = 0.82 \cdot 10^{-13}$ cm.

c) The finite cut-off model for which $h_0 = 1.0$, $d = 0.44 \cdot 10^{-13}$ cm, $b = 0.40 \cdot 10^{-13}$ cm and $a = 0.816 \cdot 10^{-13}$ cm.

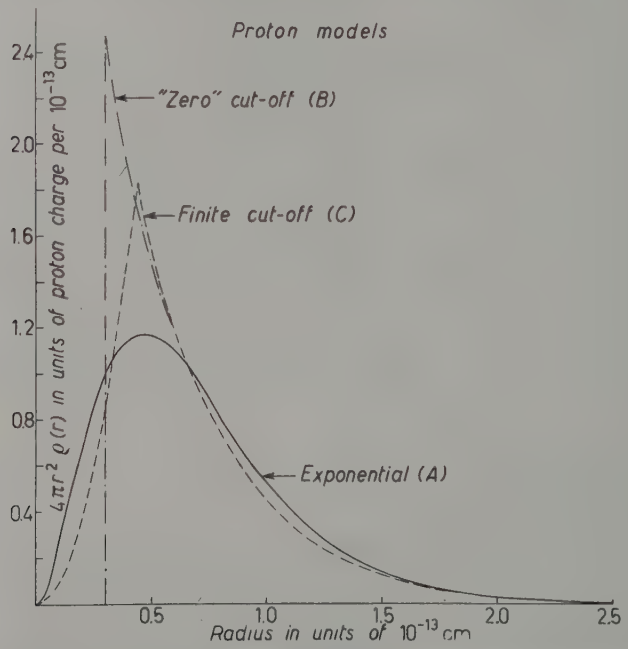

Fig. 1. – This figure shows the quantity, $4\pi r^2 \varrho(r)$, plotted against the radial distance from the center of the proton. Three models are shown corresponding to Models A, B and C of the text and Table I. The «zero» cut-off model *B* is indistinguishable on this scale from the finite cut-off model *C* beyond $0.6 \cdot 10^{-13}$ cm. All three models give very good fits with the experimental data.

Of the two new models represented in Table I model C gives slightly better agreement with the exponential case than model B but an extensive investigation of parameters for best fitting has not been made. Model C is in excellent agreement with all experiments performed to date. The current experiments have been carried as far as $q^2 \cong 18 \cdot 10^{26}$ cm^{-2}.

One can also, of course, obtain approximate agreement with experiment when, as pointed out [1], the density distribution in the middle range of radii resembles the density distribution given in Fig. 1 corresponding to an exponential distribution or to other acceptable models such as those shown in Fig. 16 of reference [1] (*). Thus a Clementel-Villi distribution will fit the data [1,7]. It has now also been found that a cut-off Yukawa II [8] model can give a good representation of the data. For this model:

$$(8) \qquad \begin{cases} \varrho = 0\,, & 0 \leqslant r \leqslant c, \\ \varrho = \varrho_0 r^{-1} \exp\left[-\frac{r}{\beta}\right], & c \leqslant r \leqslant \infty, \end{cases}$$

and the proper Fourier transform is:

$$(9) \qquad F(qa) = \left(\frac{1}{1+c_0}\right)\frac{1}{1+s^2}\left\{\cos c_0 s + \frac{1}{s}\sin c_0 s\right\},$$

where

$$(10) \qquad c_0 = \frac{c}{\beta},$$

$$(11) \qquad k^2 = \frac{2+3(c_0+1)+(c_0+1)^3}{(c_0+1)},$$

and where s is given by Eq. (6) with the value of k appearing in Eq. (11). Suitable parametric values giving an approximate fit with the experimental data are $c = 0.225 \cdot 10^{-13}$ cm, $\beta = 0.301 \cdot 10^{-13}$ cm and $a = 0.81 \cdot 10^{-13}$ cm. Further calculations have been made with other cut-off models such as

$$\varrho = \varrho_0 r^{-3} \exp\left[-r/b\right]$$

but such choices produce no qualitative changes in the above conclusions. For further comment on this model, see below.

It is worth-while to comment on the value of the range parameter « b » found in the above analysis. If the very simplest static model of a nucleon

---

(*) In Fig. 16 of reference [1] a Yukawa model with no cut-off is shown and does not fit the experimental data.

(7) E. Clementel and C. Villi: *Nuovo Cimento*, **4**, 1207 (1956).

(8) R. Hofstadter: *Rev. Mod. Phys.*, **28**, 214 (1956).

is employed ([3]) the value of b is given by:

$$b_0 = \frac{\hbar}{2\mu c}. \tag{12}$$

The numerical value of b_0 is $0.70 \cdot 10^{-13}$ cm whereas the value obtained from our analysis is $b = 0.40 \cdot 10^{-13}$ cm. However, our result is a reasonable one because the value b_0 corresponds only to the two-meson contribution to the form factor in the approach of dispersion theory ([9,10]). Higher order contributions will contribute fields whose range-parameters are smaller and the fact that our result points in this direction may imply that the higher order contributions should not be neglected.

It is possible to fit the experiments with the model of Equation (2) with larger values of b such as $0.59 \cdot 10^{-13}$ cm, almost approaching the value b_0, by including more charge in the central finite region. In fact one may place up to approximately 50% of the charge in this region if desired. However, the r.m.s. radius a is thereby increased to values about $a = (0.90 \div 0.92) \cdot 10^{-13}$ cm and it is not believed that the present experiments support an r.m.s. radius this large. In view of this possibility however, it seems very desirable to increase the accuracy of the electron scattering experiments at small q values in order to better determine an r.m.s. radius. It is also possible to obtain an excellent fit with the experimental data by using the zero-cut off model: $\varrho = \varrho_0 r^{-3} \exp[-r/b]$ mentioned above, with the « good » value of $b = 0.67 \cdot 10^{-13}$ cm and a core radius, $d = 0.34 \cdot 10^{-13}$ cm. For this case the value of $a = 0.86 \cdot 10^{-13}$ cm and the above remarks apply once again.

A few remarks about the value of the cut-off or core radius $d \cong 0.40 \cdot 10^{-13}$ cm may also be pertinent. This value is approximately of the same order found by SALZMAN ([11]) in his analysis of the neutron-electron interaction. Our value of d is also of approximately the same order as the repulsive core radius and may conceivably be connected with a common origin of the two concepts. Perhaps the cut-off radius is also one manifestation of the idea of a fundamental length.

* * *

I wish to thank Drs. SERGIO FUBINI and GEORGE SALZMAN for their constructive remarks and interest in these results.

([9]) S. D. DRELL: *Annual International Conference on High Energy Physics at CERN* (1958), pp. 28-31.

([10]) G. F. CHEW, R. KARPLUS, S. GASIOROWICZ and F. ZACHARIASEN: *Phys. Rev.*, **110**, 265 (1958).

([11]) G. SALZMAN: *Phys. Rev.*, **99**, 973 (1955).

I wish also to acknowledge with thanks the support of CERN and the J. S. Guggenheim Foundation in providing an opportunity to carry out the above studies.

RIASSUNTO (*)

Si dimostra che il fattore di forma che soddisfa i dati dello scattering elettrone-protone, che precedentemente poteva essere descritto da una distribuzione esponenziale di densità, può essere espresso in modo del tutto equivalente da uno dei molti modelli con cut-off protonico. Tali modelli hanno un comportamento asintotico teoricamente desiderabile secondo le idee attuali sulla teoria di campo.

(*) *Traduzione a cura della Redazione.*

Nucleon Correlation Effects in High Energy Electron Scattering.

R. Gatto

Istituto di Fisica e Scuola di Perfezionamento in Fisica Nucleare dell'Università - Roma
Istituto Nazionale di Fisica Nucleare - Sezione di Roma

(ricevuto l'11 Febbraio 1959)

Summary. — A detailed investigation is carried out of the role of nucleon-nucleon correlations in the inelastic scattering of high energy electrons by nuclei summed over all nuclear excitations. It is concluded that the dominant correlation effect is that caused by the exclusion principle and the differential cross section can be rather accurately predicted independently of the details of the nuclear dynamics.

1. – Introduction.

It is known that nucleon correlation effects can be directly observed in high energy electron scattering by measuring the inelastic differential cross-section summed over all nuclear excitations ([1-3]). This possibility was first pointed out in connection with experimental work on nuclear scattering of μ-mesons, but the derivation was based on the use of a Born approximation. An important advance was subsequently contributed by Schiff, who was able to sum the infinite Born series in a high energy approximation and adopting an adiabatic description for the motion of the nuclear particles ([3]). Schiff's work confirmed in general the conclusions drawn from the Born approximation approach. Nucleon correlations are also known to appear in the nuclear dispersive contributions to high energy elastic or inelastic electron scattering to a particular

([1]) R. Gatto: *Nuovo Cimento*, **10**, 1559 (1953).
([2]) J. Smith: *Phys. Rev.*, **95**, 271 (1954).
([3]) L. I. Schiff: *Nuovo Cimento*, **5**, 1223 (1957).

nuclear level ([4-6]). The difference between the summed inelastic effects considered in references ([1]) and ([2]), and the nuclear dispersive effects considered in ([4]), ([5]) and ([6]), is illustrated by the diagrams in Fig. 1, for the lowest Born approximations. Inelastic effects appear already at the first electromagnetic order, while nuclear dispersive effects appear only at the second order. In spite of their physical difference both effects can be expressed in terms of the nuclear pair correlation function. However, as remarked by SCHIFF ([3]), it seems rather difficult to identify correlation effects in the nuclear dispersive contribution, while their identification from the summed nuclear inelastic cross-section should be rather direct.

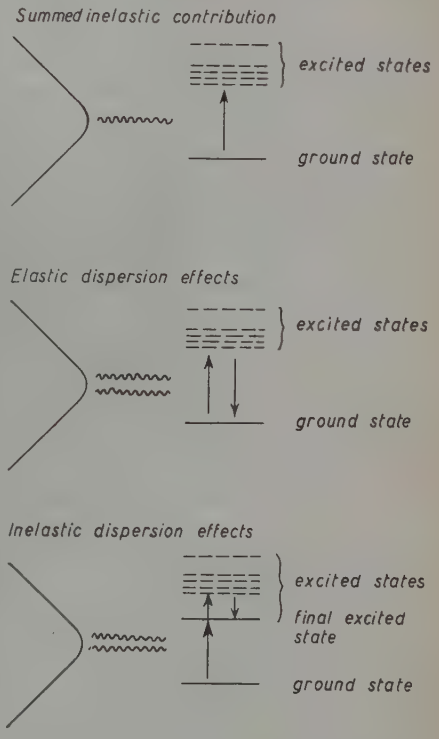

Fig. 1. – Diagrams illustrating various effects that can be expressed through the nucleon correlation function.

In the present paper we shall only be concerned with nuclear correlation effects in the summed inelastic cross-section. Our approach, already outlined in a preceding note ([7]), will be different from that followed in previous work ([1,2]), in that we shall try an evaluation of the effect without introducing *ad hoc* assumptions for the correlation function, bur rather trying to follow a consistent description of the nuclear dynamics. Correlation effects will result from the operation of the exclusion principle and of the nuclear forces. To simplify the formulation of the problem we shall ignore minor mesonic effects which become sensible at the high values of the momentum transfer. In particular before comparing with the experimental data one should include form factors for the nucleons. It is known from the interpretation of the electron deuteron experiments that the introduction of nucleon form factors produces a better agreement with ex-

([4]) L. I. SCHIFF: *Phys. Rev.*, **98**, 756 (1955).
([5]) B. W. DOWNS: *Phys. Rev.*, **101**, 820 (1956).
([6]) R. R. LEWIS: *Phys. Rev.*, **102**, 544 (1956).
([7]) R. GATTO: *Nuovo Cimento*, **2**, 669 (1955).

periment ([8]). The formal procedure for introducing nucleon form factors is well-known and can be found for instance in reference ([1]). Also neglected in our treatment are minor contributions arising from nucleon currents, including exchange currents due to the presence of charge exchange forces in the nuclear Hamiltonian. In a recent paper DRELL and SCHWARTZ ([9]) show that such contributions are quite small, but one can construct a sum rule for the energy weighted cross-section at fixed momentum transfer that turns out to be very sensitive to the presence of exchange currents. As a typical illustration of our results we report in Fig. 2 graphs of the form factor J for the summed inelastic differential cross-section, which is defined as the ratio between such a cross-section and the cross-section from the point charge Ze. The curves are calculated for a two body nuclear force of Yukawa shape. We shall try to reproduce some of the rather cumbersome mathematics that is involved in the evaluation of the correlation kernels, since our results may also be useful in connection with other problems, such as for instance correlation problems for the electron gas, where other systems of fermions must be described in similar conditions.

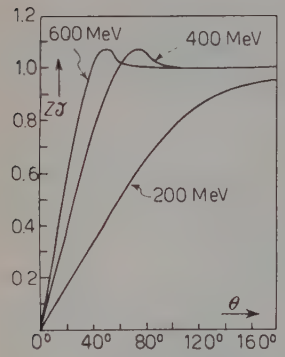

Fig. 2. – The calculated incoherent form factor J times the nuclear charge Z as a function of the scattering angle.

2. – Theoretical formulation.

We shall report here the main steps of the theory, without however going into details of calculation, since most of the results of this section were already reported in ([1]) and ([7]). A nuclear form factor R is defined as the ratio between the scattering by a nucleus with Z protons and $A-Z$ neutrons and the scattering by a point charge Ze. The form factor R is the sum of a coherent contribution C and an incoherent contribution J. Since we are interested in the summed transition probability over all excited nuclear levels we employ a closure approximation. The validity of the approximation for high energy scattering was checked in detail in ([1]) by a comparison with calculations performed in particular cases without the use of such an approximation ([10]). The

([8]) J. A. MCINTYRE and S. DHAR: *Phys. Rev.*, **106**, 1047 (1957).
([9]) S. D. DRELL and C. L. SCHWARTZ: *Phys. Rev.*, **112**, 568 (1958).
([10]) E. AMALDI, G. FIDECARO and F. MARIANI: *Nuovo Cimento*, **7**, 553 (1950).

form factors R can then be written as the mean value in the nuclear ground state of

$$(1) \qquad Z^{-2} \sum_{jl} \Gamma_{jl} \exp[i\boldsymbol{q}\cdot\boldsymbol{r}_{jl}] ,$$

where: $\boldsymbol{q}$ is the momentum transfer in the scattering process, $\boldsymbol{q} = \boldsymbol{p}_f - \boldsymbol{p}_i$ with $\boldsymbol{p}_f$ and $\boldsymbol{p}_i$ the final and initial electron momenta resepctively; $\boldsymbol{r}_{jl}$ is the relative co-ordinate of the l-th nucleon relative to the j-th one, and Γ_{jl} is unity when j and l are both protons, and zero in the other cases. It will be convenient in the following to regard Γ_{jl} as a projection operator in isotopic spin space. As in reference ([7]) the nuclear ground state is expanded as a sum of a ground configuration in which the nucleons occupy all the states inside the Fermi sphere, and of excited configurations for which individual states of the Fermi sphere are replaced by holes and correspondingly excited individual states are occupied. The major contributions to the incoherent form factor are due to the terms independent of the nuclear interaction. For large momentum transfers the whole approach would however be inadequate if the nuclear interaction is assumed to have a rigid repulsive core. It is known that different treatments may be applied to deal with such a situation. It must still be true, however, that, in the limit of large momentum transfers, effects produced directly from the binding nuclear forces shall disappear. In this limit the nucleus will scatter as an assemblage of Z independent protons and $A-Z$ independent neutrons. Furthermore, the rigid core model will not certainly reflect the true situation if the exploring wavelengths are capable to penetrate inside the core itself. One also expects specific mesonic effects to be already important at such wavelenghts, to change drastically the picture with a rigid core interaction. We assume explicitly that only two-body forces between nucleons are effective. In such a model the only excited configurations that may appear differ from the ground configuration only in the replacement of two of its individual states by two other individual states not already contained in the ground configuration. Very accurate methods of calculation are now available for the coherent contribution in the static approximation ([11]). The subtraction of such a contribution can easily be performed by considering the Z dependence. It is easily seen that there are no coherent contributions linear in the nuclear interaction. In fact such contributions would originate from terms in the total charge density which are linear in the nuclear interaction. Such terms would be given by integrals, over all the co-ordinates of all nucleons except one, of the product of the representatives of the ground configuration and of an excited configuration. However in the ground configu-

([11]) See for instance: L. I. Schiff: *Phys. Rev.*, **103**, 443 (1956); D. R. Yennie, D. G. Ravenhall and J. Tiemann: to be published.

ration there are two states different from those of the excited configuration, and thus any such integral is necessarily zero. In consequence of this result we can say that all terms linear in the nuclear interaction which contribute to the mean value of (1) in the nuclear ground state are of incoherent nature. We indicate by $J^{(1)}$ the contribution of such terms, that shall be evaluated at a fixed momentum transfer.

The main contribution is still expected to arise from the zero order term $J^{(0)}$. One may note that only one nuclear parameter having the dimensions of a length, namely the nuclear radius, or, equivalently, the mean nuclear separation, may appear in such approximation. The relevant role is indeed played by the angle η given by

$$\sin\frac{\eta}{2}=\frac{p_F}{p_i}\,, \tag{2}$$

where p_F is the Fermi momentum. In terms of the nuclear radius $r_0A^{\frac{1}{3}}$, and of the wavelength λ of the incident particle one has

$$\sin\frac{\eta}{2}=\left(\frac{9\pi}{4}\,\frac{Z}{A}\right)^{\frac{1}{3}}\frac{\lambda}{r_0}\,. \tag{3}$$

The physical meaning of the angle η is that at angles greater than η the restrictive effect of the exclusion principle to the scattering process is absent. In fact as evident from (2), for angles greater than η the nucleon struck aquires a sufficient recoil to escape from the Fermi sphere. In terms of the variable

$$\xi=\frac{\sin(\theta/2)}{\sin(\eta/2)}\,, \tag{4}$$

the incoherent form factor is expressed by

$$J^{(0)}=Z^{-1}(-\tfrac{1}{2}\,\xi^3+\tfrac{3}{2}\,\xi)\,, \tag{5}$$

for $\xi\leqslant 1$, and is constant

$$J^{(0)}=Z^{-1}\,, \tag{5'}$$

for $\xi\geqslant 1$. Let us assume for simplicity a nuclear potential of the form [12]

$$J_0v(r)O=J_0v(r)\{a_0+a_\sigma(\boldsymbol{\sigma}_1\cdot\boldsymbol{\sigma}_2)+a_\tau(\boldsymbol{\tau}_1\cdot\boldsymbol{\tau}_2)+a_{\sigma\tau}(\boldsymbol{\sigma}_1\cdot\boldsymbol{\sigma}_2)(\boldsymbol{\tau}_1\cdot\boldsymbol{\tau}_2)\}\,. \tag{6}$$

---

[12] L. Rosenfeld: *Nuclear forces* (Amsterdam, 1948), p. 160.

The mean value of (1) can be evaluated by standard techniques. One finds for $J^{(1)}$

$$(7)\qquad Z^2J^{(1)} = 4MJ_0 \sum_{b_1b_2}\sum_{d_1d_2}[b_1^2+b_2^2-d_1^2-d_2^2]^{-1}\langle b_1b_2|\cos q\cdot r|d_1d_2\rangle\cdot$$
$$\cdot[\langle b_1b_2|v(r)|d_1d_2\rangle \operatorname{Tr}[O\Gamma] - \langle b_1b_2|v(r)|d_2d_1\rangle \operatorname{Tr}[OP_\sigma P_\tau\Gamma],$$

where the momenta b are all contained in the Fermi sphere, while d are momenta not contained in the Fermi sphere. In (7) M is the nucleon mass, P_σ is the spin exchange operator and P_τ is the isotopic spin exchange operator. By evaluating explicitly the matrix elements in (7) and introducing the variables

$$(8)\qquad x = \frac{q}{p_F}, \qquad y = p_F r.$$

one can write (7) in the form

$$(9)\qquad ZJ^{(1)} = \frac{1}{2}(MJ_0r_0^2)\frac{1}{6\pi^5}\left(\frac{9\pi}{8}\right)^{\frac{1}{3}}\left(\frac{A}{2Z}\right)^{\frac{4}{3}}\cdot$$
$$\cdot\int dy \exp[ix\cdot y]f(y)\{G(x,y)\operatorname{Tr}[0P_\sigma P_\tau\Gamma] - G(x,0)\operatorname{Tr}[0\Gamma]\},$$

where

$$(10)\qquad f(y) = v\left(\frac{y}{p_F}\right).$$

The kernel function $G(x, y)$ expresses the kinematics of the system. It can be defined most simply by the following integral representation

$$(11)\qquad G(x,y) = \int_0^\infty d\omega \exp[-\omega x^2]F(\omega, x, y)F^*(\omega, -x, y),$$

where

$$(12)\qquad F(\omega, x, y) = \int dz \exp[(\omega x - iy)\cdot z],$$

the integration being extended to all those z that satisfy the two conditions

$$(13)\qquad |z|<1, \qquad |z-x|>1.$$

3. – Evaluation of the formulae.

The appearance of the function $G(\boldsymbol{x}, \boldsymbol{y})$ is typical of problems involving correlations between fermions of a degenerate system. In particular $G(\boldsymbol{x}, 0)$ essentially appears in a second order binding energy calculation for a degenerate fermion gas. Indeed it can be shown that the expression of $G(\boldsymbol{x}, 0)$ can be reduced to an integral already evaluated by Euler in his second order binding energy calculations ([13]). One finds in terms of the variable ξ of Eq. (4), which is equal to $\frac{1}{2}x$,

$$(14)\qquad G(\boldsymbol{x}, 0) - \frac{2\pi^2}{15}\left[\left(\frac{4}{\xi} + \frac{15}{2} - 5\xi^2 + \frac{3}{2}\xi^4\right)\log(1+\xi) + 29\xi - 3\xi^3 + \right.$$

$$\left. + \left(\frac{4}{\xi} - \frac{15}{2} + 5\xi^2 + \frac{3}{2}\xi^4\right)\log(1-\xi) - 40\xi\log 2\right], \quad \text{for} \quad \xi \leqslant 1,$$

$$(14')\qquad = \frac{2\pi^2}{15}\left[\left(\frac{4}{\xi} - 20\xi - 20\xi^2 + 4\xi^4\right)\log(\xi+1) + 4\xi^2 + 22 + \right.$$

$$\left. + \left(-\frac{4}{\xi} + 20\xi - 20\xi^2 + 4\xi^2\right)\log(\xi-1) + (40\xi^2 - 8\xi^4)\log\xi\right]. \qquad \text{for } \xi \geqslant 1.$$

It can be verified that the two expressions (14) and (14′) and their derivatives are continuous at $\xi = 1$.

To evaluate (9) one has than essentially to evaluate the functional

$$(15)\qquad \mathcal{G}[f] = \int \mathrm{d}\boldsymbol{y} \exp[i\boldsymbol{x}\cdot\boldsymbol{y}]\, G(\boldsymbol{x}, \boldsymbol{y}) f(y)\,;$$

which can be written in the form

$$(16)\qquad \mathcal{G}[f] = \int \mathrm{d}\boldsymbol{y}\, \mathrm{d}\boldsymbol{z}\, \mathrm{d}\boldsymbol{z}'\, f(y)[\boldsymbol{x}(\boldsymbol{x} - \boldsymbol{z} + \boldsymbol{z}')]^{-1} \exp[i(\boldsymbol{x} - \boldsymbol{z} + \boldsymbol{z}')\cdot\boldsymbol{y}]\,,$$

over all values of $\boldsymbol{y}$ and all $\boldsymbol{z}$ and $\boldsymbol{z}'$ that satisfy the limitations

$$(17)\qquad |\boldsymbol{z}| < 1, \quad |\boldsymbol{z}'| < 1, \quad |\boldsymbol{z} - \boldsymbol{x}| > 1, \quad |\boldsymbol{z}' + \boldsymbol{x}| > 1\,.$$

([13]) H. Euler: *Zeits. f. Phys.*, **105**, 553 (1937).

It will be convenient to use instead of the variables $\boldsymbol{z}$ and $\boldsymbol{z}'$ the variables $\boldsymbol{s}$ and $\boldsymbol{t}$ defined by the relations

(18) $$\boldsymbol{z} = \boldsymbol{t} - \tfrac{1}{2}(\boldsymbol{s} - \boldsymbol{x}) ,$$

(18′) $$\boldsymbol{z}' = \boldsymbol{t} + \tfrac{1}{2}(\boldsymbol{s} - \boldsymbol{x}) .$$

In terms of such variables one has

(19) $$\mathcal{G}[f] = \int \mathrm{d}\boldsymbol{s}\,\mathrm{d}\boldsymbol{t}\,\mathrm{d}\boldsymbol{y} f(y)(\boldsymbol{x}\cdot\boldsymbol{s})^{-1} \exp[i\boldsymbol{s}\cdot\boldsymbol{y}] ,$$

over all $\boldsymbol{s}$ and $\boldsymbol{t}$ that satisfy

(20) $$\pm \boldsymbol{t}^2 + |\boldsymbol{t}\cdot(\boldsymbol{s} \mp \boldsymbol{x})| \pm \tfrac{1}{4}|\boldsymbol{s} \mp \boldsymbol{x}|^2 < \pm 1$$

for the two choices of the signs. Integrating over angles one finds

(21) $$\mathcal{G}[f] = 8\pi^2 x^{-1} \int \mathrm{d}s\ \mathrm{tg}\,\gamma\,\mathrm{d}\gamma \tilde{f}(s) \int \mathrm{d}\boldsymbol{t} ,$$

where

(22) $$\tilde{f}(s) = \int_0^\infty \mathrm{d}y f(y) y \sin sy ,$$

and

(23) $$xs\ \mathrm{tg}\,\gamma = \boldsymbol{x}\boldsymbol{s} .$$

The last factor in (21) can be written in the form

(24) $$\int \mathrm{d}\boldsymbol{t} = -\frac{4}{3}\int_{C_+} \nabla\cdot(\boldsymbol{u} g(u^2))\ \mathrm{d}^2\boldsymbol{u} + \frac{4}{3}\int_{C_-} \nabla\cdot(\boldsymbol{u} g(u^2))\ \mathrm{d}^2\boldsymbol{u} ,$$

where $g(a) = a^{-1}(1-a)^{\frac{3}{2}}$ for $a < 1$ and $g(a) = 0$ for $a > 1$, and $C_\pm$ are triangular regions defined by the limitations

(25) $$\pm \tfrac{1}{2}x^2 + \boldsymbol{u}\cdot\boldsymbol{x} > 0 , \qquad \pm \tfrac{1}{2}s^2 \mp \boldsymbol{u}\cdot\boldsymbol{s} > 0 , \qquad \pm \boldsymbol{u}(\boldsymbol{s} \mp \boldsymbol{x}) - \tfrac{1}{2}|\boldsymbol{s} \mp \boldsymbol{x}|^2 > 0 .$$

The upper choice of the signs holds for C_+, the lower choice for C_-. Using Green's theorem one can finally write

(26) $$\mathcal{G}[f] = \frac{32\pi^2}{3x} \int_{l(x)}^{x+1} \mathrm{d}s \tilde{f}(s)\, \mathcal{L}(x, s) ,$$

where the lower limit $l(x)$ is zero for $x < 2$ and $x - 2$ for $x > 2$. The kernel $\mathcal{L}(x, s)$ is given by

$$\mathcal{L}(x, s) = \mathrm{P}\int_0^{\pi} \mathrm{tg}\,\alpha\,\mathrm{d}\alpha\, h(x, s, \alpha)\,, \tag{27}$$

where P denotes principal part and $h(x, s, \alpha)$ is given by

$$h(x, s, \alpha) = |\boldsymbol{s} - \boldsymbol{x}| \int_0^{a} g\left(\omega^2 + \frac{1}{4}|\boldsymbol{s} - \boldsymbol{x}|^2\right) \mathrm{d}\omega + s\int_0^{b_2} g\left(\omega^2 + \frac{1}{4}\, s^2\right) \mathrm{d}\omega + \tag{28}$$

$$+ x\int_0^{b_2} g\left(\omega^2 + \frac{1}{4}\, x^2\right) \mathrm{d}\omega\,,$$

with $a = \frac{1}{2}|\boldsymbol{s} - \boldsymbol{x}|\,\mathrm{ctg}\,\alpha$, $b_1 = (2\sin\alpha)^{-1}(x - s\cos\alpha)$, $b_2 = (2\sin\alpha)^{-1}(s - x\cos\alpha)$, α being the angle between $\boldsymbol{s}$ and $\boldsymbol{x}$.

The calculation of $\mathcal{L}(x, s)$ from (27) and (28) is now straigthtforward but very lengthy. We reproduce in the Appendix some of the steps involved and the final expressions for $\mathcal{L}(x, s)$ for the different ranges of values of the variables.

4. – Numerical applications.

From the definition of the projection operator Γ it can be shown that a trace of a product of a spin operator S, an isotopic spin operator T, and Γ, can be reduced according to

$$\mathrm{Tr}\,[STI\Gamma] = \langle T\rangle_{\text{triplet}}\,\mathrm{Tr}\,[S]\,, \tag{29}$$

where $\langle T\rangle_{\text{triplet}}$ is the mean value of T in a triplet isotopic spin state and $\mathrm{Tr}\,[S]$ is evaluated in the 4-dimensional spin subspace. From (29) it follows

$$\mathrm{Tr}\,[OP_\sigma P_\tau \Gamma] = 2(a_0 + a_\tau) + 6(a_\sigma + a_{\sigma\tau})\,, \tag{30}$$

$$\mathrm{Tr}\,[O\Gamma] = 4(a_0 + a_\tau)\,. \tag{30'}$$

In the choice of the parameters a of the nuclear interaction (6) we shall try to satisfy, on reasons of internal consistency of the model, those restrictions

which follow for the same model from the general properties of heavy nuclei ([14]). It can be seen that the necessary saturation condition by Breit and Wigner implies that $\mathrm{Tr}[O\Gamma] > 0$. From this same condition, together with the Breit-Wigner condition for the stability of isobars and with Volz's condition for α-nuclei it follows similarly that $\mathrm{Tr}[OP_\sigma P_\tau \Gamma] \geqslant 0$. Furthermore all such conditions imply $a_0 \cong 0$ and $a_\sigma \cong 0$. The remaining coefficients a_τ and $a_{\sigma\tau}$ are taken to satisfy the normalization condition

$$a_\tau + a_{\sigma\tau} = \tfrac{1}{3} ,$$

which is equivalent to define $J_0 r(r)$ as the absolute value of the effective ^3S potential. For the ratio $a_\tau/a_{\sigma\tau}$ we shall assume the choice $a_\tau \cong 0.1$, $a_{\sigma\tau} \cong 0.23$ ([14]). For such a choice $\mathrm{Tr}[O\Gamma] = 0.4$ and $\mathrm{Tr}[OP_\sigma P_\tau \Gamma] = 1.58$. The graphs reported in Fig. 2 were calculated with a potential of the form

$$J_0 v(r) = J_0 a r^{-1} \exp\left[-\frac{r}{a}\right] , \tag{31}$$

with $a = 1.4 \cdot 10^{-13}$ cm. For such a choice J_0 can be fixed from the proton-neutron triplet S scattering data and is found to be $\cong 51$ MeV. The graphs were calculated for such a choice of the parameters and for $r_0 = 1.2 \cdot 10^{-13}$ cm. It was also supposed that $Z = \frac{1}{2}A$: a smaller value of Z would lead to values for the form factors slightly smaller.

The asymptotic behaviour of $G(\boldsymbol{x}, \boldsymbol{y})$ for large $\boldsymbol{x}$ can be most easily derived directly from the original definition (11). For $|\boldsymbol{x}| > 2$ the second of the conditions (13) holds as a consequence of the first one. One then finds for large $|\boldsymbol{x}|$

$$G(\boldsymbol{x}, \boldsymbol{y}) \to \frac{1}{x^2} \left| \int \mathrm{d}\boldsymbol{z} \exp\left[-i\boldsymbol{z}\cdot\boldsymbol{y}\right] \right|^2 = \left(\frac{4\pi}{x}\right)^2 \left(\frac{1}{y} j_1(y)\right)^2 , \tag{32}$$

where j_1 is a spherical Bessel function. From (32)

$$\mathcal{G}[f] \to \left(\frac{4\pi}{x}\right)^2 \int \mathrm{d}\boldsymbol{y} \exp\left[i\boldsymbol{x}\cdot\boldsymbol{y}\right] f(y) y^{-2} j_1(y)^2 , \tag{33}$$

For large $|\boldsymbol{x}|$ the last expression is essentially

$$\frac{1}{9}\left(\frac{4\pi}{x}\right)^3 \tilde{f}(x) , \tag{34}$$

([14]) L. Rosenfeld: *Nuclear forces* (Amsterdam, 1948), p. 224.

where f has already been defined in (22). The resulting asymptotic limit for the incoherent form factor is then

$$ZJ \to 1 + \tilde{f}(x)x^{-3}\frac{16}{27\pi^2}(MJ_0r_0^2)\left(\frac{9\pi}{8}\right)^{\frac{1}{3}}\left(\frac{A}{2Z}\right)^{\frac{2}{3}}\mathrm{Tr}\,[0(P_\sigma P_\tau - 1)\Gamma]\,. \tag{35}$$

Eq. (35) exhibits clearly the dependence of the incoherent form factor on the Fourier transform of the potential for large momenta. By direct comparison with the exact calculations we have checked that for the potential (31), the approximate form (35) is a reliable approximation of the incoherent form factor for all momentum transfers $|\boldsymbol{q}|$ greater than $2p_F$. Asymptotic expansions for $\mathcal{G}[f]$ and $G(\boldsymbol{x}, 0)$ for small momentum transfers can be obtained directly from the explicit expressions given in the Appendix and from (14). We find, for small x,

$$\mathcal{G}[f] \to x4\pi^3\int_0^2 f(\omega)\left(1 - \frac{1}{\omega}\left(1 - \frac{\omega^2}{4}\right)\log\frac{1+\omega/2}{1-\omega/2}\right)\mathrm{d}\omega\,. \tag{36}$$

$$G(\boldsymbol{x}, 0) \to x\frac{8\pi^2}{3}(1 - \log 2)\,. \tag{37}$$

Comparing with the exact expressions, we propose that (36) and (37) may be used as sufficient approximations for momentum transfers $|\boldsymbol{q}| < p_F$. To obtain an idea of the effect of a strong modification of the potential on the incoherent form factor at low momentum transfers we have considered the effect of adding a short range Yukawa term to the potential (31). Taking a potential

$$J_0 a r^{-1}\exp\left[-\frac{r}{a}\right] + J_1 b r^{-1}\exp\left[-\frac{r}{b}\right], \tag{38}$$

with a as before $= 1.4\cdot10^{-13}$ cm and $b = 0.5\cdot10^{-13}$ cm we find that $J^{(1)}$ is modified by the appearance of a factor

$$1 + 0.04\,(J_1/J_0)\,. \tag{39}$$

From (39) one sees that only a very large value of J_1 would lead to a sensible modification. To exhibit explicitly in the general case the dependence of the form factor on the Fourier transform of the potential we report here the approximate expression for the incoherent cross-section obtained through (36) and (37)

$$ZJ \cong \frac{3}{4}x + \frac{1}{9\pi^2}(MJ_0r_0^2)\left(\frac{9\pi}{8}\right)^{\frac{1}{3}}\left(\frac{A}{2Z}\right)^{\frac{2}{3}}\left\{\frac{1}{2}\int_0^2\tilde{f}(\omega)\omega^2\,\mathrm{d}\omega\,\mathrm{Tr}\,[0P_\sigma P_\tau\Gamma] - \right. \tag{40}$$

$$\left. - 8(1 - \log 2)x^{-1}\tilde{f}(x)\,\mathrm{Tr}\,[0\Gamma]\right\}x\,.$$

Eq. (40) should hold as a good approximation for momentum transfers $|\boldsymbol{q}| < p_F$. Specific mesonic effects should not alter very much the results. On the other hand the result (40) may be a little altered by the inclusion of surface effects, not properly treated in the present model, which essentially replaces the problem of scattering by a finite nucleus with that of scattering by an equivalent finite portion of an infinite nuclear medium. Of course such effects will mainly be felt in the coherent contribution, not discussed in this paper. However in the limits of long wavelengths they might influence also the incoherent terms.

* * *

The author would like to thank Prof. M. Picone and Dr. W. Gross of the Istituto Nazionale per le Applicazioni del Calcolo, where most of the computations were performed. He would also like to thank Dr. D. Judd and Dr. B. Curtis of the Radiation Laboratory in Berkeley for allowing him the use of the computational facilities of that laboratory.

Appendix

It is evident from (27) and (28) that $\mathcal{L}(x, s)$ is symmetric in x and s. To evaluate $h(x, s, \alpha)$ from (28) we need the following integrals:

$$(A.1)\quad 2m\int_0^c g(\omega^2+m^2)\,\mathrm{d}\omega = -mc(1-m^2-c^2)^{\frac{1}{2}} - m(3-m^2)\operatorname{arctg}[c(1-m^2-c^2)^{-\frac{1}{2}}] + \\ + 2\operatorname{arctg}[cm^{-1}(1-m^2-c^2)^{-\frac{1}{2}}], \qquad \text{for } c^2+m^2<1;$$

$$(A.2)\quad 2m\int_0^c g(\omega^2+m^2)\,\mathrm{d}\omega = \frac{1}{2}(2-3m+m^3)\pi\varepsilon(c), \\ \text{for } c^2+m^2>1,\ m>1, \text{ with } \varepsilon(c)=c/|c|;$$

$$(A.3)\quad 2m\int_0^c g(\omega^2+m^2)\,\mathrm{d}\omega = 0. \qquad \text{for } m>1.$$

Using the above expressions one finds for x or $s>2$

$$(A.4)\quad \frac{1}{\pi}\mathcal{L}(x, s) = \frac{1}{3}\left(1-\frac{1}{2}|x-s|\right)\left[8-(x^2+s^2)+\frac{1}{2}xs-\frac{1}{2}|x-s|\right] + \\ -\frac{1}{2}(x^2+s^2)^{\frac{1}{2}}\left[3-\frac{1}{4}(x^2+s^2)\right]\left[\log(x^2+s^2+2)^{\frac{1}{2}} - \log\left((x^2+s^2)^{\frac{1}{2}}+|x-s|\right)\right] + \\ +\left[1-\frac{1}{4}(x^2+s^2)^{\frac{1}{2}}\left(3-\frac{1}{4}(x^2+s^2)\right)\right][\log 2sx - \log(x^2+s^2-4)].$$

To evaluate $\mathcal{L}(x, s)$ for x and $s < 2$ one similarly substitutes (A.1)-(A.3) into (28). It can be shown that the calculation can then be reduced to rational integrals which are readily evaluated and to integrals of the form

$$\int_0^\infty \log\left|\frac{\chi + \xi u^2}{\eta + \zeta u^2}\right| du = \frac{\pi}{\sqrt{\eta\zeta}} \log\left(\chi^{\frac{1}{2}} + (\xi\eta)^{\frac{1}{2}}\zeta^{-\frac{1}{2}}\right), \qquad \text{for } \chi > 0,$$

$$= \frac{\pi}{2\sqrt{\eta\zeta}} \log\left(-\chi + \xi\eta\zeta^{-1}\right), \qquad \text{for } \chi < 0,$$

with ξ, η, ζ all positive numbers. The final expression for x and $s < 2$ can then be written in the form

$$\text{(A.5)} \qquad \frac{1}{\pi}\mathcal{L}'(x, s) = \mathcal{L}'(x, s) + \mathcal{L}''(x, s) + \mathcal{L}'''(x, s),$$

where

$$\mathcal{L}'(x, s) = 0, \qquad \text{for } s < 2 - x,$$

$$\mathcal{L}'(x, s) = \tfrac{1}{3}[\tfrac{1}{2}(x + s) - 1][8 - (x^2 + s^2) - \tfrac{1}{2}xs - \tfrac{1}{2}(x + s)] = \mathcal{P}(x, s), \qquad \text{for } 2 - x < s < \sqrt{4 - x^2},$$

$$\mathcal{L}'(x, s) = \mathcal{P}(x, s) + \tfrac{1}{4}xs\sqrt{x^2 + s^2 - 4}, \qquad \text{for } \sqrt{4 - x^2} < s < 2,$$

$$\mathcal{L}''(x, s) = \mathcal{M}(x, s) \log\left(\sqrt{x^2 + s^2} + 2\right) + \mathcal{N}(x, s) \log\left(4 - x^2 - s^2\right), \quad \text{for } s < 2 - x,$$

$$\mathcal{L}''(x, s) = \mathcal{M}(x, s) \log\left(\sqrt{x^2 + s^2} + x + s\right) + \mathcal{N}(x, s) \log 2xs, \quad \text{for } 2 - x < s < 2,$$

where $\mathcal{M}(x, s) = -\tfrac{1}{2}\sqrt{x^2 + s^2}\,[3 - \tfrac{1}{4}(x^2 + s^2)]$,

$\mathcal{N}(x, s) = -\left\{1 - \tfrac{1}{4}\sqrt{x^2 + s^2}\,[3 - \tfrac{1}{4}(x^2 + s^2)]\right\}$,

$$\mathcal{L}'''(x, s) = 2 \log 2 + \mathcal{R}(x) + \mathcal{R}(s), \qquad \text{for } s < \sqrt{4 - x^2},$$

with $\mathcal{R}(t) = \left(1 + \frac{t}{2}\right)^2\left(1 - \frac{t}{4}\right) \log\left(1 + \frac{t}{2}\right) + \left(1 - \frac{t}{2}\right)^2\left(1 + \frac{t}{4}\right) \log\left(1 - \frac{t}{2}\right)$,

$$\mathcal{L}'''(x, s) = \mathcal{S}^{(-)}(x, s) + \mathcal{S}^{(+)}(x, s) + 2\beta \log\left[\tfrac{1}{2}xs + \sqrt{x^2 + s^2 - 4}\right], \qquad \text{for } \sqrt{4 - x^2} < s < 2,$$

where

$$\mathcal{S}^{(\pm)}(x, s) = \tfrac{1}{2}|x \pm s|[3 - \tfrac{1}{4}(s^2 \mp sx + x^2)] \log [1 + \tfrac{1}{2}\, x \pm s \mp \tfrac{1}{2}\sqrt{x^2 + s^2 - 4}]\,,$$

$$\beta = \left(1 - \frac{x}{2}\right)^2 \left(1 + \frac{x}{4}\right), \qquad \text{for } s < x,$$

$$= \left(1 - \frac{s}{2}\right)^2 \left(1 + \frac{s}{4}\right), \qquad \text{for } s > x.$$

RIASSUNTO

Viene svolto uno studio dettagliato sugli effetti di correlazione nucleone-nucleone nella diffusione anelastica di elettroni d'alta energia di nuclei sommando sugli stati d'eccitazione del nucleo. Si trova che l'effetto di correlazione dominante è quello originato dal principio di esclusione e la sezione d'urto differenziale può venire abbastanza accuratamente calcolata indipendentemente dai dettagli della dinamica nucleare.

LETTERE ALLA REDAZIONE

(La responsabilità scientifica degli scritti inseriti in questa rubrica è completamente lasciata dalla Direzione del periodico ai singoli autori)

Air Radioactivity in Catania.

B. Cantone, G. Pappalardo and R. Ricamo

Centro Siciliano di Fisica Nucleare
Istituto di Fisica dell'Università - Catania

(ricevuto il 2 Gennaio 1959)

Measurements of air radioactivity have been made using the method of dust collection by air filtration followed by measurements of the β-activity of the filter deposits. Such method has been fully illustrated by several authors [1-3].

Two sets of samples were taken: the first « short » 500 litres pumpings in 10 min, the second with (10÷60) m³ in periods of the order of hours, both for outside air and the air of enclosed spaces.

Mica-window GM counters, Philips 18505, 2.4 mg/cm², were used. β-rays self absorption in W41 filters has been determined with the incineration method. A value of 15% has been obtained.

To identify the radioactive isotopes, collected on the filter, measurements of decay were made (Fig. 1, 2), followed by measurements of β absorption to determine the maximum energy of the emitted β.

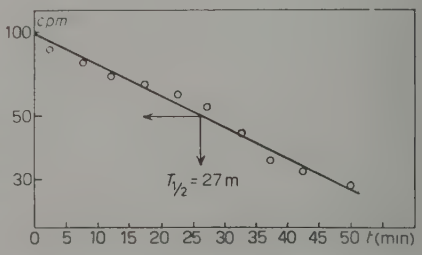

Fig. 1. – Decay of radioactive deposit obtained from inside air 10 min (500 litre) filtering, showing the presence of RaB ($T_{\frac{1}{2}}$ = 27 m).

Some decay products of radon and thoron were thus detected and their concentration determined.

(1) F. Barreira and M. Laronjeira: *Proc. of the Intern. Conf. on Peaceful Uses of Atomic Energy*, **9**, 756 (1955).

(2) A. Malvicini and C. Polvani: *Energia Nucleare*, **4**, 363 (1957); *Minerva Nucleare*, **10**, 261 (1958).

(3) L. Daddi *et al.*: *Ric. Scient.*, **27**, 3313 (1957).

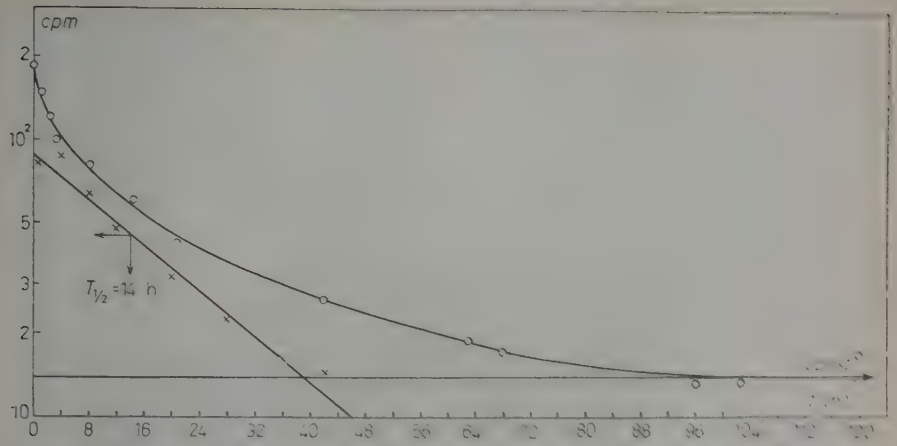

Fig. 2. - Decay of radioactive deposit obtained from open air (20 h, 60 m³) filtering., showing the presence of Tn products.

1. – Open air radioactivity.

The 500 litres, 10 min samples, taken at 10 metres from ground level for several days at intervals of a few hours show typical daily variations, with a period of 24 hours and a maximum which was usually observed at about 04.00 hrs (Fig. 3).

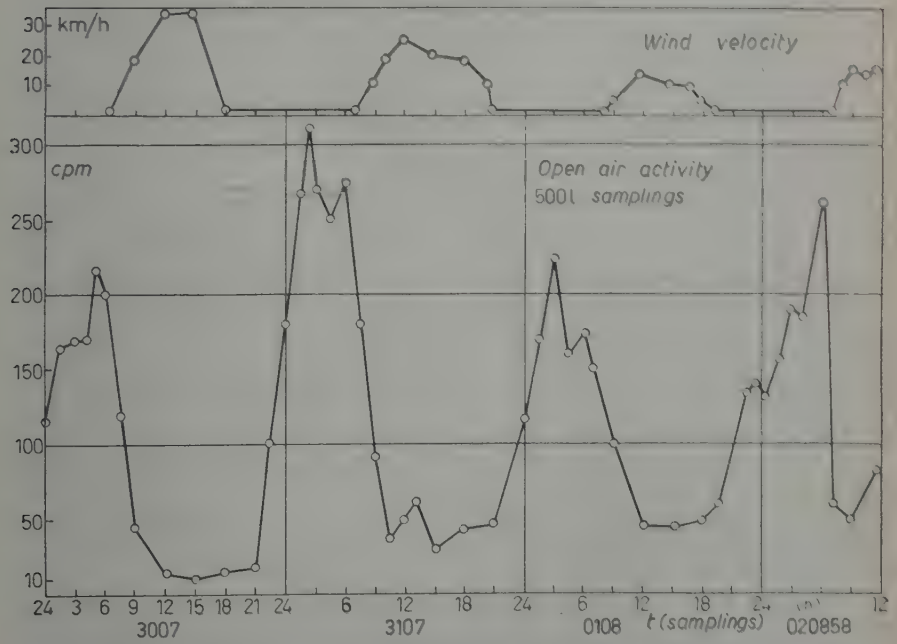

Fig. 3. – Open air β radioactivity and wind velocity at Catania in July-August 1958.

Comparing the values of air activity measured at different times, a noticeable correlation was observed between maximum radioactivity and minimum wind speed (*).

A ratio greater than 10 was frequently observed between maximum and minimum daytime activity in Catania.

that in general any assignment of the typical value of air radioactivity for a given area requires standard samples, taken at 2 hours intervals for several days and at different times of the year.

From the analysis of the decay of the radioactive products settled on filter using short (10 min) filtering, it has been

TABLE I. – *Minima and maxima concentrations of* Rn, Tn *and fission products (curies/litre) for various air samplings.*

		Outside samples		Inside samples	
		Short 500 litres	Long	Short 500 litres	Long
Rn products	min	$1.68 \cdot 10^{-13}$	$3.5 \cdot 10^{-13}$	$47 \cdot 10^{-13}$	$114 \cdot 10^{-13}$
	max	$52 \cdot 10^{-13}$	$14.2 \cdot 10^{-13}$	$220 \cdot 10^{-13}$	$179 \cdot 10^{-13}$
Tn products	min	—	$0.46 \cdot 10^{-15}$	—	$9.3 \cdot 10^{-15}$
	max	—	$5.2 \cdot 10^{-15}$	—	$35 \cdot 10^{-15}$
Fission products	min	—	$1.3 \cdot 10^{-15}$	—	$0.61 \cdot 10^{-15}$
	max	—	$1.3 \cdot 10^{-15}$	—	$2.1 \cdot 10^{-15}$

Since mean air radioactivity is 1000 times lower above open seas than above continents (4), one can presume that similar marked differences in daytime air radioactivity variations, possibly due to a particularly strong washing action by the sea winds, can be observed in other places such as sea shores or great lakes.

From what has been said it appears possible to establish the presence of ^{214}Pb(RaB), and ^{214}Bi(RaC).

After taking into account the detector's efficiency and the self-absorption, measuring the aspirated air volume, and assuming the equilibrium of the radon products (5) present in the atmospherical dust, from the measured activity on the filter the following values have been obtained for air radioactivity in a large Mt. Etna area during summer months:

$$(2 \div 50) \cdot 10^{-13} \text{ curies/litre},$$

(*) The Authors wish to thank the Sicily Air Command for making available the meteorological data used in the present paper, which were collected by the Catania Meteorological Observatory A.F.

(4) E. PICCIOTTO: *Nuovo Cimento*, **11**, 190 (1958).

(5) G. ALIVERTI, A. DE MAIO, G. LOVERA, R. PERILLI FEDELI and L. SACCHETTI: *Nuovo Cimento*, **12**, 270 (1954); **10**, 68 (1958).

which are very near to the Central Europe mean values (6) and to those observed in Leghorn (3).

Similar measurements were made on Mt. Etna 2000 metres above sea level and outside the Catania area, yielding same mean concentrations for radon products.

To measure the concentration in the air of thoron products, « long » samples were made, with pumping times between 10 and 20 hours at 50 litres/min speed. The presence of the thoron products is clearly revealed by the decay curves (Fig. 2). Once the filter-saturation was reached, from measurements of decay and absorption, a concentration was derived for thoron products in the limits $(0.5 \div 5) \cdot 10^{-15}$ curies/litre.

The concentration of the radon products deduced from the activity of the « long » samples was the same as that obtained from the « short » samples.

A ratio of about 100 : 1 was found between concentrations of radon and thoron products in the outside air. This ratio was about constant for all samples.

An activity with half life of at least 20 days was found in the « long » samples. This could be traceable to artificial radioactivity from fission products. Outside air and enclosed space samples, between 14 and 40 m³, yielded the following values for artificial radioactivity concentration:

$$(1.2 \div 2) \cdot 10^{-15} \text{ curies/litre} .$$

2. – Enclosed space activity.

Because of the marked daytime variation observed in the radioactivity of the outside air, and in order to obtain a mean of reference for checking instruments and methods, the air activity in long-closed apartment rooms has been measured.

A mean radioactivity of $6 \cdot 10^{-13}$ curies/litre was found for inhabited rooms of average ventilation. This is to be ascribed to the radon radioactive products and in lesser measure to the thoron products.

In a hermetically closed room the activity is shown to rise and reach an equilibrium value in about 3 days (Fig. 4).

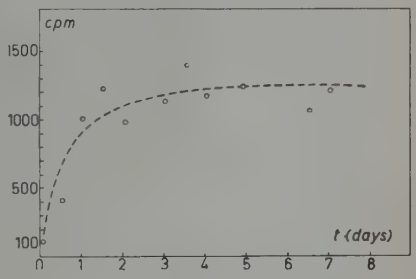

Fig. 4. – β radioactivity of the air from a closed 110 m³ room measured with 10 min sampling (500 litres) at different times after the closure.

This value is subject to fluctuation presumably in relation among other things to the mean temperature variations, and to strong winds (wall permeability and minor failures in the closing devices).

The measurements show that the maximum values of activity in 3 closed lecture rooms placed in 3 buildings in Catania up to 2 km apart and built at times separated by many decades are near to $2 \cdot 10^{-11}$ curies/litre.

The maximum allowed air radioactivity for Radon 222 at equilibrium with its products, for non professional individuals, is 10^{-11} curies/litre (7) but the measured air radioactivity in closed rooms

(6) Erster Bericht: *Sonderausschuß Radioaktivität* (Jan. 1958).

(7) AEC 1957; Nat. Bur. of Stand., Handb. 52 (1953).

at equilibrium in the Catania area is twice as great.

We are now attempting to discover what materials are responsible for this high radioactivity so as to discourage the use of them in buildings ([8]).

([8]) A. F. GABRYSH and F. J. DAVIS: *Nucleonics*, Jan. 50 (1955).

The radioactivity of air in a deep underground cavity digged in lava rock in Catania area is very near the minimum outside air activity.

It may be of interest here to note that in a closed apartment room in the town of Caltagirone (70 km from Catania) a measurement of only $7 \cdot 10^{-13}$ curies/litre at equilibrium was made.

DOMUS GALILÆANA

PISA - VIA S. MARIA, 18

È uscito il volume (19,5 cm × 26,5 cm):

CELEBRAZIONE
DELLA
ACCADEMIA DEL CIMENTO
NEL
TRICENTENARIO DELLA FONDAZIONE

Pisa, 19 Giugno 1957

Oltre a parole introduttive
di G. POLVANI, Presidente della Domus Galilaeana
il volume contiene:

6 Conferenze con numerose note bibliografiche (pag. 1-80),

G. ABETTI, dell'Università di Firenze
L'Accademia del Cimento

M. L. BONELLI, dell'Università di Firenze
Gli strumenti superstiti dell'Accademia del Cimento

A. PROCISSI, dell'Università di Firenze
I manoscritti superstiti dell'Accademia del Cimento

T. DERENZINI, dell'Università di Pisa
Giovanni Alfonso Borelli, fisico

L. BELLONI, dell'Università di Milano
Francesco Redi, biologo

B. NARDI, dell'Università di Roma
Significato del motto "provando e riprovando"

42 Tavole fuori testo,

4 Appendici con trascrizioni di manoscritti (pag. [a]-[u]).

Prezzo L. 3200

SOCIÉTÉ ITALIENNE DE PHYSIQUE

IL NUOVO CIMENTO

Fascicules spéciaux du SUPPLEMENTO aux volumes des séries IX^{ème} et X^{ème} du NUOVO CIMENTO

- **Comptes rendus de Colloques, Congrès, Conférences internationaux, organisés par la Société Italienne de Physique.**

Colloque International de Mécanique Statistique (Florence, 1949).
Congrès International sur les Rayons Cosmiques (Côme, 1949).
Colloque International sur les Ultrasons (Rome, 1950).
Colloque International d'Optique et Microondes (Milan, 1952).
Congrès International sur les particules instables lourdes et sur les événements de haute énergie dans les Rayons Cosmiques (Padoue, 1954).
Colloque International sur la Physique des solides et liquides (Varenna, 1954).
Colloque International d'études sur l'Infrarouge (Parme, 1954).
Conférence Internationale sur les particules élémentaires (Pise, 1955).
Colloque International des études sur l'ionosphère (Venise, 1955).
Colloque International sur les constantes fondamentales de la Physique (Turin, 1956).
Colloque International sur les rayons cosmiques (Varenna, 1957).
Colloque International sur l'état condensé de sistèmes simples (Varenna, 1957)

- **Cours tenus à Varenna à l'École internationale de Physique de la Société Italienne de Physique.**

Révélation des particules élémentaires, avec référence spéciale à la Radiation cosmique (Varenna, 1953).
Physique des particules élémentaires et machines accélératrices (Varenna, 1954).
Questions de Physique Nucléaire: structure et modèles du noyau, nouvelles espèces d'atomes (positronium, atomes mésiques), Optique neutronique, moments nucléaires, processus physiques du réacteur nucléaire (Varenna, 1955).
Propriétés magnétiques de la matière (Varenna, 1956).
Physique de l'état solide (Varenna, 1957).
Physique du plasma et applications astrophysiques (Varenna, 1958)*.
Theorie de l'information (Varenna, 1958)*.
Problemes mathématiques de la Théorie quantistique des particules et des champs (Varenna, 1958)*.
Physique des pions (Varenna, 1958)*.

* sous presse

- **Rapports sur des questions diverses de Physique.**

Premier, Deuxième, Troisième, Quatrième, Cinquième Rapport sur les travaux de Physique en Russie (1953, 1956).
MORPURGO et FRANZINETTI. *An Introduction to the Physics of the New Particles* (1957).

Pour les commandes s'adresser à
NICOLA ZANICHELLI - EDITORE
34, Via Irnerio - BOLOGNA

On the (γ, pn) Reaction in ^{32}S.

U. Farinelli, F. Ferrero, S. Ferroni, R. Malvano and E. Silva (*).

Istituto di Fisica dell'Università - Torino
Istituto Nazionale di Fisica Nucleare - Sezione di Torino

(ricevuto il 21 Gennaio 1959)

Recently the great importance has been pointed out of the (γ, pn) reactions in light nuclei specially in connection with the quasi-deuteron model (1) of the photonuclear reactions. Unfortunately there are only very few cases where it is possible to measure the (γ, pn) process through the residual activity method.

The ^{32}S nucleus is particularly favorable for this kind of research and actually it was the object of many earlier measurements (2-4), very carefully done especially in the threshold region. Now our interest in this case is confined in the energy region far above threshold and therefore we decided to extend the research up to the maximum X-ray energy available in this laboratory, that is, 33 MeV.

Together with the (γ, pn) process we have also measured the (γ, n) reaction and the fast neutron component, using the same experimental techniques described in ref. (5). The experimental results are collected in Table I while the cross-sections, calculated from the measured yields with the Penfold-Leiss (6) method, are shown in Fig. 1.

The results that can be emphasized are the following:

1) The (γ, pn) cross-section seems to present a maximum, very broad indeed, above 30 MeV, being this result in striking disagreement with the result of ref. (2) and (3).

(*) On leave of Universidade de S. Paulo, Brazil. Fellow of the Conselho Nacional de Pesquisas, Brazil.

(1) J. Levinger: *Phys. Rev.*, **84**, 43 (1951); K. G. Dedrick: *Phys. Rev.*, **100**, 58 (1955); K. Godtfried: *Nucl. Phys.*, **5**, 557 (1958).

(2) L. Katz and A. S. Penfold: *Phys. Rev.*, **81**, 815 (1951).

(3) L. Katz and A. G. W. Cameron: *Can. Journ. Phys.*, **29**, 518 (1951).

(4) S. S. Villaca and J. Goldemberg: *Anais Acad. Brazil. Cienc.*, **27**, 427 (1955); J. Goldemberg and L. Marquez: *Nucl. Phys.*, **7**, 202 (1958).

(5) F. Ferrero, R. Malvano, S. Menardi and O. Terracini: *Nucl. Phys.*, **9**, 33 (1958).

(6) A. S. Penfold and J. E. Leiss: *Analysis of Photonuclear Reactions*. Phys. Res. Lab. University of Illinois (Champaign, Ill.), May 1958.

TABLE I.

Reaction in ^{32}S	E_{max} (MeV)	I (MeV)	dis. cm²/mol. MeV	$\int_{30MeV}^{\infty} \sigma dE$ (MeV barns)
(γ, n)	$21 \pm .5$	6	$7.2 \cdot 10^{-5}$	0.093
(γ, pn)	> 30	—	$1.12 \cdot 10^{-5}$	0.028
$(\gamma, n) + (\gamma, pn)$	$21 \pm .05$	10.5	$8.32 \cdot 10^{-5}$	0.121
(γ, n)-fast ($E_n > 5.5$ MeV)	> 30	—	$1.91 \cdot 10^{-5}$	0.040

2) The (γ, n) contribution becomes very small at 30 MeV while the fast neutron component ($E_n > 5.5$ MeV), measured by a (n, p) silicon threshold detector, is of the same order of magnitude as the $[(\gamma, n)+(\gamma, np)]$ cross-section.

This last result is very peculiar and is difficult to be explained with a two step reaction [7], while it is more likely to be in agreement with a quasi-deuteron model. In order to put the argument on a quantitative basis other measurements are in progress in this laboratory.

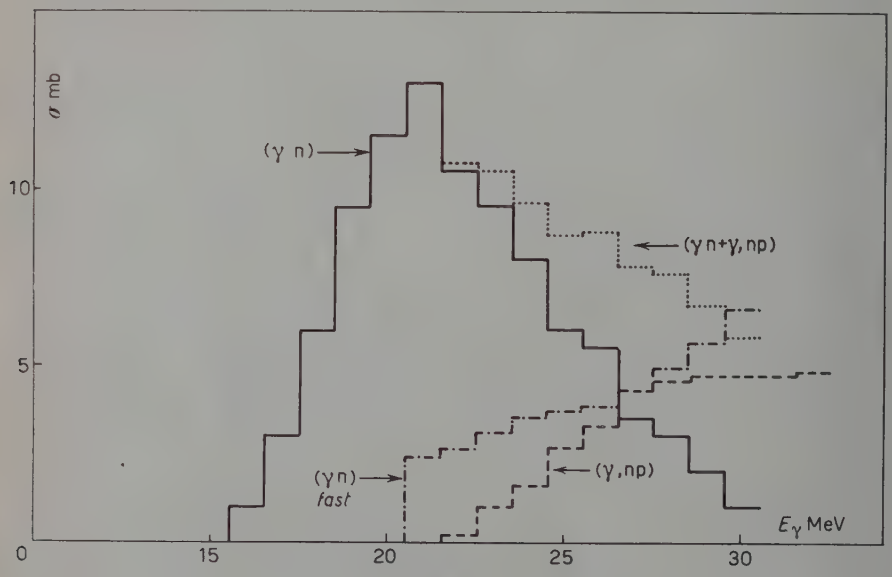

Fig. 1.

(7) A. HOFMAN and P. STOLL: *Helv. Phys. Acta*, **31**, 591 (1958).

IL NUOVO CIMENTO Vol. XII, N. 1 1° Aprile 1959

On the Observation of π-mesons Emitted in the Interaction in Emulsion of K^--mesons.

European Collaboration

M. C. Amerighi, F. Baldassare, M. Beniston, A. Bonetti, D. H. Davis, M. Di Corato, C. Dilworth, E. Ferreira (*), E. Frota-Pessoa (*), W. B. Lasich, N. Raina, M. René, J. Sacton and A. E. Sichirollo

Istituto di Fisica dell'Università - Bari
Laboratoire de Physique Nucléaire de l'Université Libre - Bruxelles
Physics Department of the University College - London
Istituto di Scienze Fisiche dell'Università - Milano
Istituto Nazionale di Fisica Nucleare - Sezione di Milano

(ricevuto l'8 Marzo 1959)

1. – Introduction.

In continuation of the work of the European Collaboration on K^- interactions at rest, a second stack has been exposed to a filtered K^- beam. This stack is of the Ilford K-5 emulsion, and presents certain advantages over the previous one for the study of fast particles, having larger dimensions, a slightly higher grain density and lower background fog.

In a preliminary survey of the material the percentage of lightly ionizing tracks observed in the K^- stars at rest appeared to be higher than in the previous work (1). This point was of immediate interest, since in the previous work two difficulties were encountered, which could be resolved if there had been a larger scanning loss of π-mesons than was estimated. These difficulties were:

1) The difficulty of attribution of about 400 out of 3024 events to either K^--N or K^--2N interactions.

2) The lack of very high energy π-mesons ($E \geqslant 100$ MeV) associated with direct production of Λ^0 hyperons in the reaction (K^-N, $\pi^-\Lambda^0$).

Four groups (Bari, Bruxelles, Milan, London) have therefore examined the question and this letter contains their preliminary results.

2. – Experimental method.

Grey tracks in the beam direction were picked up at about 1 cm from the entrance edge of the stack, and followed to their end. Those track endings falling

(*) On leave of absence from Pesquisas Fisicas, Rio de Janerio.

(1) G. Alexander *et al.* (European Collaboration): *Nuovo Cimento*, in press.

TABLE I.

(a)

Dip of π-meson	$0 \div 14.5°$	$14.5° \div 30°$	$30 \div 48.6°$	$48.6 \div 60°$
No. of events	117	104	123	58

(b)

Depth above glass of K^--stars containing a π-meson	$(50 \div 100)$ μm	$(100 \div 200)$ μm	$(200 \div 300)$ μm	$(300 \div 400)$ μm	$(400 \div 500)$ μm	$(500 \div 550)$ μm
No. of events	36	79	76	88	72	50

within 50 μm of either surface of the emulsion were discarded from the statistics.

Measurements of ionization and range were made on tracks with ϱ endings to separate $K\varrho$'s from protons.

1148 K^- interactions at rest were thus selected.

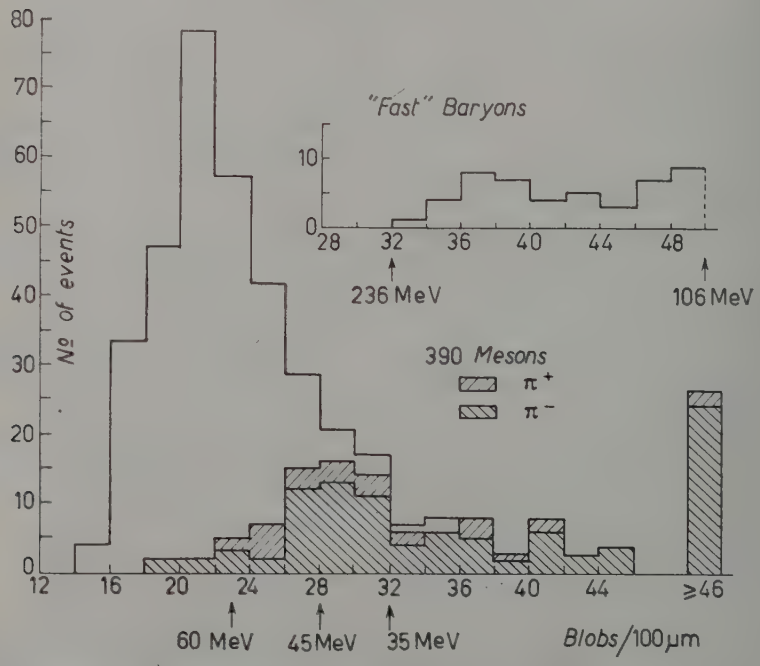

Fig. 1. – Distribution in blob density of π-mesons and «fast» baryons. All the tracks with blob density ≥ 28 blobs/100 μm were followed to such an extent as to identify the particle as either a π-meson or a baryon. No baryon with density <32 blobs/100 μm was observed.

The search for π-mesons emitted in the K^- interaction was carried out in two steps. First all black and « grey » tracks were followed to rest, and their nature and energy so determined. Then a careful search was made for « light » tracks. This care involved a scrutiny of the K^- endings by as many as 4 independent observers at different times. During the final scrutiny which lasted up to 20 min for each K^- ending the field of view was rotated slowly through 360° by rotation either of the stage or of the microscope head, or the eyepiece cross wire was similarly rotated.

In the analysis of the tracks emitted in the K^- stars, those tracks emitted at an angle of more than 60° to the plane of the emulsions were discarded, in order to avoid ambiguity in the separation of fast baryons from π-mesons. A correction for solid angle was then applied to the resulting π/K^- ratio.

The distribution in dip and depth of the π-meson tracks at their origin, is given in Table I.

On all tracks which were not followed to rest, between 500 and 1000 blobs were counted on at least three different plates, in the central 400 μm of emulsion. It was necessary to count in more than one or two plates since, due either to processing or to fluctuations in sensitivity in these new fine grain emulsions, important differences in blob density were found in certain zones of the plates.

When the blob-density of the track was equal to or greater than that corresponding to a proton of the maximum expected energy of 300 MeV (π-meson of 45 MeV), the track was followed to its end or to the point at which, if a π-meson, it would have come to rest already, and a second blob count made. No baryon with blob density lower than that corresponding to 230 MeV was observed.

Fig. 1 shows the distribution in blob density of all π-mesons and of the « fast » baryons with energy $> \sim 100$ MeV.

For particles which interacted in

TABLE II.

Authors	No. of K^- at rest	No. of π-mesons observed	π/K^- ratio (%)
BACCHELLA *et al.* [2]	391	118	30
CHADWICK *et al.* [3]	815	230	28.2
EISENBERG *et al.* [4]	548	175	32
EUROPEAN COLLABORATION [1]	3024	892	29.6 (33.2) (*)
Present work	1148	390+(12) (**)	39.2+(1.3) (**)

(*) Corrected for scanning losses.
(**) Bracketed figures refer to doubtful π-mesons.

[2] G. L. BACCHELLA, A. BERTHELOT, A. BONETTI, O. GOUSSU, F. LÉVY, M. RENÉ, D. REVEL, J. SACTON, L. SCARSI, G. TAGLIAFERRI and G. VANDERHAEGHE: *Nuovo Cimento*, **8**, 215 (1958).

[3] G. B. CHADWICK, S. A. DURRONI, P. B. JONES, J. W. G. WIGNALL and D. H. WILKINSON: *Phil. Mag.*, **3**, 1193 (1958).

[4] Y. EISENBERG, W. KOCH, M. NICOLIĆ, M. SCHNEEBERGER and H. WINZELER: *Nuovo Cimento*, **11**, 351 (1959).

flight or left the stack after a few mm, the value of $p\beta$ was determined by scattering in order to assure the separation of π-mesons from protons. Where the available track length was too short to allow scattering determination, the track was listed as doubtful. Owing to the difficulties of following close to the beam direction, some tracks had to be abandoned after a short distance. There were 3 instances of this, and these are also shown as doubtful events in Tables II and III.

TABLE III.

Class	Present work				Previous work [1]		
	No. of K^--mesons	% of total K^-	No. of π mesons (angle of dip $\leqslant 60°$)	Ratio π/K^- in the class (corrected to total solid angle) (%)	Ratio π/K^- in the class (%)	Mean Kin. Energy of π's in the class (MeV)	% Loss of π-mesons deduced from present work
$K\varrho$	112	9.8	—	—	—	—	—
$K\sigma_1$	214	18.6	66+(5)	36 +(3)	27	79	33
$K\sigma_2$	333	29.0	164+(4)	57 +(1)	51.5	52.5	10.7
$K\sigma_3$	207	18.0	64+(2)	36 +(1)	32.8	51	9.8
$K\sigma_4$	141	12.3	40+(1)	33 +(1)	22.4		
$K\sigma_5$	102	8.9	44	50	32.5	50	52
$K\sigma_{\geqslant 6}$	39	3.4	12	35	25.0		
Total	1148	—	290+(12)	39.2+ +(1.3)±2	29.6±1.1	—	32.5+ +(4.5)±2.3

2) Errors in the solid angle correction, due to errors in measurement of the dip of the particle near the cut-off, fluctuations in thickness of the plates and uncertainty in the mean thickness of the plates of this stack. The first two are random errors, the total effect on the π/K^- ratio being negligible. The third effect leads to a systematic error. Measurements made in specimen plates indicate that the true mean thickness does not differ from the nominal value by more than 10%. With a deviation of 10% from the nominal thickness, the π/K^- ratio would change by $\pm 1\%$.

3) Further observational loss. It is most probable that there still remains a scanning loss of the faster π-mesons. A general scarcity of grains in the field of view, the existence of a large gap in the π-meson track at its origin, and, associated with either of these, a high distortion in the plate, will reduce the visibility of the track below observational level. Plates were exchanged between the collaborating groups, so that a part of each sample could be re-examined. One or two additional π-mesons were found in each case, which

3. – Results.

Among 1148 K^- stars examined, 390 π-mesons were identified, and 12 particles classed as « doubtful π-mesons ». Applying the correction for the restriction of solid angle, this gives a π/K^- ratio of $[39.2+(1.3)\pm 2]\%$, a value substantially higher than that found in previous experiments (see Table II).

This value is subject to the following uncertainties:

1) Statistical fluctuations. These lead to the given error of $\pm 2\%$.

showed that while the efficiency of observation of all groups was comparable, it was always less than 100%.

In Table III are given the numbers of π-mesons in the various types of K^- stars and for comparison, the values obtained in the previous work (1). Table IV shows the percentages of π-mesons below and above 45 MeV, as well as

4. – Conclusions.

1) The value of the π/K^- ratio found in this work, $[39.2+(1.3)\pm 2]\%$, is higher than was previously estimated.

2) A comparison with the previous work of this collaboration shows that the scanning loss there was chiefly among the higher energy π-mesons in

TABLE IV.

Kinetic energy	% of π-mesons and fast baryons	
	present work	previous work (1)
π-mesons		
$0 < E \leqslant 45$ MeV	10.5 ± 1	10.0 ± 0.6
$E > 45$ MeV	28.7 ± 1.7	19.6 ± 0.8
		(23.2 ± 1) (*)
Baryons		
60 MeV $< E <$ 300 MeV	14.7 ± 1.1	14.2 ± 0.7

(*) Corrected for scanning losses.

those of «fast» baryons in the interval (60÷300) MeV, together with the corresponding values from (1).

From these two tables, some idea can be got of the cause of loss of fast particles in the previous experiment:

1) The factor of loss is higher for multi-pronged, ($\sigma \geqslant 4$) stars than in stars of one, two or three prongs. This implies that the more complex was the event, the less carefully it was examined, as might be expected.

2) Among the stars with fewest prongs, the greatest loss of π's was that among the $K\sigma_1$ events. This may be attributed to the higher mean energy of the mesons in this type of event. There is a corresponding reduction in the percentage of $K\varrho$ events. That the higher energy π-mesons are those which escape observation appears from Table IV.

$K\sigma_1$ stars and among the multi-pronged events.

3) This implies a larger proportion of hyperons produced directly in the interaction

$$K^- + N \to \pi^- + \Lambda^0,$$

and that the absorption of π-mesons is even smaller than previously estimated.

4) The importance of the loss of π-mesons in previous work requires a reassessment also in the study of Σ hyperons, of the branching ratio

$$\Sigma^+ \to \pi^+ / \Sigma^+ \to p,$$

of the sign ratio, and possibly of the lifetime.

5) The estimation of the frequency of K^--2N interactions, if based on the number of events not associated with π-mesons, is likely to lead to an overestimate.

LIBRI RICEVUTI E RECENSIONI

K. B. MATHER and P. SWAN: *Nuclear Scattering*. Cambridge University Press, 1958; pp. 469; 80 s.

È un libro completo sullo scattering nucleare, in cui il lettore trova un'ampia esposizione sia della parte propriamente tecnica, sia della interpretazione teorica dei risultati. Quanto ai risultati, l'esposizione è aggiornata al 1957.

Questo libro è senz'altro utile a chi lavora in fisica nucleare ed è, a mio parere, da consigliarsi a chi inizia delle ricerche in questo campo. La breve esposizione che segue, del contenuto dell'opera preciserà questo giudizio. Infatti la trattazione della materia segue, si può dire, le varie parti e fasi dell'esperienza.

Gli autori iniziano con la descrizione delle sorgenti di particelle veloci, dei vari tipi di bersaglio, delle misure di intensità ed energia del fascio. Essi, descrivono poi vari tipi di rivelatori di particelle (cariche e neutre) ed alcune disposizioni sperimentali d'insieme tipiche per esperienze con neutroni o protoni.

Nella seconda parte del testo gli autori espongono i risultati relativi alle interazioni nucleone-nucleone, nucleone-nucleo nei vari intervalli di energia e la interpretazione teorica di questi risultati.

Data la vastità della materia trattata nel libro, è evidente che per ulteriori precisazioni e approfondimenti il lettore dovrà rivolgersi a testi specializzati sia nel campo tecnico, che nella parte teorica.

M. GRILLI

Direttore responsabile: G. POLVANI Tipografia Compositori - Bologna

Questo Fascicolo è stato licenziato dai torchi il 10-IV-1959